

國立台灣大學醫學院暨工學院醫學工程學研究所



博士論文

Institute of Biomedical Engineering
College of Medicine and College of Engineering
National Taiwan University
Doctoral Dissertation

利用特定環境蛋白誘導毛囊新生

Inducing hair follicle organogenesis with defined
environmental proteins

范邁儀

Sabrina Mai-Yi Fan

指導教授：林頌然 博士

Advisor: Sung-Jan Lin, MD, PhD

中華民國 107 年 1 月

January 2018

國立臺灣大學博士學位論文
口試委員會審定書

利用特定環境蛋白誘導毛囊新生

Inducing hair follicle organogenesis with defined
environmental proteins

本論文係范邁儀君（學號 d98548009）在國立臺灣大學醫學工程
學研究所完成之博士學位論文，於民國107年1月26日承下列考試委員
審查通過及口試及格，特此證明

口試委員：

林 頌 然

(指導教授)

陳玉如

楊念修

楊宗霖

曹伯鈞

所長：

黃義偉

中文摘要

器官發育是一個自體組織生成的複雜過程。毛囊新生是透過角質細胞與真皮細胞間的所展開及持續的交互作用所達成。在成體狀態下誘導毛囊新生需要活化角質細胞並且誘導上皮-間質交互作用。後者可藉由毛囊真皮乳突細胞誘導，但因細胞來源有限且體外培養過程中容易喪失所需之特性。儘管現階段已有許多研究在探討相關的胚胎發育機制，但如何在成體誘發此發育機制而誘導成體器官再生仍尚未釐清。

本研究在探討可否可利用真皮細胞以誘導出生後的上皮-間質交互作用，而進一步誘導毛囊新生。本研究發現利用特定發育階段的胚胎皮膚所取得的無細胞萃取物，能夠在沒有毛囊真皮乳突細胞或新生鼠真皮細胞的幫助下，在全層皮膚傷口模型或修改的小片毛囊再生模型中誘導毛囊新生。我們發現在此毛囊新生的過程中主要是藉由影響纖維細胞而達成。成體的纖維細胞培養於胚胎皮膚萃取物後，可讓纖維細胞展現誘導毛囊新生的能力；但角質細胞利用此刺激後，並無法誘導毛囊新生。我們透過分析接觸此萃取物的纖維母細胞之磷酸化蛋白質體發現胰島素/類胰島素生長因子訊息傳遞被活化，並在實驗中確認此訊息傳遞路徑在成體纖維細胞誘導毛囊新生的過程是必需的。此外透過分析此胚胎皮膚萃取物的蛋白質體，我們尋找到三個會大量表現在胚胎皮膚的分泌型胞外蛋白，包括脫輔基蛋白質-1，半乳凝素-1 和基膜聚醣。動物實驗實驗證實利用此三個蛋白質可與表皮細胞混合後，可在活體中修改的小片毛囊再生模型中誘導毛囊新生。因此經過特定細胞外蛋白混合物短時間刺激後，成體細胞可以被誘導成具有再生能力的細胞。

器官再生可以透過施與特定的細胞外因子來建構促發組織再生反應的環境。故藉由特定器官的胚胎組織來尋找誘發此器官再生特定蛋白質組合，可以作為促進成體器官再生的重要策略。

關鍵詞：

毛囊，無細胞萃取物，新生，特異的細胞外因子，纖維細胞，重編程，蛋白質體學

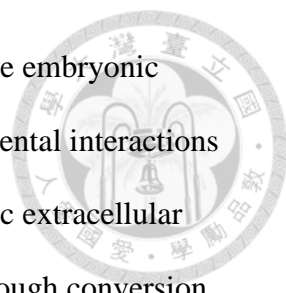
ABSTRACT



Organ development is a sophisticated process of self-organization. Hair follicle neogenesis depends on the initiation and perpetuation of crosstalk between keratinocytes and dermal cells. Regenerating new hair follicles in adults requires reactivation of epithelial-mesenchymal interactions between competent keratinocytes and inductive mesenchymal cells. The latter can be expanded from the preexisting dermal papilla fibroblasts of mature hair follicles, yet this source is limited and cells quickly lose inductive properties in culture. However, despite a growing understanding of the developmental mechanisms involved, little is known about how to reactivate them for adult organ regeneration.

We ask whether this epithelial-mesenchymal interaction for hair follicle neogenesis can be initiated without introducing inductive dermal cells in postnatal life. Here we demonstrate a new regenerative approach that does not require dermal papilla fibroblasts. We found that cell-free extract from embryonic skin of specific developmental stages was able to induce hair follicle neogenesis both in a full-thickness wound and in a modified patch assay in mice without the help of inductive dermal papilla cells or newborn dermal cells. Hair follicle neogenesis here was mediated mainly through the effect on fibroblasts. When adult fibroblasts, but not keratinocytes, were cultured with the cell-free extract, they were conferred on the ability to induce new hair follicles. In search of the molecular mechanisms involved through phosphoproteomic analysis, we found that insulin/IGF signaling was activated and required for the hair follicle inductivity in adult fibroblasts.

Finally, through proteomics analysis, we identified 3 extracellular/ secreted proteins, including apolipoprotein, galectin-1 and lumican, enriched in embryonic skin. These three proteins together were required and sufficient to induce hair follicle neogenesis in



vivo. Thus, a cocktail of organ-specific extracellular proteins from the embryonic environment can render adult cells competent to re-initiate developmental interactions for regeneration. Therefore, short-term exposure to and organ-specific extracellular protein cocktail can render adult cells competent for regeneration through conversion toward a state in which their fate can be further stably committed via re-engagement in developmental interactions. These 3 proteins show a stage-specific co-enrichment in the embryonic dermis during the peri-folliculogenetic period. Mechanistically, exposure to embryonic skin extract or a combination of the 3 proteins altered the gene expression to a hair follicle dermal papilla fibroblast-like profile and activated Igf and Wnt signaling, crucial for the regeneration process.

Organ regeneration can be initiated by creating a pro-regeneration environment with defined extracellular factors. Identification of factors to recreate tissue-specific embryonic extracellular context could become an important strategy for promoting regeneration in various adult organs.

Keywords: hair follicle, cell-free extract, neogenesis, defined extracellular factors, fibroblast, reprogramming, proteomics

目 錄



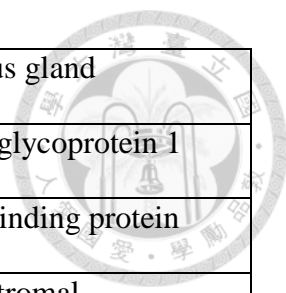
中文摘要	1
ABSTRACT	2
目 錄	4
LIST OF ABBREVIATIONS	6
LIST OF FIGURES	8
LIST OF TABLE	11
Introduction	12
Hair Follicle Structure	12
Development of a Hair Follicle.....	15
The Damaged Tissue is Often Replaced by Fibrosis with Further Functional Deterioration	18
Stem Cells and Bioartificial Organs	20
Hair Follicle Neogenesis by Dermal Papilla Cells	21
Spontaneous Regeneration of Hair Follicles.....	23
Hair Follicle Inducing Ability and Scarless Healing of Fetal Skin	24
HYPOTHESIS	26
MATERIALS AND METHODS	28
Animals	28
Preparation of Cell-Free Extract	28
Dilution and Pretreatment of Skin Extract	29
Cells and Culture	29
Standard and Modified Patch Assays	30
Hair Follicle Neogenesis in Full-Thickness Wound and Preparation of Dermal Equivalent.....	31
Real-Time PCR Analysis of Gene Expression	31
RNA-Sequencing and Analysis	33
Beta-Galactosidase Activity Assay and Alkaline Phosphatase Activity Assay.....	34
In Situ Hybridization	35
Western Blot.....	35
Recombinant Proteins.....	36
Histology and Immunofluorescence	36
Mass Spectrometry for Proteomic and Phosphoproteomic Analysis	37
Bioinformatics Analyses	40
Statistics	40
RESULTS	41
Cell-Free Extract from Stage-Specific Embryonic Skin Could Induce HF Neogenesis	41
Protein Fraction in E16.5 Skin Extract was Sufficient to Induce HF Neogenesis ..	48
Proteomic Analysis Identified Eight Secreted Proteins Enriched with Embryonic Skin	51
Apolipoprotein-A1, Galectin-1 and Lumican Together were Required and Sufficient to Induce HF Neogenesis.....	66

E16.5 Skin Extract Conferred Fibroblasts a Reversible Ability to Induce HF Neogenesis.	71
Fibroblasts become competent for hair regeneration after exposure to embryonic skin proteins	74
Activation of Insulin/IGF1 Signaling in Fibroblasts Exposed to E16.5 Skin Extract and 3 Proteins.....	79
Insulin/IGF1 and Wnt Signaling was Required for Hair Follicle Induction Ability of Fibroblasts.....	81
Discussion	92
Conclusions	97
Reference	100

LIST OF ABBREVIATIONS



Ab	antibody	HS	hair shaft
ACN	acetonitrile	HCD	higher-collisional dissociation
FBs	adult fibroblasts	IRS	inner root sheath
Anxa2	annexin A2	IGF	Insulin-like growth factor
Apoa1	apolipoprotein-A1	KC	keratinocyte
APM	arrector pili muscle	LC-MS/MS	liquid chromatography- tandem mass spectrometry
BM	basal membrane	Lum	lumican
Baso	basophil	MS/MS	mass spectra
β -cat	beta-catenin	Mast	mast cell
BMP	bone morphogenetic protein	M	matrix
CL	companion layer	NCE	normalized collision energy
CTS	connective tissue sheath	ORS	outer root sheath
DP	dermal papilla	PBS	phosphate buffer solution
DS	dermal sheath	PMN	polymorphonuclear leukocyte
E13.5	embryonic day 13.5	P1	postnatal day 1
EOS	eosinophil	PCA	Principal component analysis



ECM	extracellular matrix	SG	sebaceous gland
Fgb	fibrinogen beta chain	Psap	sulfated glycoprotein 1
FGF	fibroblast growth factor	TBP	TATA-binding protein
Fn1	fibronectin	TSLP	thymic stromal lymphopoietin
FA	formic acid	TGF- β	transforming growth factor-beta
Lgals1	galectin-1	TA	transit amplifying
Gsn	gelsolin	TFA	trifluoroacetic acid
HF	Hair follicle	TNF	tumour necrosis factor

LIST OF FIGURES



Figure 1 Histomorphology of the hair follicle.	14
Figure 2 Embryonic pelage hair follicle development in mice.	17
Figure 3 Overview of wound repair and fibrosis.	19
Figure 4 Preparation of skin extract and HF neogenesis assays	27
Figure 5 Histology of Wistar rat skin at different developmental stages.	43
Figure 6 The effect of cell-free extract prepared from different stages of skin on HF induction.	44
Figure 7 Proteins in cell-free extract from stage-specific embryonic skin induce HF neogenesis.	45
Figure 8 Alkaline phosphatase activity and HS morphology of new HFs induced by E16.5 skin extract.	46
Figure 9 Proteins in cell-free extract from stage-specific embryonic skin induce HF neogenesis.	47
Figure 10 Effect of serial dilution of E16.5 skin extract on HF inductivity.	49
Figure 11 Proteins in cell-free extract from stage-specific embryonic skin induce HF neogenesis.	50
Figure 12 Proteomic analysis identifies secreted proteins enriched in developmental skin.	53
Figure 13 Proteomic analysis identifies secreted proteins enriched in developmental skin.	63
Figure 14 Expression of the 8 proteins in E17.5 Wistar rat embryonic skin.	64

Figure 15 Expression of apolipoprotein-A1, galectin-1 and lumican genes in embryonic to postnatal skin detected by in situ hybridization.	65
Figure 16 Combination of 7 or 8 proteins to induce new HF.	67
Figure 17 Induction of HF neogenesis by defined proteins.	68
Figure 18 Induction of HF neogenesis by defined proteins.	69
Figure 19 Induction of HF neogenesis by defined proteins and mRNAs.	70
Figure 20 E16.5 skin extract confers adult fibroblasts trichogenic ability.	72
Figure 21 Effect of rat E16.5 skin extract on HF inductivity of adult human dermal fibroblasts.	73
Figure 22 Comparison of numbers of upregulated genes in indicated conditions.	75
Figure 23 Pathway analysis of all regulated phosphoproteins exposed to E16.5 skin extract or 3 proteins.	80
Figure 24 E16.5 skin extract confers adult fibroblasts trichogenic ability through activating IGF and Wnt signaling.	83
Figure 25 Alkaline phosphatase activity and gene expression of adult fibroblasts cultured in E16.5 skin extract.	85
Figure 26 Effect of the combination apolipoprotein-A1, galectin-1 and lumican on IGF and Wnt signaling in adult fibroblasts.	87
Figure 27 Alkaline phosphatase activity and gene expression of Human adult fibroblasts cultured in E16.5 skin extract.	88
Figure 28 The effect of the 3 proteins on IGF and Wnt signaling in human adult fibroblasts. Adult fibroblasts were cultured with 3 proteins.	90
Figure 29 Induction of HF neogenesis by defined proteins and mRNAs.	91

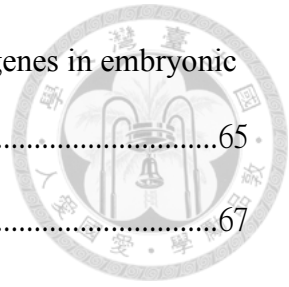


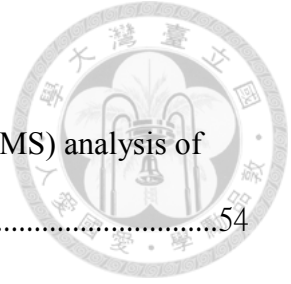
Figure 30 Depiction of the effect of embryonic environmental proteins on HF
neogenesis.....



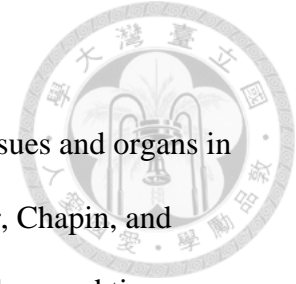
99

LIST OF TABLE

Table 1 Liquid chromatography-tandem mass spectrometry (LC-MS/MS) analysis of proteomes of E16.5 and P1 skin extract.	54
Table 2 RNA sequencing data of DP; fibroblasts before and after exposure to E16.5 skin extract and to the combination of 3 proteins of ApoA1/Lgals1/Lum mix.....	76



Introduction

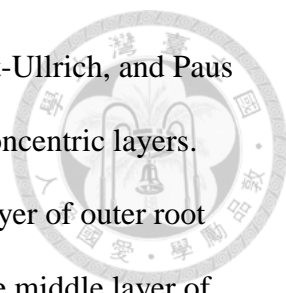


Compared with the profound spontaneous restoration of lost tissues and organs in lower vertebrates (Brockes 1997; Johnson and Weston 1995; Becker, Chapin, and Sherry 1974), mammals show limited regeneration after injury and damaged tissues are often replaced by morphological and functionally debilitating scars (Wynn and Ramalingam 2012). In adult skin, wounds are usually repaired by fibrosis rather than regeneration, leading to scarring and permanent loss of skin appendages, prominent hair follicles (HFs) (Martin 1997). Although promotion of wound healing has been attempted by transplanting cultured keratinocytes or skin equivalents (Veves et al. 2001; O'Connor et al.)

Hair loss can cause great psychosocial distress for patients. The most common cause of hair loss is androgenetic alopecia or male pattern baldness (Norwood 1975; Messenger, Slater, and Bleehen 1986). The main treatment includes systemic 5- α reductase inhibitor (Diani et al. 1992; Kaufman and Dawber 1999) or topical minoxidil (Kreindler 1987; Headington 1987). In severe cases, hair transplantation is an alternative treatment choice. It involves surgical redistribution of autologous hair follicles (HFs) from the hairy zone (e.g., occipital scalp). Hence this treatment is limited to patients with significant amount preserved. In patients with severe hair loss, regeneration of functional HFs is an unmet challenge.

Hair Follicle Structure

Skin is a large peripheral organ densely populated by Adult stem cells (SCs). It contains a huge number of hair follicles (HFs) that undergo repetitive cycles of regeneration consisting of growth (anagen), regression (catagen) and rest (telogen) phases (Muller-Rover et al. 2001). HF is a mini-organ composed of an epithelial cylinder and its



characteristic mesenchyme, dermal papilla (DP) (Schneider, Schmidt-Ullrich, and Paus 2009). The elongated epidermal strand differentiates into different concentric layers. They include: 1. the central cylinder of hair shaft (HS) 2. the outer layer of outer root sheath (ORS) that separates HF from surrounding mesenchyme 3. the middle layer of the inner root sheath (IRS) which allows the HS to penetrate upward to emerge from the skin surface. It is suggested the IRS moves outward together with the HS.

HF epithelium contains an anatomical protruding portion, named bulge. Bulge is the niche where HF stem cells reside and it is also the location where the arrector pili muscle is connected with HFs (Cotsarelis, Sun, and Lavker 1990). Bulge stem cells are able to differentiate into sebocytes and interfollicular epidermal keratinocytes. Above the bulge in the sebaceous gland (SG), a small oil-producing structure. The sebocytes of SG produce and release fatty substance to lubricate both the HS and the skin surface. Anagen HFs contain a lowermost bulbar structure, the hair bulb, which contains quickly proliferating matrix cells, which support the growth of the inner layered structure of HFs.

The dermal components of HF include the DP cells and dermal sheath (DS) cells. DP, located at the base of HFs, is composed of a group of specialized fibroblasts. DS surrounds' the HF from bulge level downward to the base of the HF and is connected with DP cells. Developmentally, both DP and DS are derived from local fibroblasts during embryonic stage through the epithelial-mesenchymal interaction of HF development.

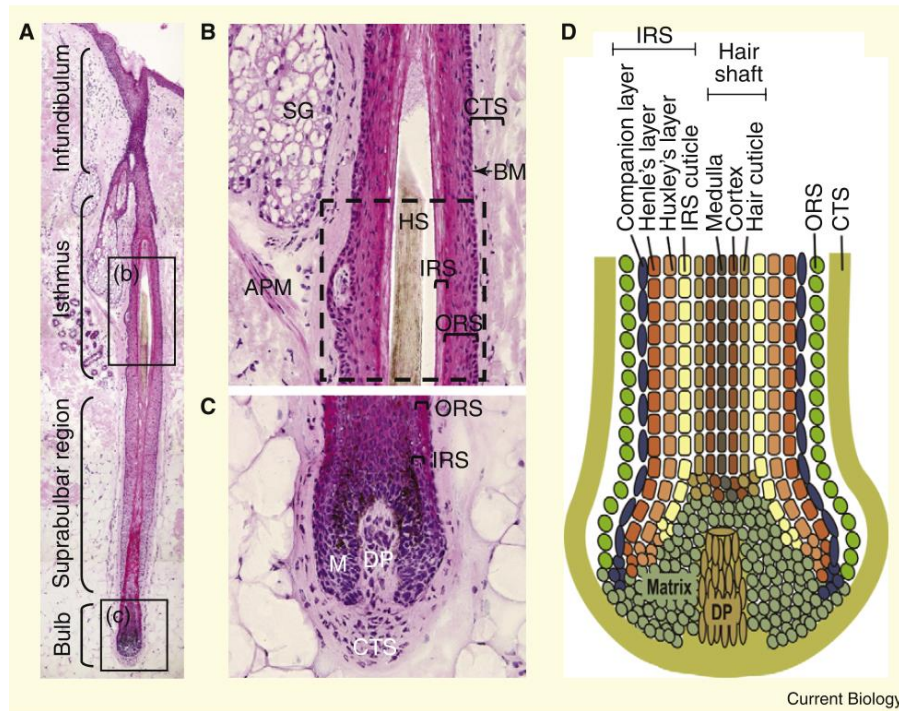


Figure 1 Histomorphology of the hair follicle.

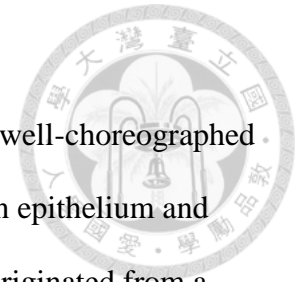
(A) Sagittal section of HF (anagen VI) showing the infundibulum, isthmus, suprabulbar and bulbar area components of the hair follicle. (B) The high magnification image of the isthmus. (C) The high magnification image of the bulb. (D) Schematic drawing illustrating the concentric layers from ORS, IRS and the shaft in the bulb. (CL: companion layer; BM: basal membrane; APM: arrector pili muscle; CTS: connective tissue sheath; M: matrix) (Schneider, Schmidt-Ullrich, and Paus 2009)

Development of a Hair Follicle

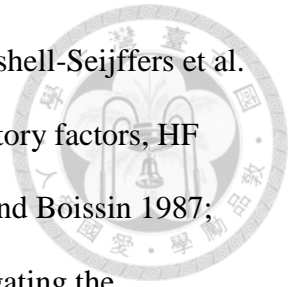
Similar to other epithelial organs, HF development depends on well-choreographed epithelial-mesenchymal interaction initiated by the crosstalk between epithelium and local fibroblasts (Schneider, Schmidt-Ullrich, and Paus 2009). It is originated from a multi-stepped process during which embryonic epidermis elongates downwards through the interaction with the mesenchyme (Hardy 1992; Millar 2002). It is proposed that the first signals for HF development are derived from the embryonic dermis and induce the above lying undifferentiated epidermis to form a thick plaque named placode. Then the placode cell signal back, causes the underlying dermal cells to aggregate into clustered cells of dermal condensate. The dermal condensate induces placode cells to proliferate and transform from an epidermal fate into a follicular fate. These transformed epithelial cells elongate downward into the dermis, forming a thorough structure of HF. The initial dermal condensate progressive committed to a dermal papilla (DP) fate.

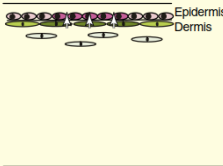
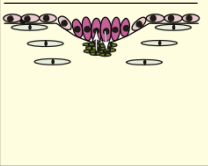

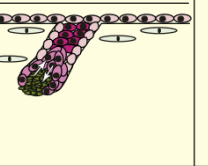
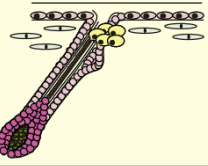
During HF morphogenesis, signals known to regulate epithelial-mesenchymal communication includes the Wnt/wingless family, the hedgehog family, members of the TGF- β /BMP (transforming growth factor-beta/bone morphogenetic protein), FGF (fibroblast growth factor) and TNF (tumor necrosis factor) families (Schneider, Schmidt-Ullrich, and Paus 2009).

Activation of each new regeneration cycle is fueled by HF stem cells (HFSCs) residing in the so-called bulge and secondary hair germ niche compartments (Cotsarelis, Sun, and Lavker 1990; Greco et al. 2009). When HFSC activity becomes suppressed, entrance to anagen is prohibited (Choi et al. 2013; Plikus et al. 2008; Chen and Chuong 2012; Kandyba et al. 2013; Kobiela et al. 2007). HFSC activity has been shown to be regulated by intrinsic intracellular factors as well as by the signals from the local and systemic environments (Ali et al. 2017; Castellana, Paus, and Perez-Moreno 2014; Chen



et al. 2015; Chen et al. 2016; Festa et al. 2011; Plikus et al. 2008; Enshell-Seijffers et al. 2010; Oshimori and Fuchs 2012). In addition to these internal regulatory factors, HF regeneration can also be altered by external cues (Maurel, Coutant, and Boissin 1987; Chen et al. 2016). Therefore, HF provides an opportunity for interrogating the mechanisms of how tissue SCs communicate with the outer environment and how the external environmental changes are perceived and transmitted to an internal SC niche.



Induction		Organogenesis		Cytodifferentiation
Stage 0	Stage 1 (placode)	Stage 2 (germ)	Stage 3–5 (peg)	Stage 6–8 (bulbous peg)
				
Interacting gradients of activators and inhibitors creating an inductive field in the epidermis (pre-germ). Specialised dermal fibroblasts gather underneath pre-germ.	Visible hair germ (placode). Promotion of placode growth: <i>Wnt/β-catenin</i> , <i>EdaA1/EdaR/NF-κB</i> , <i>Noggin/Lef-1</i> , <i>CTGF?</i> , <i>Ectodin?</i> , <i>P-cadherin</i> . Inhibition of placode fate in surrounding cells and placode growth: <i>Dkks (Dkk1, 2, and 4)</i> , <i>BMPs (2, 4 and 7)</i>	Proliferation of epidermal hair germ cells: <i>Shh/Smo/Gli2</i> , <i>Wnt (10b,10a)/Lef-1</i> , <i>FGFs/FGF2R-IIIb</i> , <i>TGFβ2?</i> , <i>Follistatin?</i> Formation of dermal papilla: <i>Shh/Smo/Gli2</i> , <i>PDGF-A</i> .	See Table 2 for molecular controls of ORS, IRS and hair shaft formation, polarity, shaping, innervation etc.	See Table 2 for molecular controls of ORS, IRS and hair shaft formation, polarity, shaping, innervation etc.

Current Biology

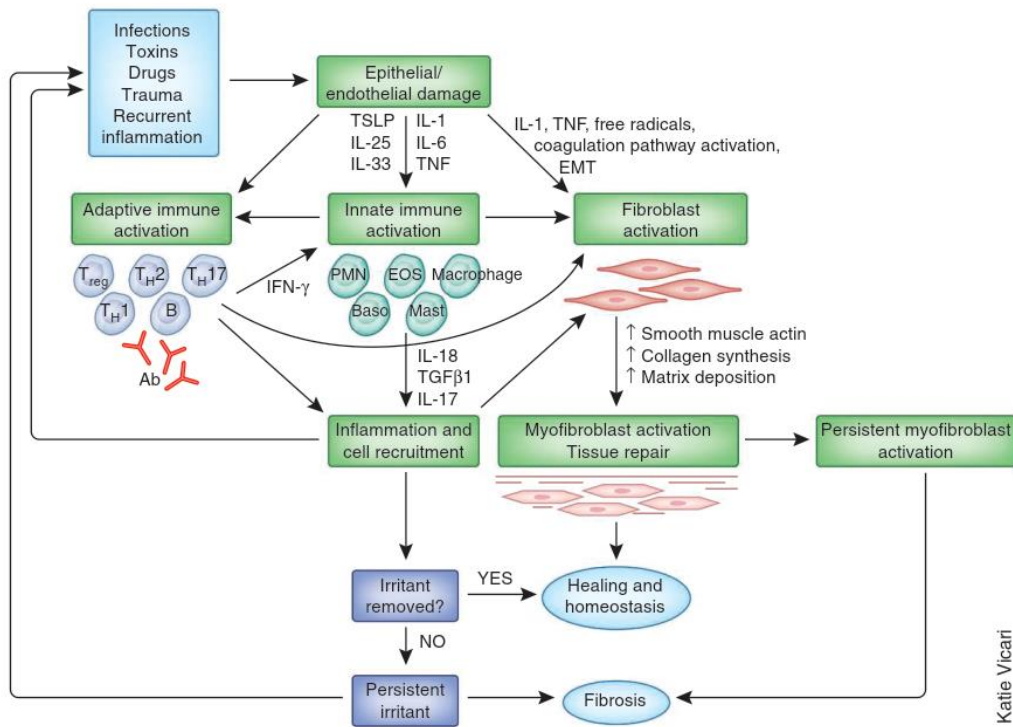
Figure 2 Embryonic pelage hair follicle development in mice.

Their three phases in Murine HF development: Induction, organogenesis and cytodifferentiation. The most important stages of HF morphogenesis in prenatal HF development (stages 0-8). At E14 is the primary guard hair development status. And then two major waves in HF development in one of which is intermediate awl and auchene hairs at E16.5 and downy zigzag hairs around P0. At stage 1, HF placode has formed, the inductive signal involves local HF activators (such as *Wnt/β-catenin* signaling) suppress HF inhibitors which between the epidermis and the underlying dermis. The dermal condensate and DP form at follow stages. And the placode growth since the BMP signaling has been down-regulated with the developing placode. In the following stages 3–8, began to develop different hair lineages (Schneider, Schmidt-Ullrich, and Paus 2009).

The Damaged Tissue is Often Replaced by Fibrosis with Further Functional Deterioration

In adult skin, wounds are usually repaired by fibrosis rather than regeneration, leading to scarring and permanent loss of skin appendages, prominent hair follicles (HFs) (Martin 1997). Mammals show limited regeneration when injured (Wynn and Ramalingam 2012). The damaged tissue is often replaced by fibrosis with further functional deterioration (Wynn and Ramalingam 2012). Various injuries caused epithelial and/or endothelial damage. The programs of wound-healing to restore homeostasis. At the first, the coagulation pathway which functions to prevent blood loss. Followed by adaptive immune activation and innate immune activation. Because the activation of the adaptive immune response, stimulating the Epithelial and innate immune cells to produce cytokines. Tissue damage can also directly eliciting the adaptive immune response. In the process, there are some inflammatory and immune mediators (cytokines, chemokines and free radicals) try to eliminate the inciting factor. At the same time the reaction activates the quiescent fibroblasts into myofibroblasts. And promote orchestrate angiogenesis and production of extracellular matrix (ECM) components. Activation of Wnt- β -catenin signaling increases the synthesis of ECM components in mouse and human lung fibroblasts (Baarsma et al. 2011). If they failed to eliminate the inciting factors can exacerbate the inflammatory response and cause to a chronic wound-healing, with continued tissue damage, repair and regeneration, in the end resulting in fibrosis (Wynn and Ramalingam 2012).





Katie Vicari

Figure 3 Overview of wound repair and fibrosis.

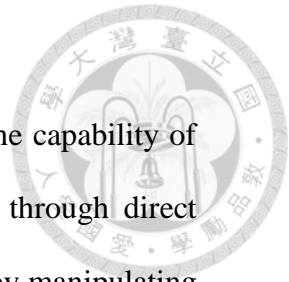
Ab, antibody; Baso, basophil; EOS, eosinophil; Mast, mast cell; PMN, polymorphonuclear leukocyte; TSLP, thymic stromal lymphopoietin (Wynn and Ramalingam 2012).

Stem Cells and Bioartificial Organs

The results of previous studies of attempts to gain or restore the capability of certain cell types for specific purpose have been achieved either through direct conversion with transcriptional factors (Vierbuchen et al. 2010), or by manipulating cellular microenvironment (Higgins et al. 2013), or by culturing cells with defined growth factors.

Cell differentiation during development of the majority is found in an irreversible. But the 2006 results show that mouse and human fibroblasts can make use of in combination with the four transcription factors (Oct3/4, Sox2, c-Myc, and Klf4) after reprogramming to a pluripotent state. (Takahashi and Yamanaka 2006; Vierbuchen et al. 2010). These transcription factors are adequate to cause pluripotency in primary fibroblasts proved that fully differentiated cells can be induced to experience dramatic cell fate changes (Takahashi and Yamanaka 2006). Changes in transcriptional activity could also cause to genome-wide regulation of inhibiting and active epigenetic features such as DNA methylation, histone modifications and changes of chromatin remodeling complexes (Zhou and Melton 2008; Jaenisch and Young 2008).

Another way to create reproductive organs, previous studies utilize coronary perfusion with detergents to create decellulized cadaveric hearts, or can also use the direct immersion way to deal with a less complex tissues to generate a cellular scaffold (Rieder et al. 2004; Dellgren et al. 2002; Ketchedjian et al. 2005; Chen et al. 2004; Gilbert, Sellaro, and Badylak 2006). And the function of neonatal cardiac cells or rat aortic endothelial cells repopulated the decellularized rat hearts can be simulated organ maturation (Gerecht-Nir et al. 2006). This technique is known can be used in mammalian organs including lung, liver, kidney and muscle (Ott et al. 2008). With such



efforts, incorporation of transplanted cells for functional organ regeneration is still among the most challenging issues in regenerative medicine (Segers and Lee 2008).

In addition to cell transplantation, regeneration can theoretically be induced *in situ*, a process of spontaneous restoration of lost organs more often seen in amphibians and fish (Brockes 1997; Johnson and Weston 1995; Becker, Chapin, and Sherry 1974). Adult urodeles can take advantage of blastemal or mesenchymal growth zone and then regenerate their limbs. Production process blastemal cells depends on the local extracellular environment and the differentiated state after injury and wounding. However, the molecular basis related is not fully understood, but proximodistal identity in newt blastemal cells may be respecified by signaling through a retinoic acid receptor isoform (Brockes 1997).

Hair Follicle Neogenesis by Dermal Papilla Cells

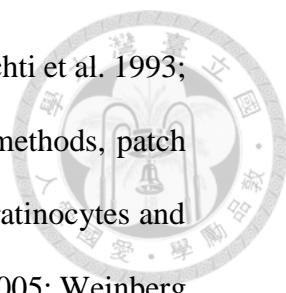
HFs provide a paradigm for studying postnatal tissue and organ regeneration. Similar to other ectodermal mini-organs, HF development depends on well-choreographed epithelial-mesenchymal interactions initiated by the crosstalk between epithelial and dermal embryonic skin progenitors (Millar 2002; Dhouailly 1973; Hardy 1992; Schneider, Schmidt-Ullrich, and Paus 2009). During HF morphogenesis, epithelial progenitors gradually adopt a follicular fate, whereas dermal progenitors differentiate into DP fibroblasts. DP cells play a key part on the mesenchymal side, and the keratinocyte located on top is responsible for the development of the epidermal components in the embryonic stage (Oliver 1966; Jahoda, Horne, and Oliver 1984; Horne, Jahoda, and Oliver 1986). The most important breakthrough was the aggregation DP cells in cultured were able to induce a new HF when they were put in close to the epithelium *in vivo* (Jahoda, Horne, and

Oliver 1984). Continue study found that cultured DP cells possess the ability to “transform” epidermal cells into follicular epithelium (Reynolds and Jahoda 1992).

In normal adult skin, new HFs generally cannot form (Schneider, Schmidt-Ullrich, and Paus 2009). As an exception, HFs can regenerate spontaneously in the center of very large wounds and with low efficiency in humans via incompletely understood mechanisms (Ito et al. 2007; Seifert et al. 2012; Kligman and Strauss 1956; Gay et al. 2013; Nelson et al. 2015). Such examples indicate that, in principle, the potential for HF neogenesis is preserved in adult mammals and can possibly be unleashed.

To induce new HFs in adults, Oliver et al. demonstrated that microdissected DP could induce new HFs from epidermis when transplanted into the subepidermal space (Oliver 1970). Following this seminal work, HF neogenesis in adults has largely relied on culture-expanded DP fibroblasts, which are capable of reinitiating developmental epithelial-mesenchymal interactions with competent keratinocytes (Jahoda, Reynolds, and Oliver 1993; Huang et al. 2013; Yang and Cotsarelis 2010; Higgins et al. 2013). The HF-inducing ability of cultured DP fibroblasts is easily lost during culture and this limits their use for large-scale HF regeneration (Jahoda, Reynolds, and Oliver 1993). In addition to adult DP cells, freshly isolated newborn murine dermal fibroblasts have also been demonstrated to be capable of inducing HF neogenesis (Yang and Cotsarelis 2010; Weinberg et al. 1993; Morris et al. 2004; Blanpain et al. 2004; Lei et al. 2017), but such HF inductivity of dermal fibroblasts are quickly lost in postnatal life.

To achieve large amount of HF regeneration or neogenesis, both dermal parts and epidermal parts should be taken to consider carefully. Several animal models for generating new hairs have been introduced and are readily applicable in hair regeneration researches. Among them, chamber model, patch assay, sandwich and flap model, and wound model are most well-known and practical (Inamatsu et al.



2006; Zheng et al. 2005; Morris et al. 2004; Weinberg et al. 1993; Lichti et al. 1993; Reynolds and Jahoda 1992; Ohyama et al. 2010). Most published methods, patch assay, simply mix the dissociated state dermal cells and separate keratinocytes and implant them into the subcutis or dermis of nude mice (Zheng et al. 2005; Weinberg et al. 1993; Yen, Chan, and Lin 2010; Osada et al. 2007; Toyoshima et al. 2012; Qiao et al. 2009; Lichti, Anders, and Yuspa 2008). An alternative strategy for inducing new HFs is through the use of embryonic skin (Ferraris, Bernard, and Dhouailly 1997). In contrast to adult skin, wounded embryonic skin heals without scarring and with extensive HF neogenesis (Longaker and Adzick 1991). When embryonic dermal tissues are combined with postnatal epithelium, they are able to induce new HFs (Ferraris, Bernard, and Dhouailly 1997). On the other hand, it has also been suggested that embryonic tissues create unique extracellular environments conducive to regeneration (Longaker and Adzick 1991; Badylak 2005). The extracellular matrix from embryonic and adult tissue has been shown to enhance tissue regeneration (Badylak 2005; McGann, Odelberg, and Keating 2001).

Spontaneous Regeneration of Hair Follicles

Though rarely observed, spontaneous organ regeneration in mammals does occur through mechanisms not well understood (Ito et al. 2007; Seifert et al. 2012; Borgens 1982; Porrello et al. 2011). It indicates that organogenetic potential is preserved in mammals and can potentially be unleashed.

The mammalian HF is a complex ‘mini-organ’ only in the development process of formation (Schmidt-Ullrich and Paus 2005); an adult follicle loss is considered permanent. And the results of other studies surmise skin wounding may induce hair follicle develop on rabbits (Billingham and Russell 1956; Breedis 1954), mice

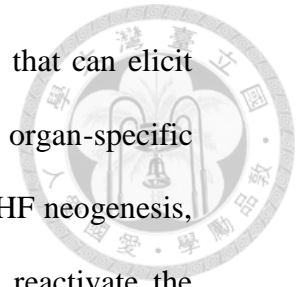
(Lacassagne and Latarjet 1946) and even humans fifty years ago (Kligman and Strauss 1956). And previous studies have found treating acute wounds with modulators of the Wnt pathway to decrease scar formation, and regenerating follicles through wounding and Wnt pathway activation (Ito et al. 2007).

There are two known species of African spiny mouse (*Acomys kemp*i and *Acomys percivali*), they use readily shed portions of their skin as a predator escape behavior. Experimental data show that in *Acomys* regeneration reparative ear is a balance between premature reformation of the dermis (scarring) and maintenance of cell proliferation within a pro-regenerative environment. In contrast, *Mus* not to form (or maintain) a wound epidermis, which is coincident with the precocious formation of the basement membrane and stratification of the epidermis. This results in loss of cell proliferation, increased collagen type I deposition (in lieu of collagen type III), myofibroblast activation and eventually it will form scar (Seifert et al. 2012).

Hair Follicle Inducing Ability and Scarless Healing of Fetal Skin

Compared with adults, embryonic skin exhibits robust regeneration. Embryonic dermis is capable of inducing new HFs when combined with keratinocytes of skin and even non-skin origins (Ferraris, Chaloin-Dufau, and Dhouailly 1994; Ferraris, Bernard, and Dhouailly 1997). Once wounded, embryonic skin undergo scarless healing with extensive HF neogenesis (Longaker and Adzick 1991). It has been suggested that extracellular environment can be key to regeneration (Seifert et al. 2012; Longaker and Adzick 1991; McGann, Odelberg, and Keating 2001; Badylak 2005). Here we test whether embryonic environmental factors can re-elicite epithelial-mesenchymal crosstalk for postnatal HF organogenesis.

Isolation of defined factors present in the extracellular matrix that can elicit neogenesis of an organ can open novel, therapeutically amenable organ-specific regeneration protocols. To bypass the need for embryonic cells for HF neogenesis, we tested whether extracellular factors from embryonic skin can reactivate the epithelial-mesenchymal crosstalk between adult skin cells to elicit HF neogenesis.



HYPOTHESIS



Hair follicle neogenesis comply with the start and continuation of crosstalk between epidermis-mesenchymal cells in embryonic development and hair reconstitution assay. And dermal signals seem to be able to change the fate of the special groups of epithelial cells. Therefore, we ask whether this epithelial-mesenchymal interaction can be initiated without introducing inductive dermal cells in postnatal life. Unlike previously described assays in which mix postnatal day 1 keratinocytes and DP cells, we directly mixed postnatal day 1 keratinocytes and embryonic skin extract in different stages before they were injected subcutaneously on the nude mouse (Fig 4). We found that cell-free extract from embryonic skin of the specific developmental stage was able to induce hair follicle neogenesis both in a full thickness wound and a modified patch assay in mice without the help of inductive dermal papilla cells or newborn dermal cells. Because previous studies have shown the initiation of HF morphogenesis by dermal signals and the embryonic skin scarless healing with extensive HF neogenesis after wounded. For this reason suggested that extracellular environment can be key to regeneration. And by our results also identified specific stages of embryonic skin extracts can induce HF regeneration. Therefore, we speculated whether with specific factors can induce HF regeneration in the specific stage of embryonic skin extract. We use proteomics analysis to compare the postnatal and the embryonic 16.5 skin extract, we identified several extracellular proteins which together were induced hair follicle neogenesis in vivo. This experiment is the main effect of hair follicle neogenesis on fibroblasts. Therefore, we tested adult fibroblasts, but not keratinocytes, were cultured with the cell-free extract, they were conferred the ability to induce new hair follicles. To prove these factors are adequate to induce cell fate changes. In order to further understand the molecular mechanisms involved through

phosphoproteomic analysis, we found that insulin/IGF signaling was activated and required for the hair follicle inductivity in adult fibroblasts. Therefore, organ regeneration can be initiated by creating a pro-regeneration environment with defined extracellular factors.

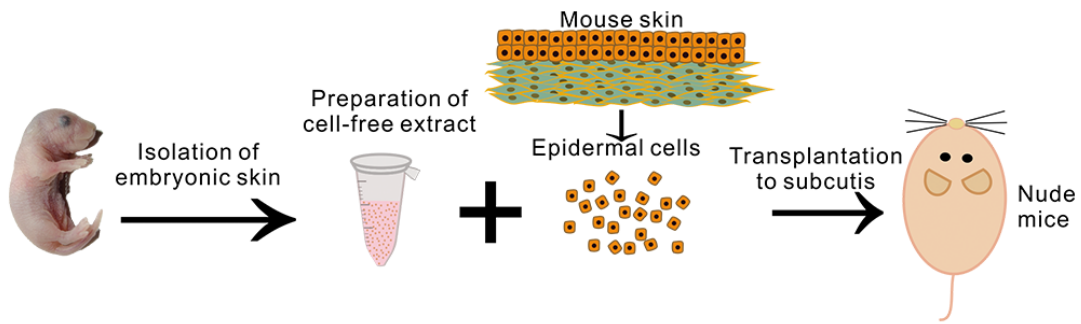
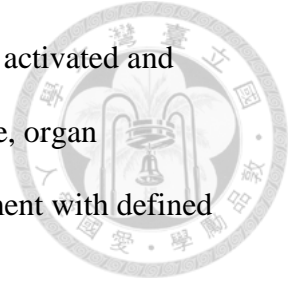


Figure 4 Preparation of skin extract and HF neogenesis assays

MATERIALS AND METHODS



Animals

All animal experiments were approved by Institutional Animal Care and Use Committee at National Taiwan University. Mice and rats were housed in animal facilities of National Taiwan University on a 12-hour light/dark cycles and were fed ad lib. Wistar rats and C57BL/6 mice were purchased from BioLASCO Taiwan Co., Ltd and nude mice (BALB/cAnN-Foxn1nu/CrINarl) were obtained from Taiwan National Laboratory Animal Center. *Z/AP* mice expressing the *lacZ* reporter gene to overexpress beta-galactosidase was from Jackson lab (Lobe et al. 1999). For invasive experimental procedures, animals were anesthetized by intramuscular injection of a mixture of Zolazepam (Zoletil vet, Virbac Laboratories) and Xylazine (Rompun, Bayer) (4:1, v/v).

Preparation of Cell-Free Extract

The whole skin containing epidermis and dermis was isolated from Wistar rats (from embryonic day 13.5 (E13.5) to postnatal stages). The skin tissue was minced and mixed with phosphate buffer solution (PBS) containing protease inhibitor (1X Protease Arrest, G-Biosciences). The samples were repeatedly frozen at -80°C and thawed on ice and then homogenized by repeated passages through a 25G needle. Cell breakage was examined under a phase contrast microscope to ensure that more than 90% cells were broken. Subsequent cell culture from the skin extract yielded no cell growth. To prepare cell-free extract from epidermis or dermis along, the whole skin was incubated in dispase (2mg/ml in PBS, Sigma-Aldrich) at 37°C for 1h and then the epidermis and dermis were separated by a forceps before further extraction. The protein concentration of cell-free extract was quantified by protein assay dye reagent (Protein Assay dye reagent concentrate, Bio-Rad Laboratories). The protein concentration was about 1-2µg/µL under our preparation procedure. The protein concentration was adjusted with

PBS containing proteinase inhibitor to the concentration of 1 $\mu\text{g}/\mu\text{L}$ for use in patch assay if not stated otherwise. If not used, the protein extract solution was stored at -80°C and was used within 1 month of preparation.



Dilution and Pretreatment of Skin Extract

E16.5 skin extract was serially diluted in PBS or pretreated with RNases A (2 $\mu\text{g}/\text{ml}$, Sigma-Aldrich), DNase I (100U/ml, Sigma-Aldrich), proteinase K (400 $\mu\text{g}/\text{ml}$, Sigma-Aldrich) for 10 min at 37°C or inactivated at 70°C for 10 min before being tested in patch assays. Removal of apolipoprotein-A1, galectin-1 and lumican from the skin extract by immunodepletion was performed by the use of protein G-agarose beads (Sigma-Aldrich) according to the instruction from the manufacturer. Antibodies used include anti-apolipoprotein A-1 (Novus, NB600-609), anti-galectin-1 (Abcam, ab138513), anti-lumican (Santa Cruz, sc-33785) and control rabbit IgG (GeneTex, GTX35035). The efficiency of immunodepletion for individual proteins was confirmed by Western blot.

Cells and Culture

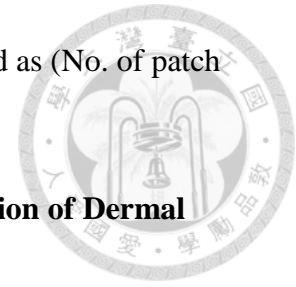
Postnatal day 1 (P1) keratinocytes were isolated from dorsal skin of C57BL/6 mice as described (Weinberg et al. 1993), and adult keratinocytes were isolated from the hairless areas of footpads of 7 to 8-week-old C57BL/6 mice. The cells were centrifuged at 1500 RPM for 10 min in a 50 ml centrifugal tube. The isolated cells were transferred to a 5-cm plastic dish and examined under a phase contrast microscope to make sure that undissociated hair germ-like tissues were removed. DP cells were expanded from vibrissae of 7-week-old C57BL/6 mice as we previously described (Li et al. 2015), and DP cells at passage 3 were used for the following experiments. Mouse adult fibroblasts were prepared from the dorsal skin of 7 to 8-week-old C57BL/6 mice (Li et al. 2015), and fibroblasts of passages 5 were used for the following experiments. To test the effect

of E16.5 skin extract on cells, P1 keratinocytes and adult fibroblasts were cultured with media (DMEM with 10% PBS for fibroblasts) containing E16.5 skin extract (2 μ g/mL) for 3 days. For washout, fibroblasts were further cultured without E16.5 skin extract for 3 days. IGF1R inhibitor (NVP-AEW541, 10nM, Selleck Chemicals) and Wnt inhibitor (XAV-939, 5 μ M, Selleck Chemicals) were also used in fibroblast culture.

Standard and Modified Patch Assays

Hair neogenesis was tested in patch assays in 7-week-old female nude mice as previously described with modification (Zheng et al. 2005). For standard patch assay with inductive mesenchymal cells, 1 $\times 10^6$ mesenchymal cells were mixed with 1 $\times 10^6$ keratinocytes in 200 μ l PBS and injected to the hypodermis of nude mice by an 18G needle. For negative controls, only keratinocytes were injected. Mice were sacrificed about 2 weeks later and the skin was removed for photography and further processed for histological examination or immunostaining. For the modified assay, no inductive mesenchymal cells were used. 1 $\times 10^6$ keratinocytes were suspended in the cell-free skin extract solution or in solutions containing defined proteins to the volume of 200 μ l and injected to the hypodermis of nude mice. The protein concentration of cell-free skin extract was 1 μ g/ μ L or serially diluted for testing. The concentration of each defined protein was 100ng/ μ L or serially diluted for testing. For defined proteins, each defined protein was initially serially diluted for testing. We ultimately used a concentration of 100 ng/ μ l for each protein because protein concentrations below this had lower or no inductive effects (data not shown). For fibroblasts transfected with mRNAs of *Lgals* (NM_008495.2), *Apoa1*(NM_009692.4) and *Lum* (NM_008524.2), 1 $\times 10^6$ mRNA transfected fibroblasts cells were mixed with 1 $\times 10^6$ keratinocytes in 200 μ l PBS and injected into the hypodermis of nude mice. For comparison of HF neogenesis between

different experimental groups, the rate of HF neogenesis was defined as (No. of patch assays with HF neogenesis)/(No. of total patch assays performed).




Hair Follicle Neogenesis in Full-Thickness Wound and Preparation of Dermal

Equivalent

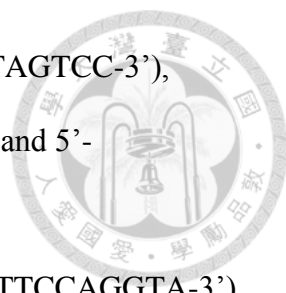
A full thickness wound (1cm × 1cm) was made by scissors on back of female nude mice and covered by a Tegaderm™ (3M) membrane. 200µl of E16.5 skin extract containing 2×10^6 P1 keratinocytes was injected into the wound with an 18G needle. For dermal equivalent preparation, adult dermal fibroblasts were suspended in the culture medium (DMEM: Ham's F-12=1:1 v/v supplemented with 10% FBS) containing E16.5 skin extract and collagen solution (E16.5 skin extract solution: collagen solution=1:10, final protein concentration of E16.5 skin extract=1µg/ml; *collagen I solution*, BD Biosciences) on ice and then transferred to an incubator for further culture for 3 days. The dermal equivalent was transferred to a full-thickness wound (1cm x 1cm) on the back of female nude mice and covered with a Tegaderm™ (3M) membrane. 2×10^6 P1 keratinocytes were injected into the top of the dermal equivalent by an 18G needle. To analyze HF neogenesis, mice were sacrificed 4 weeks later and the skin was removed for photography and further processed for histological examination and staining.

Real-Time PCR Analysis of Gene Expression

Total RNA was extracted using Trizol reagent (Invitrogen) according to the manufacturer's instructions. cDNAs were synthesized with a RevertAid H Minus First Strand cDNA synthesis Kit (Thermo Scientific). Quantitative real-time PCR (qPCR) was performed as we previously described (*Lin et al. 2013*). The sequences of the primer of murine genes sets used in this study were as following: *Akp2* (NM_001287172.1, 5'-TTGGGCAGGCAAGACACAGA-3' and 5'-TTGGCAACCCTGGGTAGACAG-3'); *Bmp6* (NM_007556.2, 5'-



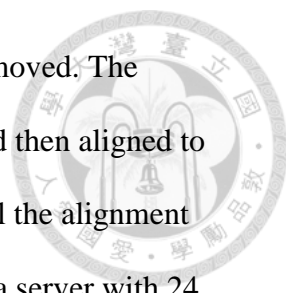
CTGCGCACCAACCAAACCTGAA-3' and 5'-TTGGGGGAGGCGAACATTAGGTA-3'); *Gapdh* (GU214026.1, 5'-CGTAGACAAAATGGTGAAGGTCGG-3' and 5'-AAGCAGTTGGTGGTGCAGGATG-3'); *Heyl* (NM_010423.2, 5'-AGCGCCGACGAGACCGAATCAATA-3' and 5'-TGGGGCAGCAGCAGAGGGTGTG-3'); *Insulin* (NM_008386.4, 5'-GAAGTGGAGGACCCACAAGTG-3' and 5'-CTGAAGGTCCCCGGGGCT-3'); *Wnt10a* (NM_009518.2, 5'-GCGCTCCTGTTCTTCTACT-3' and 5'-ATGCCCTGGATAGCAGAGG); *Wnt10b* (XM_006520893.2, 5'-TGTAATGAAGGTGAGCCTCGC-3' and 5'-TGCCCTCTGTCCTTTTCCAACC-3'); *Wnt11* (NM_009519.2, 5'-CAGTGAAGTGGGGAGACAGG-3' and 5'-ACCACTCTGTCCGTGTAGGG-3'); *Lef1* (NM_010703.4, 5'-CGCTAAAGGAGAGTGCAGCTA-3 and 5'-GCTGTCTCTTTCCGTGCT-3'); *Igfl* (NM_010512.5, 5'-GGATGCTCTTCAGTTCGTGT-3' and 5'-CTTCTCCTTTGCAGCTTCGT-3'); *Shh* (NM_009170.3, 5'-CCA ACTCCGATGTGTTCC-3' and 5'-CCTGGCTCTTCTCCTTCC-3') and Versican (XM_011244471.1, 5'-GTGACTATGGCTGGCACAAATTCC-3' and 5'-GGTTGGGTCTCCAATTCTCGTATTGC-3'). The sequences of the primers of human genes were as follows: *Shh* (NM_000193.2, 5'-ACCGAGGGCTGGGACGAAGA-3' and 5'-ATTTGGCCGCCACCGAGTT-3'), Versican (NM_001164098.1, 5'-TGGAATGATGTTCCCTGCAA-3' and 5'-AAGGTCTTGGCATTCTTCTACAACAG-3'), *Gapdh* (NM_001289746.1, 5'-ATGGGGAAGGTGAAGGTCG-3' and 5'-TAAAAGCAGCCCTGGTGACC-3'), *Bmp-6* (NM_001718.4, 5'-CAGCCTGCAGGAAGCATGAG-3' and 5'-CAAAGTAAAGAACCGAGATG-3'), *Alp* (XM_005245820.2, 5'-CCTCGTTGACACCTGGAAGAG-3' and 5'-TTCCGTGCGGTTCCAGA-3'), *Heyl* (NM_012258.3, 5'-



GCCAGCATGAAGCGAGCTC-3' and 5'-GGGTCAGAGGCATCTAGTCC-3'),
Wnt10a (XM_011511930.1, 5'-GGCAACCCGTCAGTCTGTCT-3' and 5'-
CATTCCCCACCTCCCATCT-3'), *Wnt10b* (XM_011538722.1, 5'-
CTTTTCAGCCCTTGCTCTGAT-3' and 5'-CCCCTAAAGCTGTTTCCAGGTA-3'),
Wnt11 (XR_950037.1, 5'-GGCTTGTGCTTTGCCTTCA-3' and 5'-
TTTGATGTCCTGCCCTCCTT-3'), *Lef1* (XM_006714233.1, 5'-
CAACTGGCATCCCTCATC-3' and 5'-GCAACGACATTCGCTCTC-3'), *Igf1*
(XR_944534.1, 5 TCTTGAAGGTGAAGATGCACACCA -3' and 5'-
AGCGAGCTGACTTGGCAGGCTTGA-3') and *Insulin* (NM_001291897.1, 5'-
GCAGCCTTTGTGAACCAACA-3' and 5'-TTCCCCGCACACTAGGTAGAGA-3')

RNA-Sequencing and Analysis

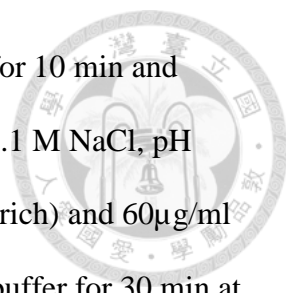
Total RNA was extracted using Trizol Reagent (Invitrogen, Carlsbad, CA, USA) and isolated by RNeasy mini-columns (Qiagen, Germantown, MD, USA). RNA quality was assessed by spectrophotometry. A fragmentation buffer (100 mM ZnCl₂ in 100 mM Tris-HCl pH7) was added to cut mRNAs into short fragments. Fragmented RNA was reverse-transcribed to first-strand cDNA with reverse transcriptase (Invitrogen) in the presence of a random hexamer-primer (Invitrogen) and dNTPs for 50 min at 42°C. The second-strand cDNA was synthesized using DNA polymerase I in a buffer containing dNTPs and RNaseH. The short DNA fragments were purified using the QiaQuick PCR extraction kit (Qiagen) and resolved with an elution buffer (10 mM Tris-Cl, pH 8.5) for end repair and the addition of a poly (A) fragment to both ends. The short fragments were connected with sequencing adapters and then separated in gels by electrophoresis. The fragments with a size suitable for sequencing were cut from gels and eluted for PCR amplification by using adapter primers. The cDNA libraries were sequenced from both the 5' and 3' ends on the Illumina GA II following the



manufacturer's instructions. The low-quality raw sequences were removed. The remaining short reads with their adaptor sequences were trimmed and then aligned to UCSC mouse genome version 10 with STAR (Dobin et al. 2013). All the alignment parameters were set to default value. The process was performed on a server with 24 cores and 128 GB of memory. The average alignment rate of samples was around 95%. Analysis data for expression changes by Cufflinks pipeline (Trapnell et al. 2012), which included cufflinks, cuffmerge, and cuffdiff were performed to quantify the expression value of transcripts and genes. Stranded library type was set. The read counts of genes in samples were further normalized as RPKM (Reads Per Kilobase per Million mapped reads). Principle Component Analysis was performed with “prcomp” in the software R (Ihaka and Gentleman 1996), and visualized with “ggplot” (Wickham 2006). CummeRbund were also used to examine the results of RPKM in each sample. RNA-seq raw data have been submitted to <http://www.ncbi.nlm.nih.gov/geo> (GEO: [GSE85303](https://www.ncbi.nlm.nih.gov/geo/query/acc.cgi?acc=GSE85303)). To identify the cellular processes/signaling pathways upregulated in fibroblasts after treatment with selected protein(s) or E16.5 skin extract, genes with greater than 1.2-fold increase were analyzed by DAVID Bioinformatics Resources 6.7 (<https://david.ncifcrf.gov/>).

Beta-Galactosidase Activity Assay and Alkaline Phosphatase Activity Assay

Beta-galactosidase activity was detected as described (Tam et al. 1997). The tissue sections were incubated in freshly prepared X-gal solution (1.3 mg/ml potassium ferrocyanide, 1 mg/ml potassium ferricyanide, 0.2% Triton X-100, 1 mM MgCl₂, and 1 mg/ml X-Gal in PBS [pH 7.2]) for 1hr at 37°C. Then, samples were rinsed with PBS three times before being counterstained with eosin. Alkaline phosphatase activity was detected as we previously described (Hughes et al. 2014). Mouse DP cells and fibroblast were plated in 12-well plates at 7.5×10⁴ cells per well. After 24h, cells were treated with



E16.5 skin extract for 72 h, and then fixed in 4% paraformaldehyde for 10 min and washed with PBS. Cells were rinsed in TN buffer (0.1 M Tris-HCl, 0.1 M NaCl, pH 9.5), then incubated in 120 μ g/ml 4-nitroblue tetrazolium (Sigma-Aldrich) and 60 μ g/ml BCIP (5-bromo-4-chloro-3-indolyphosphate, Sigma-Aldrich) in TN buffer for 30 min at 25°C and then rinsed with PBS twice before being imaged (Axiovert 200M; Carl Zeiss, Gottingen, Germany).

In Situ Hybridization

Paraffin sections were prepared for *in situ* hybridization as we described (Lin et al. 2013). Digoxigenin-labeled probes against rat apolipoprotein-A1 (nucleotides 44-700; NM_012738.1), galectin-1 (nucleotides 72-479; NM_008495.2) and lumican (nucleotides 417-1727; NM_008524.2) were synthesized by a digoxigenin RNA labeling kit according to the instructions from the manufacturer (DIG RNA Labeling kit, Roche) (Lin et al. 2013). The sections were counterstained with eosin.

Western Blot

Western blot was performed by using the following antibodies: Akt (Cell Signaling, 9272, 1:1000), phospho-Akt (Cell Signaling, 9271S, 1:1000), apolipoprotein-A1 (Novus, NB600-609, 1:1000), β -actin (Santa Cruz, sc-47778), β -catenin (BD Biosciences, 610153, 1:1000), Erk (Cell Signaling, 9102S, 1:1000), phospho-Erk (Cell Signaling, 4370S, 1:1000), GADPH (Millipore, MAB374), galectin-1 (Abcam, ab138513, 1:1000), IGF1 (Santa Cruz, sc-9013), IGF1R (LSBio, LS-C24709), IRS2 (LifeSpan BioSciences, LS-C33930, 1:1000), phospho-IRS2 (Novus, NBP1-72215, 1:1000), lumican (Santa Cruz, sc-33785, 1:1000) and TATA binding protein (Cell Signaling, 8515S, 1:1000). Fractionation of cells into nuclear and cytoplasmic content was performed by NE-PER Nuclear and Cytoplasmic Extraction Kit (Thermo

Scientific) supplemented with Protease Inhibitor Cocktails (Thermo Scientific) as we previously described (Chan et al. 2015).



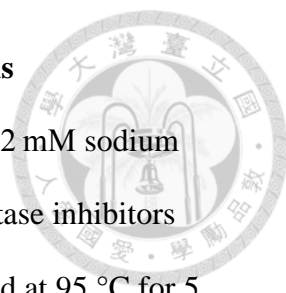
Recombinant Proteins

The recombinant proteins used for patch assays and cell culture were listed as follows: apolipoprotein-A1 (PeproTech, Cat:350-11), galectin-1 (Novoprotein, C285), lumican (Novoprotein, C372), annexin A2 (PROSPEC, PRO-777), gelsolin (Abnova, H00002934-P01), fibrinogen beta-chain fragment (American Peptide Company, AP42-1-33A), fibronectin (Innovative Research, Inc., IHFBN) and sulfated glycoprotein 1 (Psap) (Abnova, H00005660-P01).

Histology and Immunofluorescence

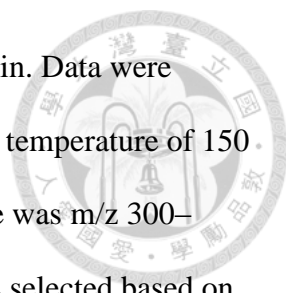
Skin samples were fixed in 4% paraformaldehyde overnight at 4°C, serially dehydrated and embedded in paraffin. The specimens were sectioned and stained with hematoxylin and eosin (H&E). Immunofluorescent staining was performed with routine antigen retrieval as suggested by the antibody manufacturer (Lin et al. 2013). The slides were examined under a confocal microscope (Meta 510, Carl Zeiss, Gottingen, Germany). The primary antibodies for immunostaining used in this study were listed as follows: fibrinogen beta-chain fragment, Abcam, EPR3083, 1:200), sulfated glycoprotein 1 (Abcam, ab68466, 1:200), galectin-1 (Abcam, ab138513, 1:200), lumican (Abcam, ab168348, 1:200), annexin A2 (Genetex, GTX101902, 1:200), gelsolin (Genetex, GTX101185, 1:200), apolipoprotein-A1 (Novus, NBP1-77008, 1:200) and fibronectin (Genetex, GTX61207, 1:200). Secondary antibodies were Alexa Fluor 594 donkey anti-mouse IgG (H+L) (Jackson ImmunoResearch, 715-585-151, 1:500), Cy3-conjugated AffiniPure donkey anti-rabbit IgG (Jackson ImmunoResearch, 711-165-152, 1:500) and Alexa Fluor 594-AffiniPure $F(ab')_2$ Fragment Rabbit Anti-Chicken IgY (IgG) (H+L) (Jackson ImmunoResearch, 303-586-003, 1:500).

Mass Spectrometry for Proteomic and Phosphoproteomic Analysis



Cells were lysed in lysis buffer (12 mM sodium deoxycholate, 12 mM sodium lauroyl sarcosinate, protease inhibitor cocktail (Roche), and phosphatase inhibitors (Sigma-Aldrich) in 100 mM Tris-HCl, pH 9.0). Cells were first heated at 95 °C for 5 min then sonicated and subjected to methanol and chloroform precipitation prior to trypsin digestion as previously described (Lin, Sugiyama, and Ishihama 2015). The protein pellet was dissolved in 8 M urea followed by protein reduction (10 mM *dithiothreitol*) and alkylation (50 mM *iodoacetamide*). The alkylated protein was diluted 5 times with 50 mM ammonium bicarbonate for overnight trypsin digestion (50:1, w/w). The resulting peptide mixture was acidified with trifluoroacetic acid (TFA) and desalted with a SDB-XC (poly(*styrene-divinylbenzene*) copolymer) solid-phase extraction cartridge. The phosphopeptides were enriched as described previously (Tsai et al. 2008; Tsai et al. 2014). Briefly, the Ni²⁺ ions in IMAC tip were removed by 50 mM EDTA in 1 M NaCl. The tip was then activated with 100 mM FeCl₃ and equilibrated with loading buffer (6% (v/v) acetic acid at pH 3.0). Tryptic peptides were reconstituted in loading buffer and loaded onto the IMAC tip. After successive washes with 6% (v/v) acetic acid, 25% ACN and 6% (v/v) acetic acid, the bound phosphopeptides were eluted by 200 mM NH₄H₂PO₄. The eluent was acidified with TFA and desalted with a SDB-XC StageTip.

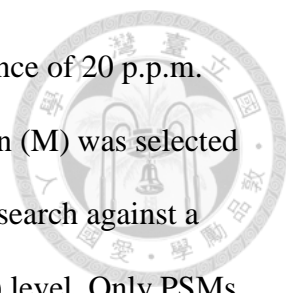
For proteome analysis, the setting of TripleTOF 5600 system (AB SCIEX, Concord, ON, Canada) equipped with a nanoACQUITY UPLC (Waters Corporation, Milford, MA, USA). The 3 μm ReproSil-Pur C18-AQ particles (Dr Maisch, Ammerbuch, Germany) were packed into a 15 cm self-pulled column with a 100 μm inner diameter. The LC system consisted of water with 0.1% formic acid (FA) (buffer A) and acetonitrile (ACN) with 0.1% FA (buffer B). Peptides were separated through a



gradient of up to 80% buffer B over 120 min at flow rate of 500 nl/min. Data were acquired using an ion spray voltage of 2.6 kV and an interface heater temperature of 150 °C. For information dependent acquisition, the MS survey scan range was m/z 300–1,500, and data were acquired for 200 ms. Top 15 precursor ions was selected based on threshold of 150 counts per second in each MS survey scan, and each acquisition scan was performed for 150 ms. The collision energy was automatically adjusted by the rolling CID function of Analyst TF 1.5. To minimize repeated scans, dynamic exclusion was set for 6 seconds, and the precursor was then removed from the exclusion list.

For phosphoproteome analysis, Orbitrap Fusion Tribrid mass spectrometer (Thermo Scientific, San Jose, CA), was coupled with an Ultimate 3000 RSLCnano system (Thermo Fisher Scientific). Peptide mixtures were loaded onto a 75µm × 250 mm Thermo Scientific™ Acclaim™ PepMap™100 C18 Nano *LC Column*. The mobile phases consisted of (A) 0.1% formic acid and (B) ACN with 0.1% formic acid. Peptides were separated through a gradient of up to 85% buffer B over 135 min at flow rate of 500 nL/min. Data were acquired in data-dependent acquisition mode with a top 15 method. MS spectra were acquired at a target value of 4×10^5 and a resolution of 120,000, and the higher-collisional dissociation (HCD) tandem mass spectra (MS/MS) were recorded at a target value of 5×10^4 and with a resolution of 30,000 with a normalized collision energy (NCE) of 35%. The maximum MS1 and MS2 injection times both were 50 millisecond. The precursor ion masses of scanned ions were dynamically excluded from MS/MS analysis for 60 seconds.

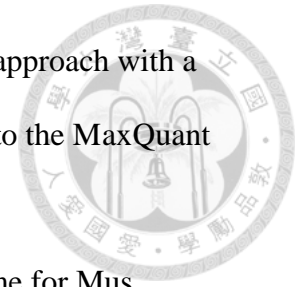
For proteome data analysis, the raw MS/MS data was processed as described previously (Tsai et al. 2015). Protein identification was were performed against the SwissPort database (version 57.8, *Rattus sapiens*) by using Mascot (Matrix Science, London, UK; version 2.3). Allowing for tryptic peptides with up to two missed cleavage



sites, a fragment ion mass tolerance of 0.1 Da and a parent ion tolerance of 20 p.p.m. Carbamidomethyl (C) was selected as fix modifications and oxidation (M) was selected as variable modifications. The false discovery rate was evaluated by search against a randomized decoy database at the peptide–spectrum matches (PSMs) level. Only PSMs with p value <0.01 were accepted. The FDR at PSMs level is 2%. Label-free quantitative analysis was performed by IDEAL-Q software as previously described (Wang et al. 2010; Tsou et al. 2010). Alignment of elution time was then performed based on the peptide information list using linear regression in different LC-MS/MS runs followed by correction of aberrational chromatographic shift across fragmental elution-time domains. To increase correct assignment, the detected peptide peaks are validated by (a) signal-to-noise (S/N) ratio > 3 and (b) accurate charge state. Only protein with at least two identified peptides was selected for quantitation. The estimated protein abundance were obtained by TOP 3 approach. The TOP3 abundance was calculated as the mean of the three highest peptides areas measured for each protein. If fewer than three peptides have intensity values, the intensities were also presented as averaged value of two identified peptides. Bioinformatics analysis was performed by Perseus (version 1. 5. 0. 15) (Xiang, Zhang, and Huang 2012). Two-sample t test (Volcano plot in Fig. 12, FDR=0.05; S0=0.6) was applied to compare across all data sets.

For phosphoproteome data analysis, all raw data was analyzed using MaxQuant (version 1.5.0.30) with an FDR < 0.01 at the level of proteins, peptides and modifications, using default settings with the following minor changes: Trypsin/P specificity allowing up to 2 missed cleavages; fixed modification of carbamidomethyl (C); and variable modifications of oxidation (M), acetylation (protein N-term), and phosphorylation (STY). Match between runs was performed with 1 min match time

window. Proteins and peptides were identified using a target-decoy approach with a reversed database, using the Andromeda search engine integrated into the MaxQuant environment (Cox et al. 2011).



Searches were performed against the UniProt reference proteome for *Mus musculus* (4 Sept 2014, proteins) and quantification of peptides and proteins was performed by MaxQuant (Cox and Mann 2008). Bioinformatics analysis was performed by Perseus (version 1. 5. 0. 15) (Xiang, Zhang, and Huang 2012). The statistical significance (two-sample t test) was calculated with the FDR set to 0.05 and the S0 parameter set to 0.2 (Fig. 22). All of the identification results and raw files have been deposited to the ProteomeXchange Consortium (Vizcaino et al. 2014) via the PRIDE partner repository with the dataset identifier PXD003131". Reviewer account details: Username: reviewer91290@ebi.ac.uk Password: hNOEjrHI

Bioinformatics Analyses

The significant entries at phosphoprotein level were subjected into STRING to analyze its signaling networks. High confident interaction hits (score ≥ 0.7) were further analyzed by Cytoscape 3.2.1 using ClueGO app. KEGG pathway analysis was enriched at p-value ≤ 0.05 .

Statistics

Data are expressed as mean \pm standard error of the mean (SEM). Comparisons between groups were performed by using a paired t-test and p-values were considered significant when less than 0.05. The rate of HF neogenesis between different groups was compared using Fisher's exact test and p < 0.05 was considered statistically significant.

RESULTS

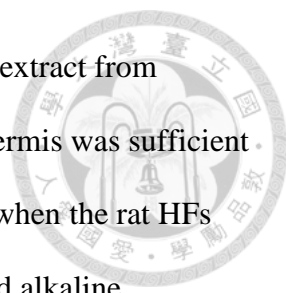


Cell-Free Extract from Stage-Specific Embryonic Skin Could Induce HF Neogenesis

We first determined whether cell-free extracts from embryonic skin can induce HF neogenesis. Wistar rat, HFs started to develop with placode formation at E15.5. Formation of hair germs with dermal condensate could be seen on E17.5. HFs developed into short hair pegs on E18.5 (Fig. 5). In the HF neogenesis assay, the contamination of preformed HFs in keratinocytes can lead to HF formation without co-administration of inductive mesenchymal cells (Weinberg et al. 1993).

Whole-skin cell-free extract of Wistar rat embryos from E13.5 to P1 was tested in a modified patch assay (Fig. 6). Whole skin extract from E15.5 to E17.5 induced new HFs from P1 keratinocytes. In E16.5 skin, extract from dermis only but not from epidermis had only been able to induce HF neogenesis from P1 keratinocytes, indicating that factors present in the dermis were sufficient to induce new HFs. E16.5 skin extract also marginally induced new HFs from adult keratinocytes from non-hairy skin of the foot pads (Fig.6).

In conventional patch assay (Zheng et al. 2005), keratinocytes were mixed with inductive mesenchymal cells, such as newborn dermal cells or DP cells (Fig. 6), before being injected into the subcutis of nude mice. We replaced the inductive mesenchymal cells with skin extract. Extract from E15.5 to E17.5 skin induced new HFs from P1 keratinocytes (Fig. 6). In E16.5 skin, extract from dermis only but not from epidermis had only was able to induce HF neogenesis from P1 keratinocytes, indicating that factors present in the dermis were sufficient to induce new HFs, with highest inductivity from E16.5 skin (70%). E16.5 skin extract also induced HF neogenesis from adult keratinocytes but at a lower rate compared with P1 keratinocytes (Fig. 6).



When the embryonic epidermis and dermis was separated, only extract from dermis induced new HFs (Fig. 6), suggesting factors present in the dermis was sufficient for the inductive effect. Histologically, E15.5 to E17.5 was the time when the rat HFs initially developed (Fig. 5). The new HFs from patch assays exhibited alkaline phosphatase activity (blue color) in the proximal hair bulbs (Fig. 7), indicating that the new DP also expressed functional alkaline phosphatase. The new HFs showed a normal HF architecture (Fig. 7) with DP exhibiting alkaline phosphatase activity and produced HSs protected by overlapping cuticles. (Fig. 8). Neogenic HFs showed a normal morphology, complete with alkaline phosphatase+ DPs and HSs with cuticles (Fig. 8). The results show the new HFs formed from lacZ⁺ keratinocytes exhibited beta-galactosidase activity in HF epithelium, including SG but not in DP and New HFs formed from lacZ⁺ dermal cell exhibited beta-galactosidase activity in HF DP (Fig.7). Therefore, the patch assay with LacZ⁺ keratinocytes transplanted into nude mice showed that only the epithelial cells of regenerated HFs were positive for beta-galactosidase activity, indicating that the new DP cells were derived from host mesenchyme, possibly local fibroblasts. We further tested HF inductivity in full-thickness wounds. Treatment with keratinocytes plus E16.5 extract and treatment with keratinocytes plus dermal equivalents containing E16.5 extract both induced new HFs (n=3) whereas no HF neogenesis was observed in the control groups without addition of E16.5 extract (Fig. 9).

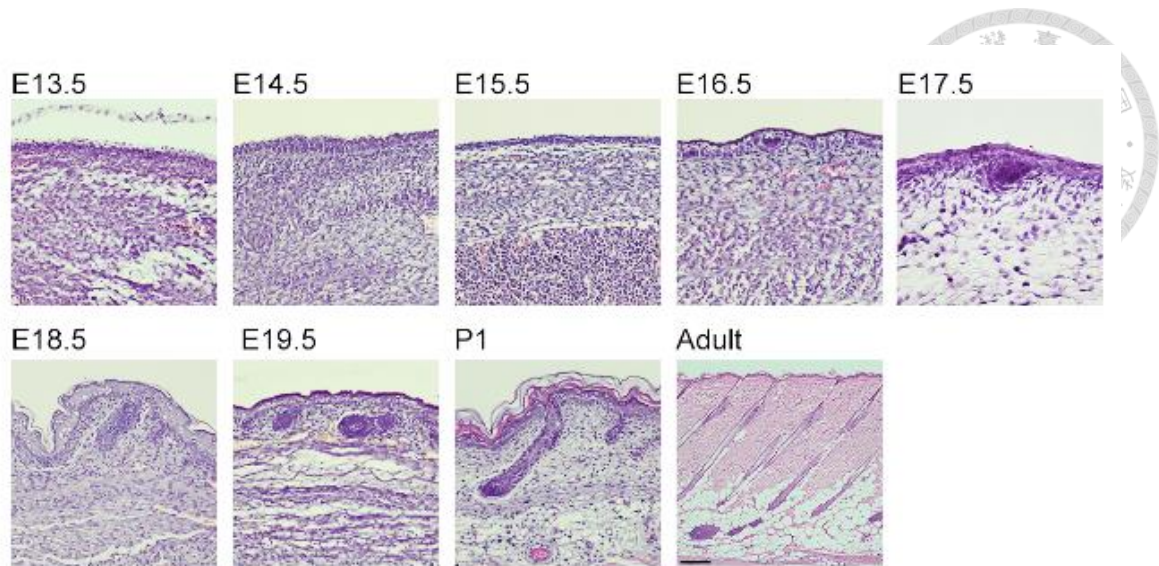


Figure 5 Histology of Wistar rat skin at different developmental stages.

Bar: 100 μ m.

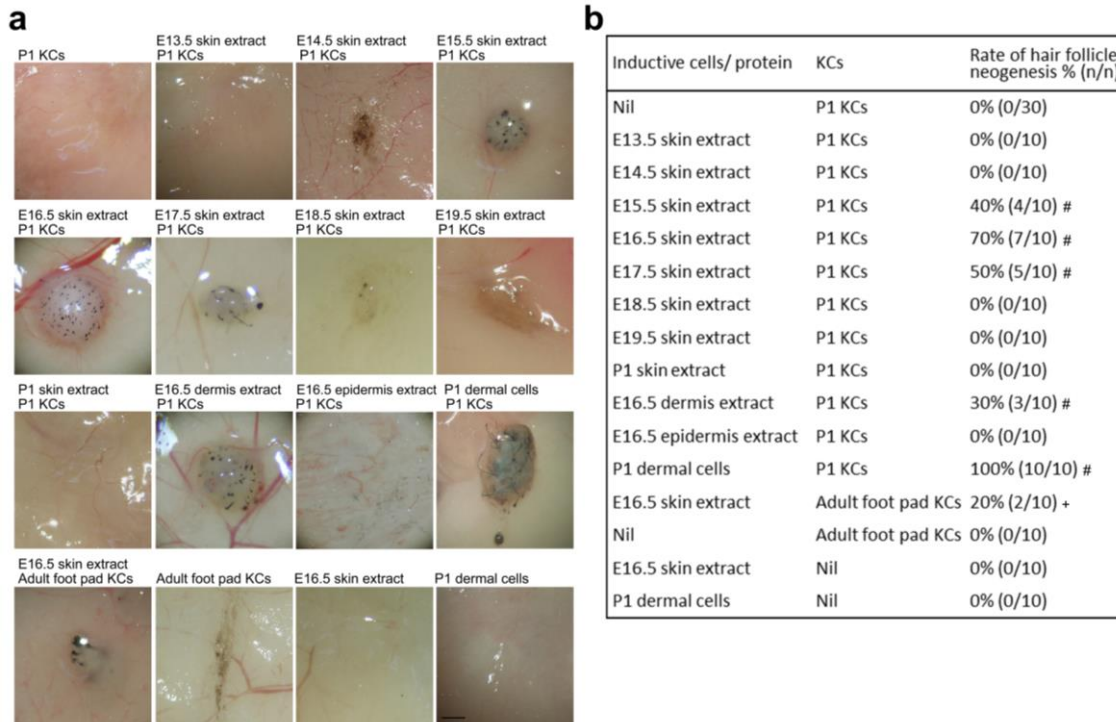


Figure 6 The effect of cell-free extract prepared from different stages of skin on HF induction.

(a) Representative photos of patch assays. (b) Results of patch assays. E16.5 skin extract also marginally induced new HF's from adult keratinocytes from non-hairy skin of foot pads (+ $p=0.0767$). # $p<0.05$, compared with P1 KCs only.

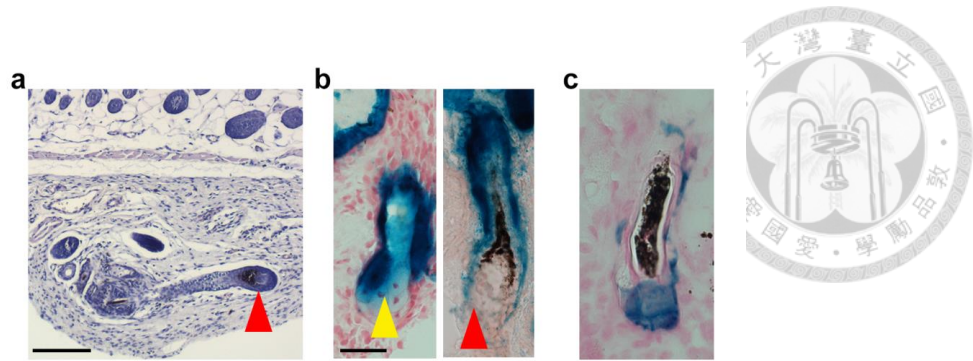


Figure 7 Figure Proteins in cell-free extract from stage-specific embryonic skin induce HF neogenesis.

(a) E16.5 skin extract induced new HF containing a DP structure (red arrowhead). (b) New HF formed from *lacZ*⁺ keratinocytes exhibited beta-galactosidase activity in HF epithelium including SG (yellow arrowhead) but not in DP (red arrowhead). (c) New HF formed from *lacZ*⁺ dermal cell exhibited beta-galactosidase activity in HF DP.

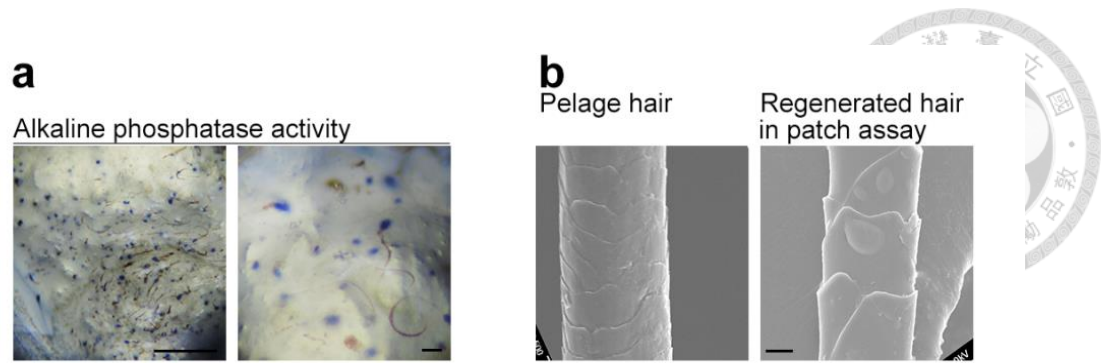


Figure 8 Figure Alkaline phosphatase activity and HS morphology of new HF induced by E16.5 skin extract.

(a) The new HF from patch assays exhibited alkaline phosphatase activity (blue color) in the proximal hair bulbs, indicating that the new DP also expressed functional alkaline phosphatase. The right panel showed magnified image from the left panel. (b) Scanning electron micrographs of normal pelage hair and regenerated hair both showed overlapping cuticles covering the HSs. Bar: 100 μ m in a, 10 μ m in b.

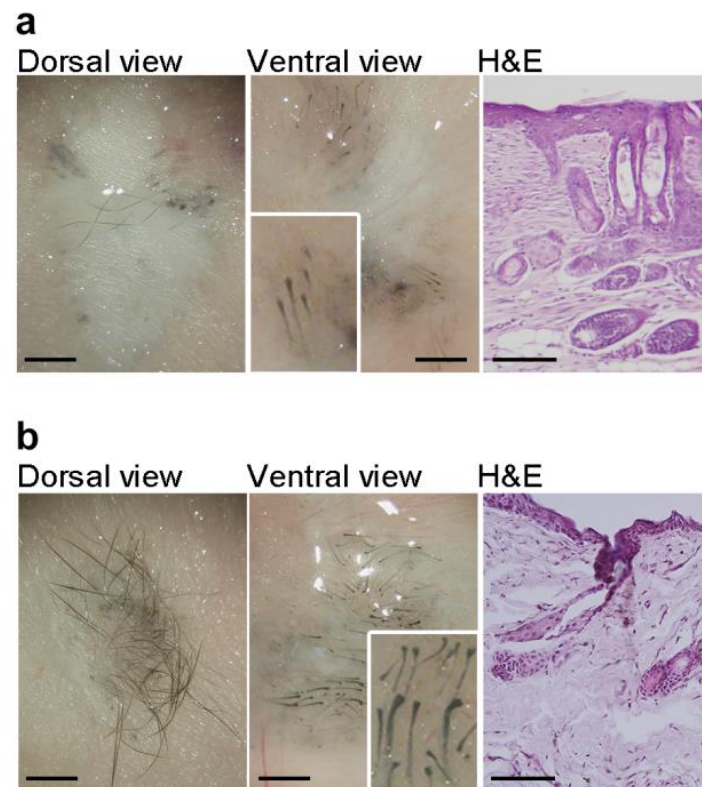


Figure 9 Figure Proteins in cell-free extract from stage-specific embryonic skin induce HF neogenesis.

(a) E16.5 skin extract induced HF neogenesis from transplanted C57BL/6 mouse keratinocytes in full-thickness wounds in nude mice. (b) Dermal equivalents containing E16.5 skin extract induced HF neogenesis from transplanted C57BL/6 mouse keratinocytes in full-thickness wounds in nude mice. All insets showed enlarged images of regenerated HF. Bar: 100 μ m in histology and 500 μ m in gross images.

Protein Fraction in E16.5 Skin Extract was Sufficient to Induce HF Neogenesis

Protein concentration E16.5 skin extract was serially diluted from 1 $\mu\text{g}/\mu\text{L}$ (1x) to 1×10^{-3} $\mu\text{g}/\mu\text{L}$ (1/1000). Upon serial dilution, HF inductivity of E16.5 skin extract gradually lost its ability to induce HFs, which disappeared completely by the 1/1000 dilution (Fig. 10). With serial dilution, the E16.5 extract gradually lost its HF inductivity.

Because the crude whole skin cell-free extract might contain substances other than proteins, we pretreated the extract with RNase, DNase, proteinase and heat denaturation and found HF neogenesis was abolished when proteins were digested or heat-denatured (Fig. 11). Inactivation of proteins by heat and proteinase K inhibited hair formation (Fig. 11). The findings above suggested that protein factor in skin of peri-folliculogenetic stages were able to induce HF neogenesis.

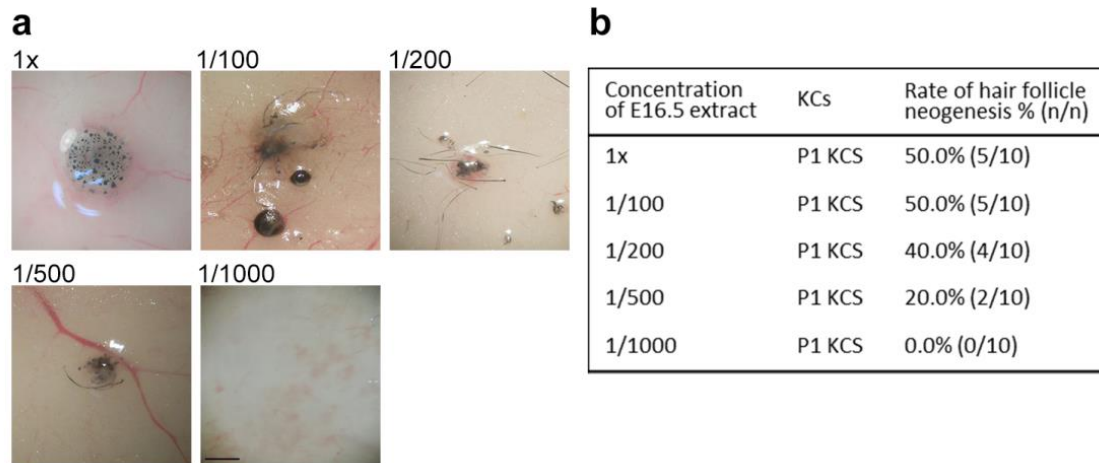
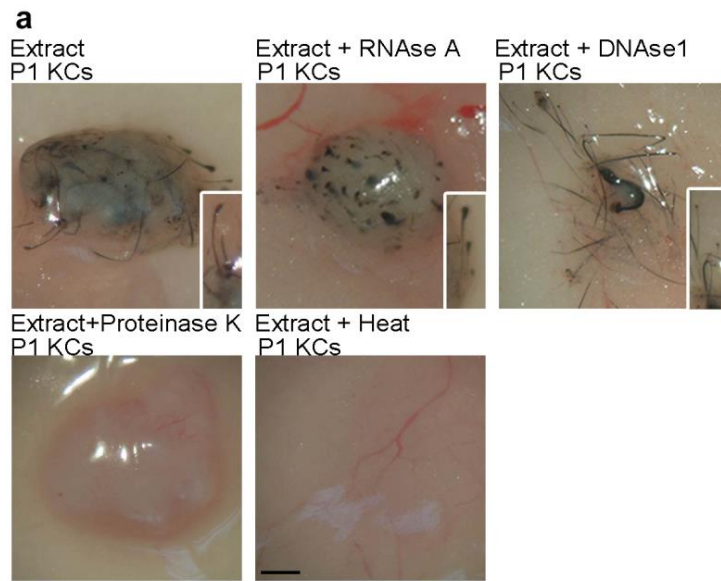


Figure 10 Effect of serial dilution of E16.5 skin extract on HF inductivity.

(a) Representative photos of patch assays. (b) Results of patch assays. Protein concentration E16.5 skin extract was serially diluted from $1\mu\text{g}/\mu\text{L}$ (1x) to $1 \times 10^{-3}\mu\text{g}/\mu\text{L}$ (1/1000). Upon serial dilution, HF inductivity of E16.5 skin extract gradually diminished. Bar: $500\mu\text{m}$.



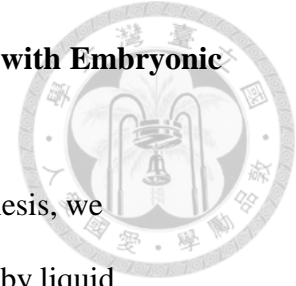
b

Skin extract and pretreatment	KCs	Rate of hair follicle neogenesis % (n/n)
E16.5 skin extract	P1 KCs	70.0% (7/10)
E16.5 skin extract + RNase A	P1 KCs	75.0% (8/12)
E16.5 skin extract + DNase 1	P1 KCs	70% (7/10)
E16.5 skin extract + Proteinase K	P1 KCs	0.0% (0/10) #
E16.5 skin extract + Heat	P1 KCs	0.0% (0/10) #

Figure 11 Proteins in cell-free extract from stage-specific embryonic skin induce HF neogenesis.

(a)-(b) Effect of various pretreatment on the HF inductivity of E16.5 skin extract. # $p < 0.05$, compared with E16.5 skin extract without pretreatment. Bar: gross images, 500 μm .

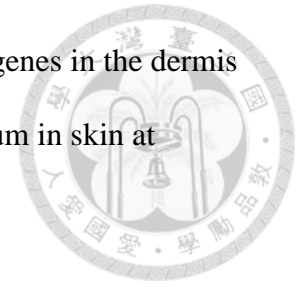
Proteomic Analysis Identified Eight Secreted Proteins Enriched with Embryonic Skin

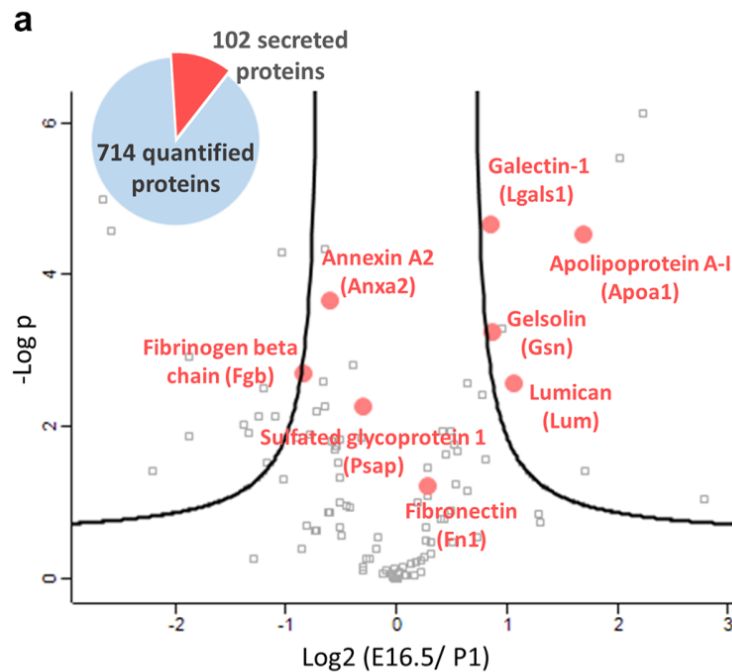


To identify the defined proteins capable of inducing HF neogenesis, we quantitatively compared the proteomes of E16.5 and P1 skin extract by liquid chromatography-tandem mass spectrometry (LC-MS/MS) (Table 1). LC-MS/MS analysis of the E16.5 and P1 skin extract proteomes and identification of key secreted proteins. The volcano plot shows the distribution of quantified proteins according to a *t*-test ($p < 0.05$) and fold change. The data points located to the left of the left curve and to the right of the right curve indicate significantly down- and up-regulated proteins, respectively. Among the 714 quantifiable proteins, we looked for secreted proteins enriched in E16.5 skin extract that were abundant in the dermis (Fig. 12).

Immunostaining verified that the 8 proteins, including apolipoprotein-A1 (Apoa1), galectin-1 (Lgals1), lumican (Lum), gelsolin (Gsn), fibronectin (Fn1), annexin A2 (Anxa2), sulfated glycoprotein 1 (Psap), and fibrinogen beta chain (Fgb), were amply present in the dermis of E16.5 and E17.5 skin (Fig. 13 and Fig. 14). The results show where Gsn, Fn1, Anxa2 and Fgb in the epidermis and dermis of E16.5 and P1 skin. Apoa1 and Lum expression mainly in HF of P1 skin. Lgals1 the main performance in the dermis of E16.5 and P1 skin. Compared with other 7 proteins, Lgals1 had a more preferential distribution in the dermis. Apoa1, Lgals1 and Lum were also abundant in the dermal condensate of the developing HFs (Fig. 13 and Fig. 14). And Western blot analysis confirmed the increased expression of Apoa1, Lgals1 and Lum during peri-folliculogenetic stages (Fig. 15). Connection with to confirm the expression of apolipoprotein-A1, galectin-1 and lumican genes in the skin at different stages by in situ hybridization. All three genes are highly expressed in the mesenchyme of E16.5 and E17.5 embryonic skin. Expression of apolipoprotein-A1 in the epithelium were also

observed in E16.5 and E17.5 skin. The expression level of all three genes in the dermis diminishes in P1 skin (Fig. 15). Expression of Apoa1, Lgals1 and Lum in skin at different ontogenetic stages.





b

AccNo	Description	E16.5/p1
P04639	Apolipoprotein A-I, Apoa1	1.70
P51886	Lumican, Lum	1.07
P11762	Galectin-1, Lgals1	0.85
Q68FP1	Gelsolin, Gsn	0.86
P04937	Fibronectin, Fn1	0.28
P10960	Sulfated glycoprotein 1, Psap	-0.31
Q07936	Annexin A2, Anxa2	-0.60
P14480	Fibrinogen beta chain, Fgb	-0.83

Figure 12 Proteomic analysis identifies secreted proteins enriched in developmental skin.

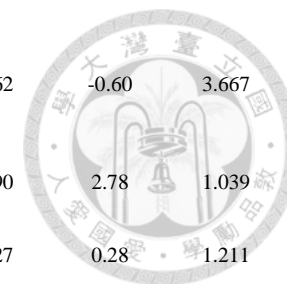
(a) LC-MS/MS analysis of proteomes of E16.5 and P1 skin extract and identification of key secreted proteins. Volcano plot showed the distribution of quantified proteins according to the t-test (p -value < 0.05) and fold change. Black curve lines indicated the significance level (false discovery rate (FDR) = 0.05; $s_0 = 0.6$). The proteins represented in red dots have been selected for the following biological validation. (b) Eight proteins enriched in embryonic skin were identified.

Table 1 Liquid chromatography-tandem mass spectrometry (LC-MS/MS) analysis of proteomes of E16.5 and P1 skin extract.

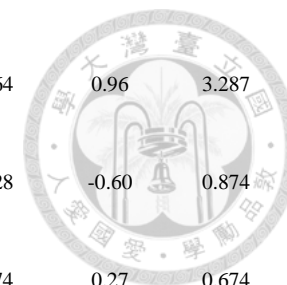


Protein index	AccNO	Description	Score	Mass	# of IDed (spectrum)	# of samples IDed	XIC area of TOP 3 identified peptides						Fold Change	-Log Log2(E16.5/p1) (P-value)	Significant	
							Total peps	E16.5 replicate 1	E16.5 replicate 2	E16.5 replicate 3	P1 replicate1	P1 replicate2				P1 replicate3
1	P02773	Alpha-fetoprotein OS=Rattus norvegicus GN=Afp PE=2 SV=1	5046	70166	393	6	62	83794	90435	88368	18286	18139	19250	2.24	6.120	+
2	P02770	Serum albumin OS=Rattus norvegicus GN=Alb PE=1 SV=2	3379	70682	357	6	63	20596	16328	29491	63316	44717	61058	-1.37	2.019	+
7	P06761	78 kDa glucose-regulated protein OS=Rattus norvegicus GN=Hspa5 PE=1 SV=1	1984	72473	169	6	35	5533	6016	5414	4624	3786	3717	0.49	1.937	
15	P12346	Serotransferrin OS=Rattus norvegicus GN=Tf PE=1 SV=3	1365	78512	175	6	39	13524	14525	13089	10801	10950	9141	0.42	1.931	
19	P63039	60 kDa heat shock protein, mitochondrial OS=Rattus norvegicus GN=Hspd1 PE=1 SV=1	1271	61088	72	6	22	5677	5609	5191	3715	2263	3655	0.81	1.564	
28	Q7TMA5	Apolipoprotein B-100 OS=Rattus norvegicus GN=Apob PE=1 SV=1	1021	537740	101	5	56	16409	5691	18521	3091	3668	4388	1.71	1.419	+
42	P02651	Apolipoprotein A-IV OS=Rattus norvegicus GN=Apoa4 PE=2 SV=2	922	44429	87	6	26	8895	8132	7755	6635	6327	7436	0.28	1.451	
43	P24090	Alpha-2-HS-glycoprotein OS=Rattus norvegicus GN=Ahsg PE=1 SV=2	1231	38757	79	6	15	4565	4709	4460	7344	6914	7147	-0.64	4.336	

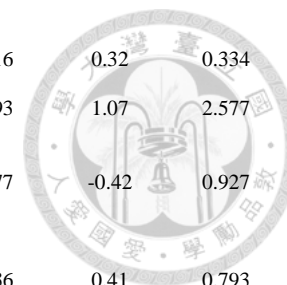
50	Q07936	Annexin A2 OS=Rattus norvegicus GN=Anxa2 PE=1 SV=2	837	38939	65	6	19	3078	3130	2916	4665	4390	4762	-0.60	3.667	
52	Q9QXQ0	Alpha-actinin-4 OS=Rattus norvegicus GN=Actn4 PE=1 SV=2	723	105306	80	6	25	63050	4792	64275	3014	4702	4190	2.78	1.039	+
60	P04937	Fibronectin OS=Rattus norvegicus GN=Fn1 PE=1 SV=2	678	275990	62	6	27	1527	1584	1705	1156	1402	1427	0.28	1.211	
64	P04639	Apolipoprotein A-I OS=Rattus norvegicus GN=Apoa1 PE=1 SV=2	499	30100	58	6	17	12447	13233	13399	4428	3733	3905	1.70	4.520	+
70	P18418	Calreticulin OS=Rattus norvegicus GN=Calr PE=1 SV=1	535	48137	59	6	14	4981	4904	5100	2843	5057	3137	0.49	0.886	
73	P31044	Phosphatidylethanolamine-binding protein 1 OS=Rattus norvegicus GN=Pebp1 PE=1 SV=3	626	20902	33	6	7	2883	2604	2114	3802	3833	3201	-0.52	1.527	
81	P02650	Apolipoprotein E OS=Rattus norvegicus GN=ApoE PE=1 SV=2	445	35788	33	6	10	3909	3634	3323	2934	3171	3392	0.19	1.001	
83	P01048	T-kininogen 1 OS=Rattus norvegicus GN=Map1 PE=1 SV=2	778	48828	46	6	9	2793	2502	2223	15487	16031	15493	-2.65	4.981	+
92	P08932	T-kininogen 2 OS=Rattus norvegicus PE=1 SV=2	896	48757	48	6	12	1813	1651	1759	8600	8292	8136	-2.26	5.976	+
93	Q9Z1P2	Alpha-actinin-1 OS=Rattus norvegicus GN=Actn1 PE=1 SV=1	405	103466	14	6	4	1629	1805	1590	6639	6389	6355	-1.95	5.285	+
100	P45592	Cofilin-1 OS=Rattus norvegicus GN=Cfl1 PE=1 SV=3	438	18749	31	6	9	8698	8546	8819	5706	4253	5367	0.78	2.408	
102	P17475	Alpha-1-antitrypsin OS=Rattus norvegicus GN=Serpina1 PE=1 SV=2	439	46278	41	6	11	5347	4983	4551	5890	6328	6182	-0.31	1.855	
103	P11762	Galectin-1 OS=Rattus norvegicus GN=Lgals1 PE=1 SV=2	338	15189	26	6	7	3173	3211	3191	1858	1714	1729	0.85	4.667	+
110	P85972	Vinculin OS=Rattus norvegicus GN=Vcl PE=1 SV=1	330	117112	45	6	21	2655	4686	5386	6617	6835	5344	-0.62	0.866	



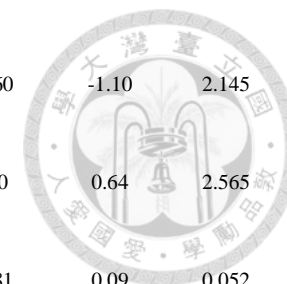
113	P38983	40S ribosomal protein SA OS=Rattus norvegicus GN=Rpsa PE=1 SV=3	557	32917	30	6	7	3303	3083	3211	1566	1536	1864	0.96	3.287	+
118	Q99376	Transferrin receptor protein 1 (Fragment) OS=Rattus norvegicus GN=Tfrc PE=2 SV=1	316	70337	28	3	12	1993	1645	2049	2892	1979	4128	-0.60	0.874	
122	Q6P6V0	Glucose-6-phosphate isomerase OS=Rattus norvegicus GN=Gpi PE=1 SV=1	313	62958	34	6	12	3507	3995	3552	2655	2731	3874	0.27	0.674	
127	P63159	High mobility group protein B1 OS=Rattus norvegicus GN=Hmgb1 PE=1 SV=2	303	25049	23	6	10	4884	4924	3855	6112	6471	6815	-0.51	1.838	
129	P10111	Peptidyl-prolyl cis-trans isomerase A OS=Rattus norvegicus GN=Ppia PE=1 SV=2	428	18091	37	6	12	9143	9273	9181	9226	9766	8909	-0.01	0.141	
142	P62963	Profilin-1 OS=Rattus norvegicus GN=Pfn1 PE=1 SV=2	295	15119	23	6	6	2370	2129	2028	2153	2085	1189	0.31	0.475	
159	P05065	Fructose-bisphosphate aldolase A OS=Rattus norvegicus GN=Aldoa PE=1 SV=2	311	39783	40	6	13	2882	3510	2870	4717	4855	4966	-0.66	2.584	
163	Q68FP1	Gelsolin OS=Rattus norvegicus GN=Gsn PE=1 SV=1	254	86413	21	6	10	752	754	680	379	383	442	0.86	3.253	+
167	P06238	Alpha-2-macroglobulin OS=Rattus norvegicus GN=A2m PE=2 SV=2	609	165107	83	6	25	2377	2587	2499	3907	4122	6218	-0.90	1.863	
186	P14480	Fibrinogen beta chain OS=Rattus norvegicus GN=Fgb PE=1 SV=4	262	54828	32	6	16	1100	1306	1161	2269	2232	1865	-0.83	2.696	
196	P02680	Fibrinogen gamma chain OS=Rattus norvegicus GN=Fgg PE=1 SV=3	209	51228	17	6	7	2110	1697	1845	1894	1753	1890	0.02	0.089	
207	P31211	Corticosteroid-binding globulin OS=Rattus norvegicus GN=Serpina6 PE=1 SV=2	201	44813	15	3	7	5507	5698	5818	1469	1414	1310	2.02	5.527	+
217	P02454	Collagen alpha-1(I) chain OS=Rattus norvegicus GN=Coll1a1 PE=1 SV=5	475	138895	37	6	9	1750	2608	2279	3443	3831	3993	-0.78	1.905	



222	P18292	Prothrombin OS=Rattus norvegicus GN=F2 PE=1 SV=1	188	71792	18	6	10	1787	1696	2116	1186	1114	2516	0.32	0.334	
223	P51886	Lumican OS=Rattus norvegicus GN=Lum PE=2 SV=1	255	38654	28	6	8	2191	2569	2491	994	1101	1393	1.07	2.577	+
224	Q9ERB4	Versican core protein (Fragments) OS=Rattus norvegicus GN=Vcan PE=2 SV=2	234	301874	23	6	9	1916	2564	2423	3816	2897	2577	-0.42	0.927	
243	P08934	Kininogen-1 OS=Rattus norvegicus GN=Kng1 PE=2 SV=1	205	71972	12	6	5	1777	1832	1145	1060	1322	1136	0.41	0.793	
245	P63029	Translationally-controlled tumor protein OS=Rattus norvegicus GN=Tpt1 PE=1 SV=1	172	19564	15	6	4	923	972	952	1083	1375	1659	-0.51	1.334	
249	P07150	Annexin A1 OS=Rattus norvegicus GN=Anxa1 PE=1 SV=2	333	39147	22	6	9	1932	2683	1351	3620	3924	912	-0.30	0.148	
274	P04638	Apolipoprotein A-II OS=Rattus norvegicus GN=Apoa2 PE=2 SV=1	155	11489	6	3	3	857	1307	895	722	499	728	0.65	1.149	
292	P26644	Beta-2-glycoprotein 1 OS=Rattus norvegicus GN=Apoh PE=2 SV=2	284	34316	20	5	5	2388	2921	2152	2839	1305	3944	0.01	0.009	
299	P10960	Sulfated glycoprotein 1 OS=Rattus norvegicus GN=Psap PE=1 SV=1	187	62908	22	6	3	1446	1421	1326	1653	1711	1819	-0.31	2.265	
304	Q64240	Protein AMBP OS=Rattus norvegicus GN=Ambp PE=1 SV=1	139	39738	7	4	3	742	772	751	404	703	957	0.22	0.239	
311	P14841	Cystatin-C OS=Rattus norvegicus GN=Cst3 PE=1 SV=2	247	15655	13	6	4	1070	779	896	987	999	2139	-0.50	0.565	
340	Q5RKI0	WD repeat-containing protein 1 OS=Rattus norvegicus GN=Wdr1 PE=1 SV=3	139	66824	25	6	7	1699	1117	1728	3001	4943	2537	-1.17	1.527	+
345	P01015	Angiotensinogen OS=Rattus norvegicus GN=Agt PE=1 SV=1	170	52177	17	6	5	1011	1329	1765	860	3004	1186	-0.12	0.073	



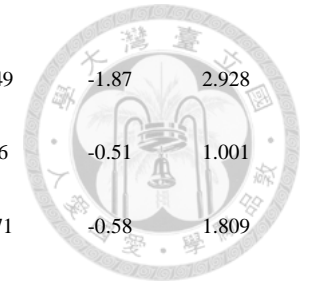
347	P29315	Ribonuclease inhibitor OS=Rattus norvegicus GN=Rnh1 PE=1 SV=2	306	51653	25	6	11	1065	1279	1629	2685	3292	2460	-1.10	2.145	+
350	P35053	Glypican-1 OS=Rattus norvegicus GN=Gpc1 PE=1 SV=1	133	62721	6	3	3	637	695	681	486	399	410	0.64	2.565	
364	P02466	Collagen alpha-2(I) chain OS=Rattus norvegicus GN=Col1a2 PE=1 SV=3	214	129999	19	6	6	1184	2279	617	1012	999	1381	0.09	0.052	
409	P13941	Collagen alpha-1(III) chain OS=Rattus norvegicus GN=Col3a1 PE=2 SV=3	134	140162	14	6	4	1309	1568	716	1545	1191	1308	-0.24	0.263	
437	Q4FZX7	Signal recognition particle receptor subunit beta OS=Rattus norvegicus GN=Srprb PE=2 SV=1	90	29722	3	2	3	366	498	575	929	1341	1118	-1.24	2.144	+
438	P00762	Anionic trypsin-1 OS=Rattus norvegicus GN=Prss1 PE=1 SV=1	107	26627	13	6	3	888	928	965	603	767	571	0.53	1.760	
461	Q9QX79	Fetuin-B OS=Rattus norvegicus GN=Fetub PE=2 SV=1	189	42361	13	5	6	1475	1394	1166	2282	1847	1808	-0.56	1.701	
462	P47853	Biglycan OS=Rattus norvegicus GN=Bgn PE=2 SV=1	83	42079	5	4	3	475	437	424	607	1607	491	-0.81	0.703	
473	O08628	Procollagen C-endopeptidase enhancer 1 OS=Rattus norvegicus GN=Pcolce PE=2 SV=1	81	50837	9	6	5	1189	1058	1337	1114	1801	2402	-0.51	0.682	
484	P0C5H9	Mesencephalic astrocyte-derived neurotrophic factor OS=Rattus norvegicus GN=Manf PE=1 SV=1	89	20831	9	6	3	1534	1708	769	2511	2659	2507	-1.02	1.317	
495	Q9R1S9	Midkine OS=Rattus norvegicus GN=Mdk PE=2 SV=1	100	15966	4	2	3	755	777	599	331	103	689	1.30	0.738	
510	P12843	Insulin-like growth factor-binding protein 2 OS=Rattus norvegicus GN=Igfbp2 PE=1 SV=3	107	33917	5	3	3	1098	481	760	576	702	580	0.26	0.294	
516	P49134	Integrin beta-1 OS=Rattus norvegicus GN=Itgb1 PE=2 SV=1	141	91687	8	4	5	1067	1033	812	608	736	629	0.56	1.675	
527	Q01129	Decorin OS=Rattus norvegicus GN=Dcn PE=1 SV=1	152	40122	8	4	4	1075	904	1592	896	1620	1864	-0.27	0.265	



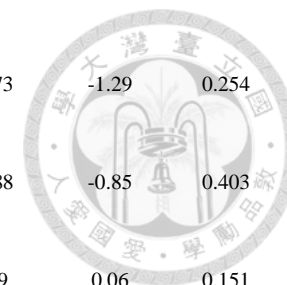
533	P00787	Cathepsin B OS=Rattus norvegicus GN=Ctsb PE=1 SV=2	272	38358	16	6	3	775	609	708	1099	1286	1045	-0.71	2.206	
535	P04276	Vitamin D-binding protein OS=Rattus norvegicus GN=Gc PE=1 SV=3	109	55106	7	3	5	988	961	1607	1779	913	944	0.00	0.002	
545	P07632	Superoxide dismutase [Cu-Zn] OS=Rattus norvegicus GN=Sod1 PE=1 SV=2	263	16073	18	6	5	1880	1442	1566	10162	9583	9366	-2.58	4.582	+
584	P06399	Fibrinogen alpha chain OS=Rattus norvegicus GN=Fga PE=1 SV=3	187	87373	25	6	12	2722	3626	3440	3756	3485	3610	-0.16	0.535	
602	Q63041	Alpha-1-macroglobulin OS=Rattus norvegicus GN=A1m PE=1 SV=1	167	168388	13	5	6	2195	2382	1332	1708	2060	1348	0.18	0.228	
612	Q9JI03	Collagen alpha-1(V) chain OS=Rattus norvegicus GN=Col5a1 PE=1 SV=1	80	184558	2	2	2	2419	711	2726	5496	1153	1377	-0.30	0.115	
634	Q9JI85	Nucleobindin-2 OS=Rattus norvegicus GN=Nucb2 PE=2 SV=1	102	50173	12	6	7	1332	1621	1020	1391	1046	519	0.51	0.482	
640	P21744	Insulin-like growth factor-binding protein 4 OS=Rattus norvegicus GN=Igfbp4 PE=1 SV=2	108	28867	5	3	3	874	1292	753	1801	719	677	-0.01	0.010	
647	P07943	Aldose reductase OS=Rattus norvegicus GN=Akr1b1 PE=1 SV=3	143	36230	12	6	7	1098	966	988	2368	1867	2867	-1.20	2.510	+
660	Q6IUR5	Neudesin OS=Rattus norvegicus GN=Nenf PE=2 SV=1	89	18980	5	4	2	1390	1096	1165	447	2268	1882	-0.04	0.016	
661	P06765	Platelet factor 4 OS=Rattus norvegicus GN=Pf4 PE=1 SV=1	63	11507	2	2	2	201	166	232	114	191	145	0.43	0.778	
685	Q8VHK7	Hepatoma-derived growth factor OS=Rattus norvegicus GN=Hdgf PE=1 SV=2	108	26586	4	3	3	1382	850	1132	5056	5493	2349	-1.87	1.883	+
695	P16975	SPARC OS=Rattus norvegicus GN=Sparc PE=1 SV=4	50	35129	3	3	2	959	1083	909	707	893	826	0.29	1.079	



700	P97690	Structural maintenance of chromosomes protein 3 OS=Rattus norvegicus GN=Smc3 PE=1 SV=1	65	138761	6	3	3	1052	1090	754	3683	4047	2849	-1.87	2.928	+
723	Q9WVH8	Fibulin-5 OS=Rattus norvegicus GN=Fbln5 PE=2 SV=1	86	52408	4	3	2	171	158	232	211	273	316	-0.51	1.001	
737	Q01177	Plasminogen OS=Rattus norvegicus GN=Plg PE=2 SV=2	146	93214	8	4	5	1867	1553	1820	2234	2940	2671	-0.58	1.809	
761	P25304	Agrin OS=Rattus norvegicus GN=Agrn PE=1 SV=2	79	216549	5	3	5	1123	881	1158	1607	1398	1570	-0.54	1.750	
798	P05371	Clusterin OS=Rattus norvegicus GN=Clu PE=1 SV=2	75	51970	3	3	3	468	821	1213	1595	802	1679	-0.73	0.629	
828	P04916	Retinol-binding protein 4 OS=Rattus norvegicus GN=Rbp4 PE=1 SV=1	87	23547	5	3	3	901	2130	3204	796	1183	1419	0.73	0.548	
858	P01026	Complement C3 OS=Rattus norvegicus GN=C3 PE=1 SV=3	859	187825	40	6	20	8703	8447	2558	10416	2502	4571	0.22	0.094	
875	P62161	Calmodulin OS=Rattus norvegicus GN=Calm1 PE=1 SV=2	220	16827	24	6	4	4589	5021	4527	2990	3417	3971	0.45	1.632	
886	P02767	Transthyretin OS=Rattus norvegicus GN=Tr PE=1 SV=1	161	15824	9	5	4	2542	2514	2323	3132	3367	3205	-0.40	2.817	
901	Q6P7R8	Estradiol 17-beta-dehydrogenase 12 OS=Rattus norvegicus GN=Hsd17b12 PE=2 SV=1	81	34990	2	2	2	122	329	462	1562	669	1765	-2.21	1.421	+
927	P05539	Collagen alpha-1(II) chain OS=Rattus norvegicus GN=Col2a1 PE=2 SV=2	78	135001	2	2	2	365	551	383	69	321	238	1.29	0.850	
938	Q9R1J8	Prolyl 3-hydroxylase 1 OS=Rattus norvegicus GN=Lepre1 PE=1 SV=1	54	83193	3	3	3	1314	1057	1477	1695	1510	972	-0.09	0.120	
962	Q6IE64	Complement C1r subcomponent-like protein OS=Rattus norvegicus GN=C1rl PE=2 SV=1	41	51930	2	2	2	3512	3659	3469	3284	4411	2343	0.13	0.189	



964	P29534	Vascular cell adhesion protein 1 OS=Rattus norvegicus GN=Vcam1 PE=2 SV=1	41	82278	2	2	2	1002	813	55	108	2669	2273	-1.29	0.254	
1025	Q6IUU3	Sulfhydryl oxidase 1 OS=Rattus norvegicus GN=Qsox1 PE=1 SV=1	46	83158	3	2	3	177	487	1199	814	533	1388	-0.85	0.403	
1061	Q6P734	Plasma protease C1 inhibitor OS=Rattus norvegicus GN=Serpina1 PE=2 SV=1	73	55804	4	2	4	982	723	881	829	772	869	0.06	0.151	
1091	P85973	Purine nucleoside phosphorylase OS=Rattus norvegicus GN=Np PE=1 SV=1	43	32566	2	2	2	13084	1539	1331	2914	2501	2620	0.16	0.053	
1147	P05544	Serine protease inhibitor A3L OS=Rattus norvegicus GN=Serpina3l PE=1 SV=3	697	46419	40	3	13	2962	3505	3573	5252	5690	4704	-0.64	2.265	
1148	P05545	Serine protease inhibitor A3K OS=Rattus norvegicus GN=Serpina3k PE=1 SV=3	459	46760	13	3	6	1013	991	1110	2060	2193	2141	-1.04	4.290	+
1152	P13635	Ceruloplasmin OS=Rattus norvegicus GN=Cp PE=2 SV=3	229	121562	16	3	9	2008	1313	2114	2433	2444	2393	-0.45	0.969	
1153	Q03626	Murine globulin-1 OS=Rattus norvegicus GN=Mug1 PE=2 SV=1	223	166590	12	3	9	1490	2229	1651	1898	1875	2242	-0.18	0.395	
1163	O08619	Coagulation factor XIII A chain OS=Rattus norvegicus GN=F13a1 PE=2 SV=3	144	83120	12	3	8	1263	1658	2510	1848	2525	980	0.07	0.046	
1165	Q63416	Inter-alpha-trypsin inhibitor heavy chain H3 OS=Rattus norvegicus GN=Itih3 PE=2 SV=1	141	99378	8	3	3	634	563	278	467	887	1053	-0.71	0.624	
1197	A2RUV9	Adipocyte enhancer-binding protein 1 OS=Rattus norvegicus GN=Aebp1 PE=2 SV=1	38	128723	2	2	2	392	440	302	275	475	441	-0.05	0.056	
1199	Q9WUW3	Complement factor I OS=Rattus norvegicus GN=Cfi PE=2 SV=1	52	69534	5	3	3	1859	1977	1676	1723	1126	1839	0.26	0.492	



1230	P14046	Alpha-1-inhibitor 3 OS=Rattus norvegicus GN=A1i3 PE=1 SV=1	158	165038	2	2	2	2517	1823	1718	1571	1219	1357	0.53	1.243	
1239	P35559	Insulin-degrading enzyme OS=Rattus norvegicus GN=Ide PE=1 SV=1	39	118376	3	2	2	613	280	417	629	605	687	-0.62	0.875	
1264	P70564	Serpin B5 OS=Rattus norvegicus GN=Serpib5 PE=2 SV=1	94	42379	2	1	2	578	1128	679	1774	2219	1813	-1.34	1.909	+



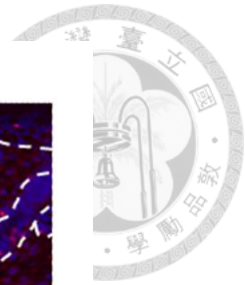
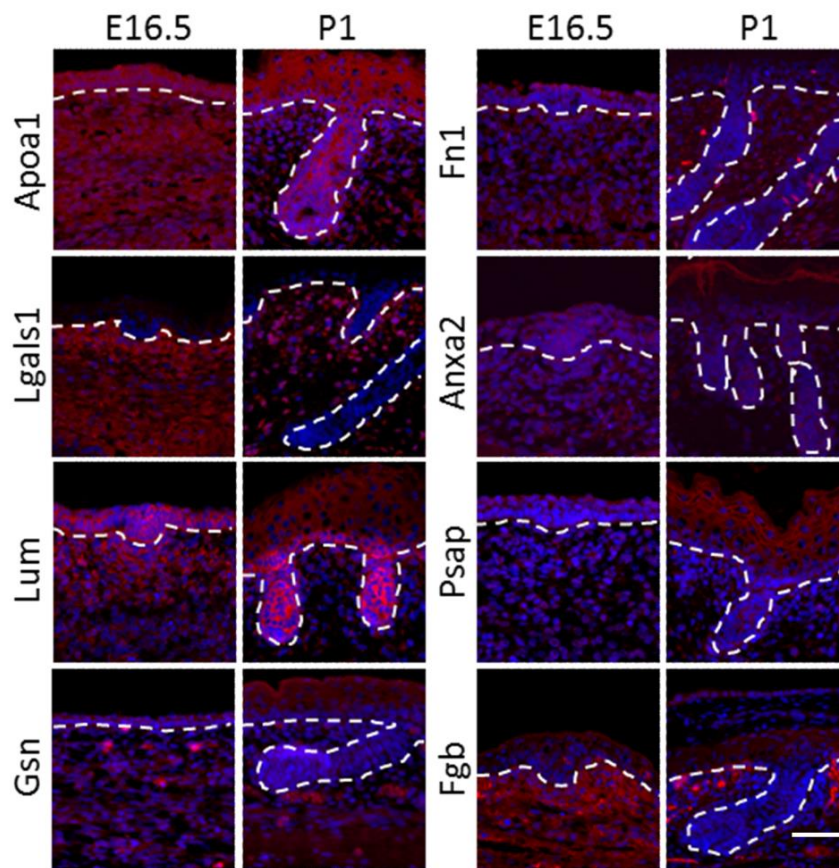


Figure 13 Proteomic analysis identifies secreted proteins enriched in developmental skin.

Immunostaining of the 8 proteins in E16.5 and P1 skin. Red: specific protein; blue: nuclear DAPI staining; dashed line: basement membrane. Bar: 100 μ m.

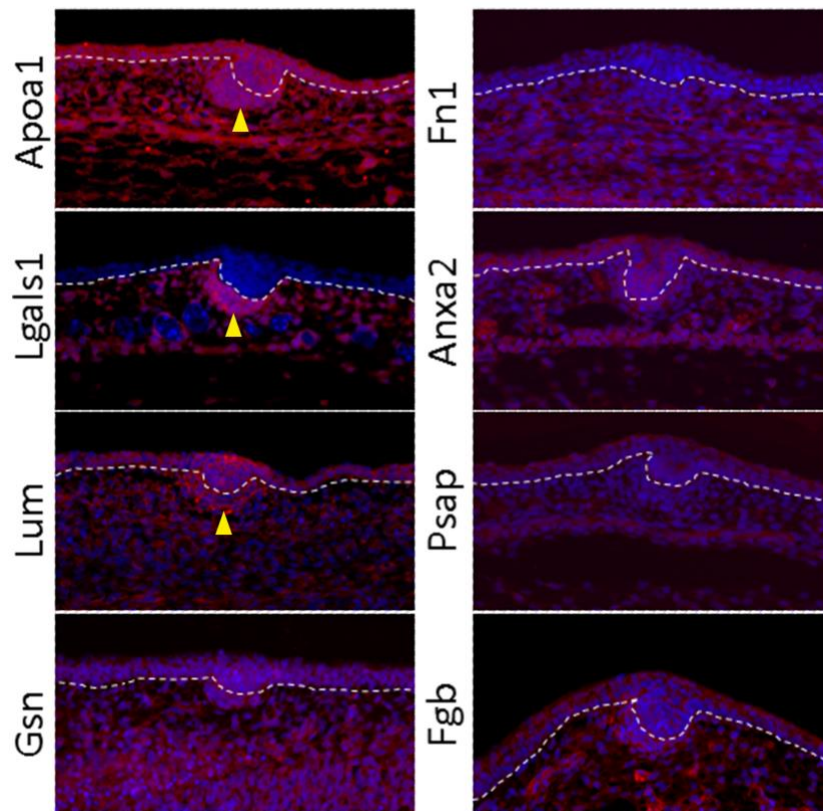


Figure 14 Expression of the 8 proteins in E17.5 Wistar rat embryonic skin.

Immunostaining showed that, compared with other 7 proteins, galectin-1 had a more preferential distribution in the dermis. Apolipoprotein-A1, galectin-1 and lumican were also abundant in the dermal condensate (yellow arrowheads) of the developing HF.

Red: specific protein; blue: nuclear DAPI staining; dashed line: basement membrane.

Bar: 100 μ m.

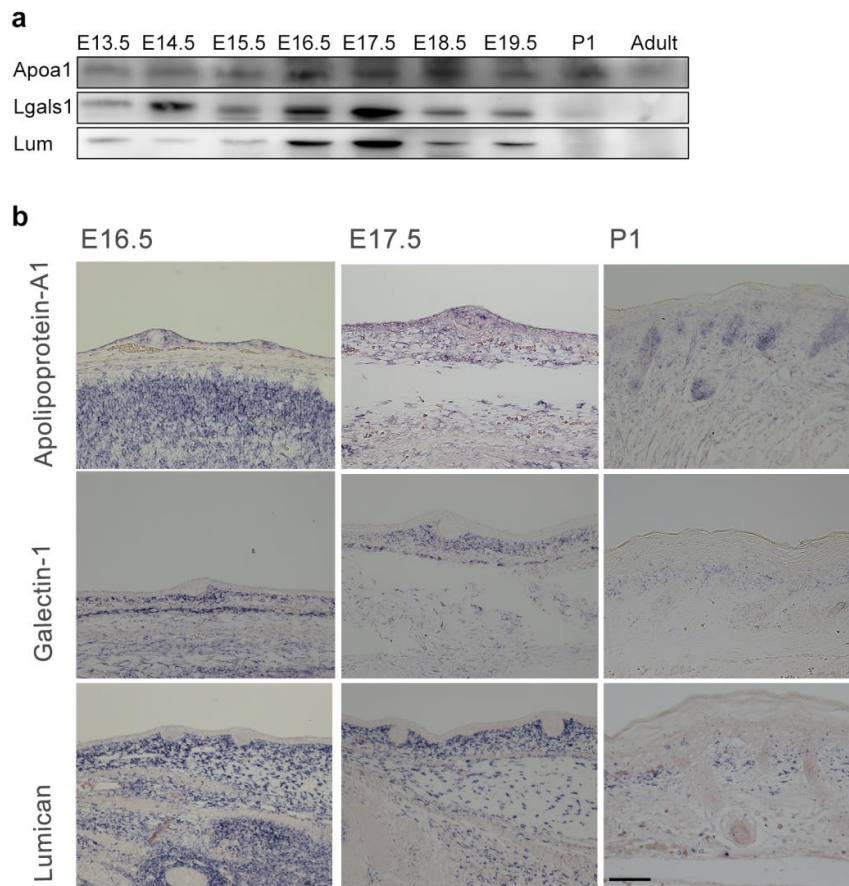


Figure 15 Expression of apolipoprotein-A1, galectin-1 and lumican genes in embryonic to postnatal skin detected by in situ hybridization.

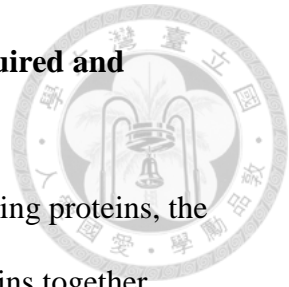
(a) Protein expression of Apoa1, Lgals1 and Lum in different stages of skin. (b) *In situ* hybridization for the expression of apolipoprotein-A1, galectin-1 and lumican genes in the skin at different stages. All the three genes were highly expressed in the dermal mesenchyme in E16.5 and E17.5 skin. Bar: 100 μ m.

Apolipoprotein-A1, Galectin-1 and Lumican Together were Required and Sufficient to Induce HF Neogenesis.

To determine whether HF neogenesis could be induced by defining proteins, the combination of the 8 proteins was tested in patch assays. The 8 proteins together induced new HFs (Fig. 16). The removal of each protein of apolipoprotein-A1, galectin-1 or lumican from the 8 proteins combination inhibited HF inductivity. To evaluate the effect of individual proteins, we subtracted each of the 8 proteins and found a different degree of suppression on HF regeneration; complete suppression was observed when ApoA1, Lgals1 and Lum was individually removed (Fig. 16).

Depletion of the E16.5 whole skin extracts of either on. Removal of ApoA1, Lgals1 or Lum from E16.5 skin extract with specific antibodies ablated the ability to induce effects on HF neogenesis induction. The removal of each of the 3 proteins from E16.5 skin extract also eliminated HF inductivity (Fig. 17).

The results indicated that ApoA1, Lgals1 and Lum were essential for HF induction. We further tested whether these 3 proteins together were sufficient to induce new HFs. Each protein alone or combinations of two of the 3 proteins did not induce new HFs (Fig. 18). Only the combination of the 3 proteins induced new HFs (Fig.18) but with a lower efficiency compared with either 8 protein combination or E16.5 skin extract. Here we demonstrated that these 3 proteins collectively promote the competency of adult fibroblasts for HF neogenesis (Fig. 18). In addition, we also demonstrated a novel way to induce HF neogenesis by transfecting adult fibroblasts with of mRNAs of these three genes, *ApoA1/Lgals1/Lum* (Fig. 19).



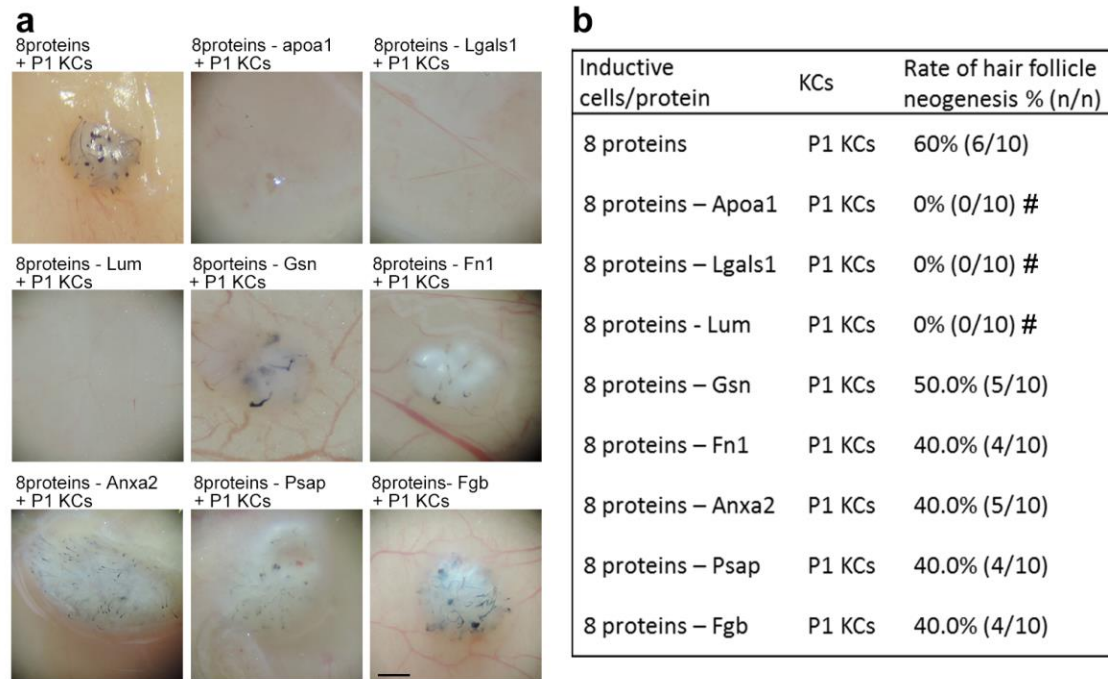


Figure 16 Combination of 7 or 8 proteins to induce new HF.

(a) Representative photos from patch assays. (b) Results of patch assays. The removal of each protein of apolipoprotein-A1, galectin-1 or lumican from the 8 proteins combination inhibited HF inductivity. # $p < 0.05$, compared with 8 proteins. Bar: 500 μ m.

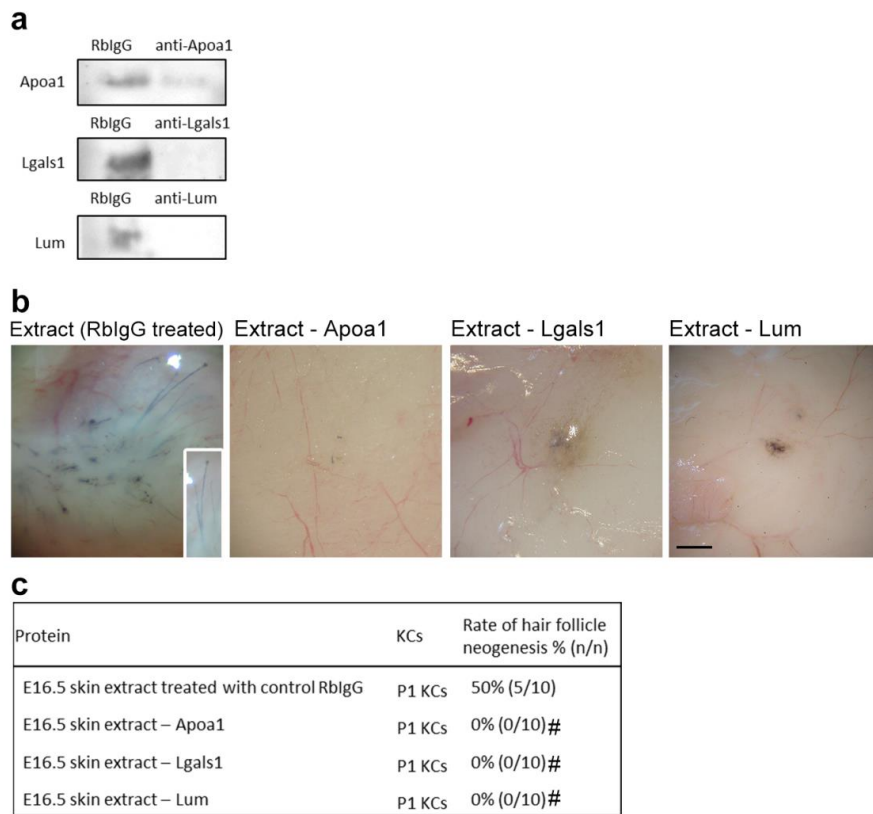
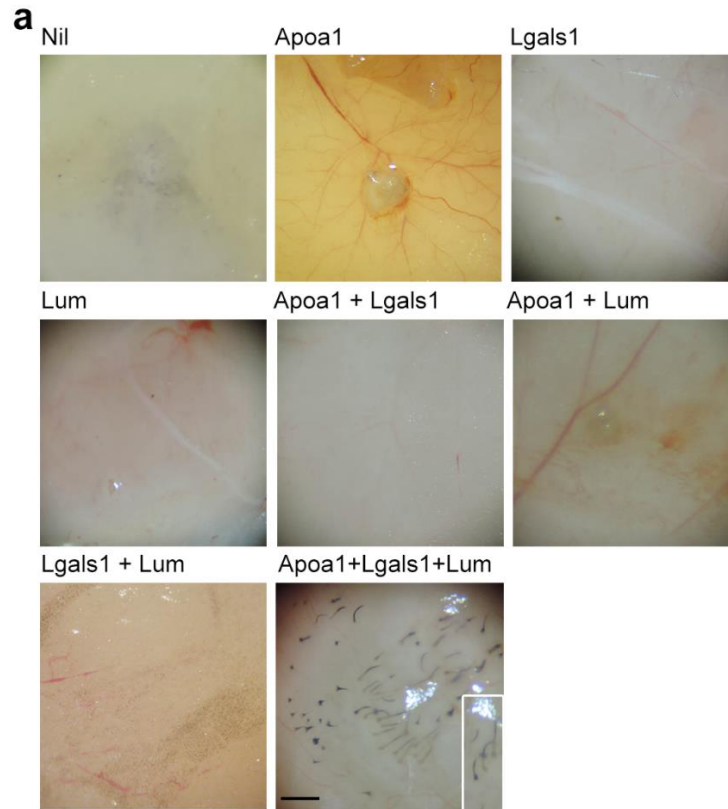


Figure 17 Induction of HF neogenesis by defined proteins.

P1 keratinocytes were suspended in solutions containing specific proteins for patch assays. (a)-(c) Removal of Apoa1, Lgals1 or Lum from E16.5 skin extract with specific antibodies and the effects on HF induction. # $p < 0.05$, compared E16.5 skin extract treated with RbIgG. RbIgG: control rabbit IgG. Bar: 500 μ m.



b

Protein	KCs	Rate of hair follicle neogenesis % (n/n)
Nil	P1 KCs	0% (0/10)
Apoa1	P1 KCs	0% (0/10)
Lgals1	P1 KCs	0% (0/10)
Lum	P1 KCs	0% (0/10)
Apoa1 + Lgals1	P1 KCs	0% (0/10)
Apoa1 + Lum	P1 KCs	0% (0/10)
Lgals1 + Lum	P1 KCs	0% (0/10)
Apoa1 + Lgals1+ Lum	P1 KCs	40.0% (4/10) #

Figure 18 Induction of HF neogenesis by defined proteins.

P1 keratinocytes were suspended in solutions containing specific proteins for patch assays. (a)-(b), Effect of 1-protein, 2-proteins and 3-proteins combination on HF induction. # $p < 0.05$, compared with P1 KCs only. Insets showed enlarged images of regenerated HFs. Bar: 500 μ m.

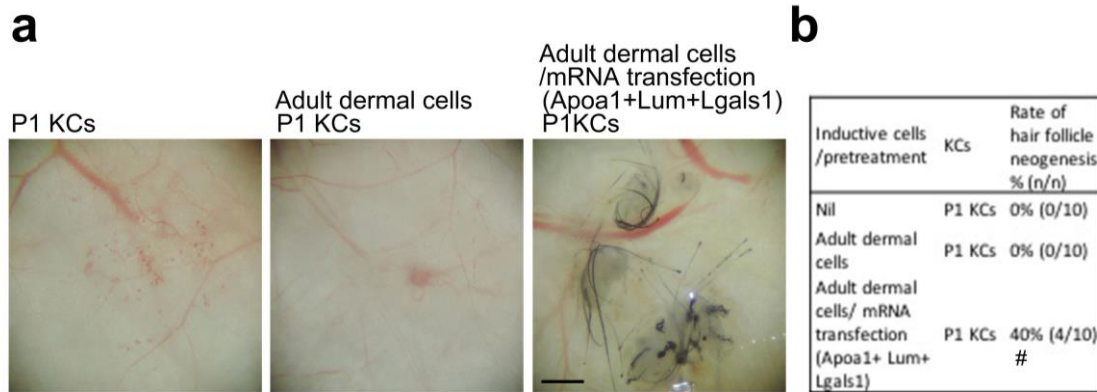


Figure 19 Induction of HF neogenesis by defined proteins and mRNAs.

P1 keratinocytes were used for all patch assays. (d, d') The effect of mRNA transfection of the three genes *Apoa/Lgals1/Lum* to adult dermal fibroblasts on HF neogenesis. # $p < 0.05$ with Fisher's test, compared with P1 KCs only (n=10).

E16.5 Skin Extract Conferred Fibroblasts a Reversible Ability to Induce HF Neogenesis.

Comparison of gene expression of DP cells with E16.5 skin extract-treated fibroblasts and E16.5 skin extract-treated fibroblasts with washout. To explore the mechanisms of how HFs were induced, P1 keratinocytes and adult dermal fibroblasts were cultured with E16.5 extract for 3 days before being tested in patch assays (Fig. 20).

The keratinocytes exposed to E16.5 extract along failed to regenerate HFs, but fibroblasts exposed to E16.5 extract induced HF neogenesis when combined with keratinocytes (Fig. 20). Fibroblasts, but not keratinocytes, acquired hair-forming competence in response to this culture condition (Fig. 20), suggesting that fibroblasts are the target cells of these proteins. The trichogenic ability of fibroblasts was lost when they were further cultured for another 3 days in the absence of skin extract (Fig. 20).

Then we also tested the adult human fibroblast exposed to E16.5 skin extract induced HF neogenesis when combined with keratinocytes (Fig. 21).

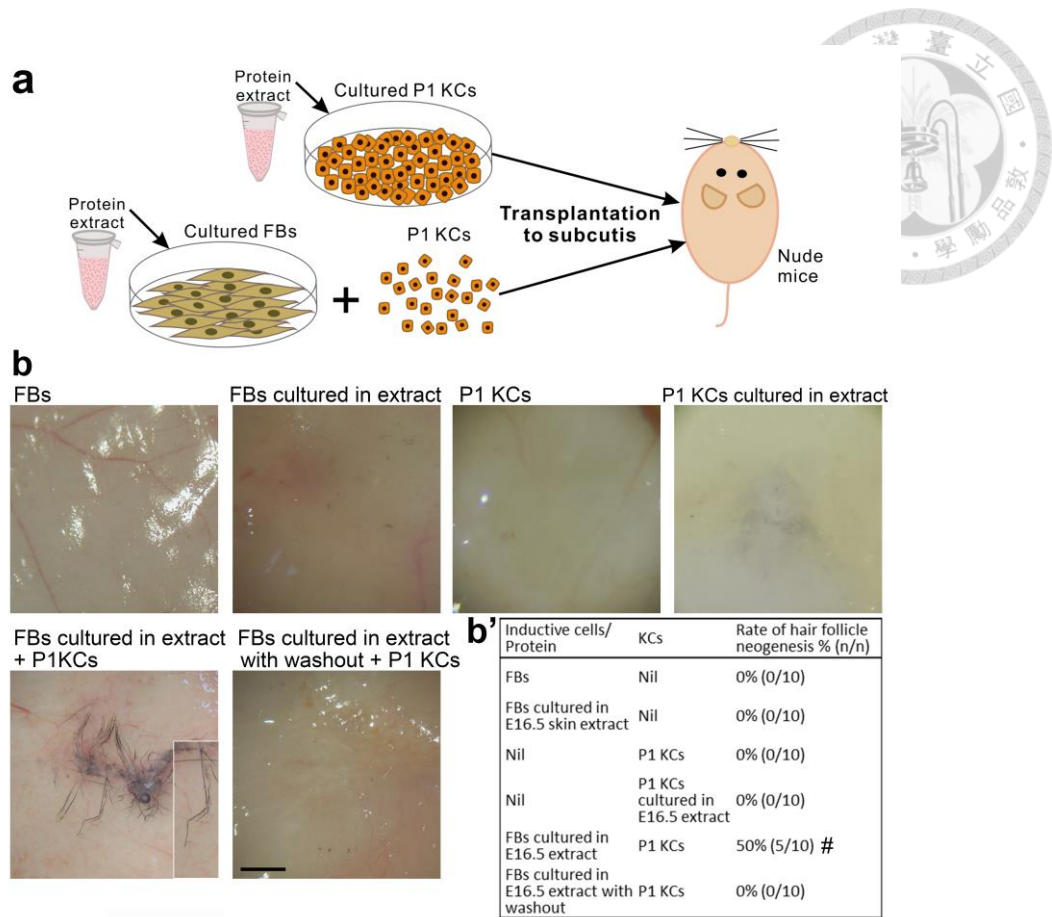
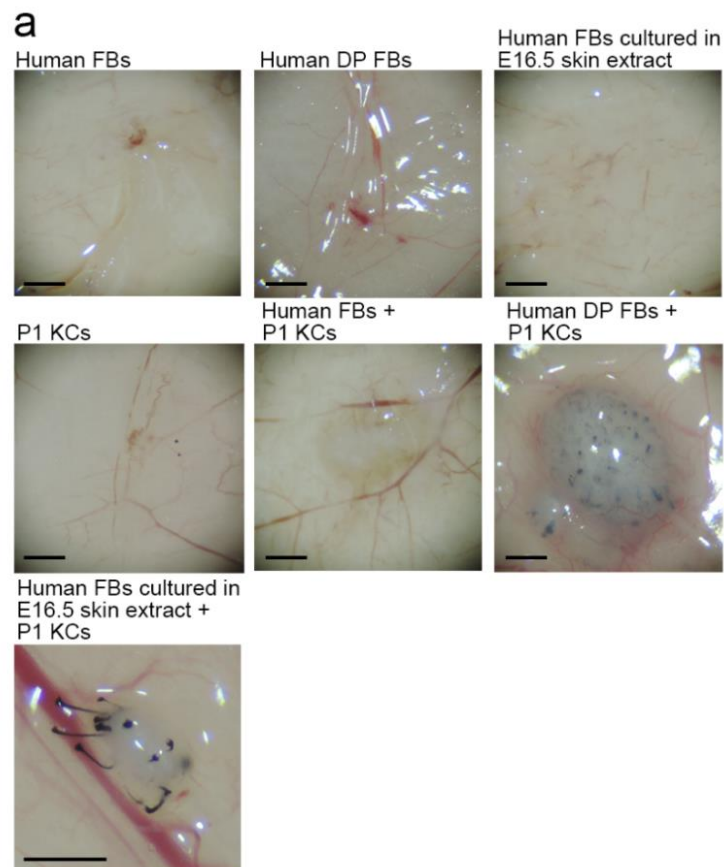


Figure 20 E16.5 skin extract confers adult fibroblasts trichogenic ability.

(a) Culturing keratinocytes and fibroblasts with E16.5 skin extract for HF neogenesis assays. (b)-(b'), Effect of exposure to E16.5 skin extract on HF inductivity of adult fibroblasts. # $p < 0.05$, compared with fibroblasts cultured in E16.5 skin extract. Bar: 500 μ m.



b

Inductive cells/ Protein	KCs	Rate of hair follicle neogenesis % (n/n)
Human FBs	Nil	0% (0/10)
Human DP FBs	Nil	0% (0/10)
Human FBs cultured in E16.5 skin extract	Nil	0% (0/10)
Nil	P1 KCs	0% (0/10)
Human FBs	P1 KCs	0% (0/10)
Human DP FBs	P1 KCs	50% (5/10) *
Human FBs cultured in E16.5 extract	P1 KCs	40% (4/10) *

Figure 21 Effect of rat E16.5 skin extract on HF inductivity of adult human dermal fibroblasts.

Adult human foreskin dermal fibroblasts were cultured in E16.5 skin extract for 3 days and then co-injected with P1 mouse keratinocytes in patch assays. (a) Representative patch assays. (b) Summary of patch assay results. Bar, 500 μm .

Fibroblasts become competent for hair regeneration after exposure to embryonic skin proteins

To clarify how adult fibroblasts became trichogenic, we compared the transcriptomes of adult fibroblasts before and after exposure to E16.5 skin extract and the combination of Apo1, Lgals1 and Lum and DP cells by RNA sequencing (Table 2).

Gene expression of adult fibroblasts exposed to E16.5 skin extract and the gene expression of adult fibroblast exposed to the 3 proteins changed notably and became more DP-like (Fig. 22 and Table 2) and alkaline phosphatase activity, which is characteristic of inductive DP fibroblasts *in vitro* (Rendl, Lewis, and Fuchs 2005), was present (Fig. 25). The results above show that E16.5 protein extract and the Apo1/Lgals1/Lum mix alter the gene expression of adult dermal fibroblasts toward a DP-like profile and render them competent to regenerate HFs.

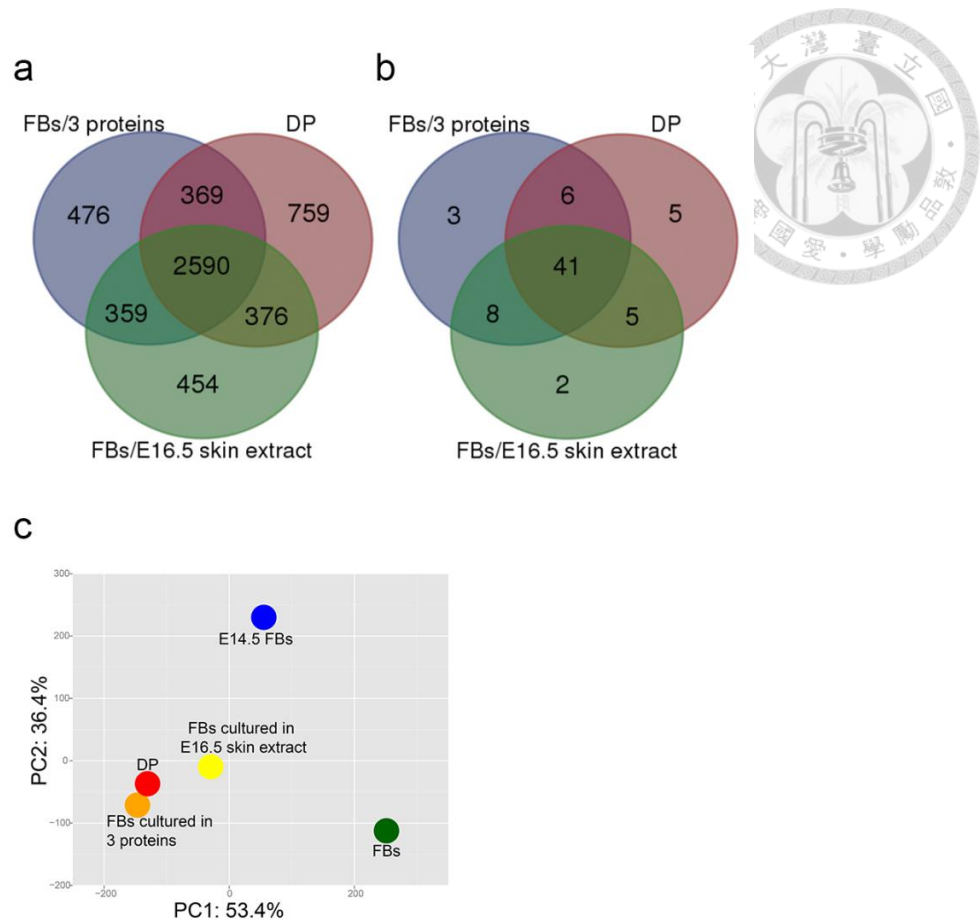
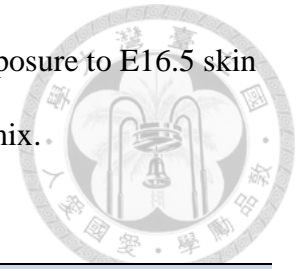
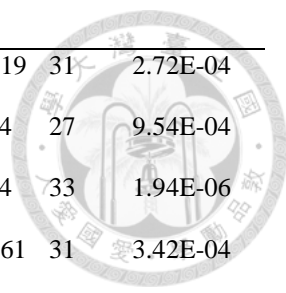


Figure 22 Comparison of numbers of upregulated genes in indicated conditions. Analysis of transcriptomes of DP and murine fibroblasts exposed to E16.5 skin extract or 3 proteins. (a), Comparison of numbers of upregulated genes in indicated conditions. Genes with 1.2-fold increase were included. Exposure to 3 proteins or E16.5 skin extract shared most genes upregulated in DP cells. Compared to exposure to 3 proteins, exposure to each of the 3 proteins only increased the expression of a minor number of genes upregulated in DP cells. (b), Numbers of significantly upregulated pathways were depicted in Genes with 1.2-fold increase (FDR ,0.05) were analyzed by DAVID Bioinformatics Resources 6.7 (<https://david.ncifcrf.gov/>). (c) PCA of transcriptomes. PCA1 and PCA2 represent top 2 dimensions of the genes showing differential expressions among these cells (fibroblasts exposed to E16.5 skin extract and 3 proteins for 6 hr)

Table 2 RNA sequencing data of DP; fibroblasts before and after exposure to E16.5 skin extract and to the combination of 3 proteins of ApoA1/Lgals1/Lum mix.



Term	DP		Extract		3pt	
	Count	p-value	Count	p-value	Count	p-value
Pathways in cancer	95	2.94E-05	93	1.86E-06	95	2.30E-06
Focal adhesion	77	7.40E-10	81	7.68E-14	86	1.25E-15
Regulation of actin cytoskeleton	73	1.87E-06	69	1.18E-06	73	1.78E-07
MAPK signaling pathway	72	0.0033245	64	0.0111778	75	1.27E-04
Chemokine signaling pathway	53	0.0027563	51	0.0010778	44	0.0567373
Endocytosis	56	0.0064591	48	0.0369667	49	0.042177
Axon guidance	41	0.0022535	48	8.53E-07	52	4.14E-08
Ubiquitin mediated proteolysis	42	0.0025996	44	8.80E-05	41	0.0015629
Wnt signaling pathway	39	0.0544948	43	0.0015374	45	8.50E-04
Insulin signaling pathway	36	0.0674455	38	0.0070447	39	0.0069422
Neurotrophin signaling pathway	36	0.0308246	36	0.0080541	45	2.61E-05
TGF-beta signaling pathway	33	1.72E-04	36	1.04E-06	33	5.35E-05
Tight junction	36	0.0512136	35	0.0244138	38	0.0083014
Cell cycle	44	1.64E-04	34	0.0189523	38	0.003205
Lysosome	41	2.70E-04	34	0.0061697	36	0.00299
Small cell lung cancer	33	1.03E-04	32	4.36E-05	30	5.22E-04
Prostate cancer	26	0.0437417	32	1.50E-04	32	2.80E-04
ECM-receptor interaction	39	7.17E-08	31	7.01E-05	36	6.14E-07
Melanogenesis			31	0.0025022	35	1.92E-04
ErbB signaling pathway	28	0.0087017	30	4.58E-04	32	1.38E-04
Gap junction	25	0.0451991	30	3.68E-04	33	4.10E-05
Vascular smooth muscle contraction	34	0.0264292	29	0.0887665	36	0.0034801
Progesterone-mediated oocyte maturation	31	6.15E-04	29	7.07E-04	29	0.0012096
T cell receptor signaling pathway			29	0.074751		



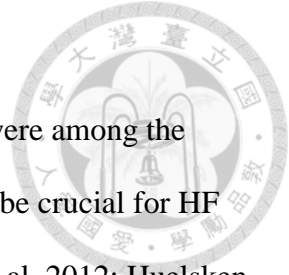
Colorectal cancer	25	0.0451991	28	0.0019619	31	2.72E-04
Chronic myeloid leukemia	24	0.0200292	28	2.22E-04	27	9.54E-04
Adherens junction	30	1.64E-04	27	5.68E-04	33	1.94E-06
Apoptosis	27	0.0164891	27	0.0049861	31	3.42E-04
Renal cell carcinoma	24	0.0070715	27	1.26E-04	29	2.68E-05
Arrhythmogenic right ventricular cardiomyopathy (ARVC)	31	4.54E-05	24	0.0056759	25	0.004038
Pancreatic cancer			24	0.0032194	20	0.069149
Dilated cardiomyopathy	36	3.84E-05	23	0.0984099	31	9.90E-04
Phosphatidylinositol signaling system	32	1.57E-05	23	0.0117944	29	1.15E-04
B cell receptor signaling pathway	31	1.83E-04	23	0.0249603		
Ribosome			23	0.0733341	23	0.0975351
Acute myeloid leukemia	22	0.0021337	22	6.25E-04	18	0.0287587
Endometrial cancer	17	0.0411489	21	4.38E-04	18	0.0114443
Long-term depression	22	0.0377281	20	0.0522667	22	0.020831
p53 signaling pathway	21	0.0445387	20	0.0351041		
NOD-like receptor signaling pathway	20	0.0287702	20	0.0114591		
Melanoma	20	0.0984746	20	0.0459952		
Glioma			20	0.0162612	22	0.0050096
RNA degradation			20	0.007859	21	0.0049935
Long-term potentiation	20	0.0877461	19	0.0719034	22	0.0151331
mTOR signaling pathway	18	0.0290523	19	0.0052872	16	0.0680024
Inositol phosphate metabolism	22	9.58E-04	18	0.0123349	19	0.0075428
Non-small cell lung cancer			18	0.0123349		
Aldosterone-regulated sodium reabsorption	14	0.0593901	16	0.0051221	13	0.0804654
Bladder cancer	17	0.0047865	15	0.0131745	15	0.0174341
Type II diabetes mellitus	17	0.0239894	15	0.0489774	16	0.0308559
N-Glycan biosynthesis			14	0.0611574	15	0.0380488
Lysine degradation	14	0.0497207	13	0.0555417	16	0.0054499

Amino sugar and nucleotide sugar metabolism			13	0.0884998		
Dorso-ventral axis formation			13	1.30E-04	11	0.0037454
Prion diseases	13	0.0327558	12	0.0405687	15	0.0027908
Chondroitin sulfate biosynthesis	9	0.0544028	8	0.0882868		
Calcium signaling pathway	52	0.012605			46	0.0543852
Leukocyte transendothelial migration	35	0.0138792			34	0.0102051
Hypertrophic cardiomyopathy (HCM)	32	2.02E-04			26	0.0094814
Toll-like receptor signaling pathway	31	0.0085201				
Fc gamma R-mediated phagocytosis	30	0.0135361				
Oocyte meiosis	30	0.0951453			31	0.0317058
GnRH signaling pathway	27	0.0597137			29	0.0098068
Cardiac muscle contraction	23	0.0481601				
Hematopoietic cell lineage	23	0.0967238				
Aminoacyl-tRNA biosynthesis	14	0.0593901			13	0.0804654
Glycosaminoglycan degradation	9	0.0693977				
Non-small cell lung cancer					18	0.0169431
Notch signaling pathway					15	0.071985
Sphingolipid metabolism					14	0.0392843
Steroid biosynthesis					7	0.0820248

Activation of Insulin/IGF1 Signaling in Fibroblasts Exposed to E16.5 Skin Extract and 3 Proteins

Follow the above experiment, Wnt signaling and IGF signaling were among the shared pathways (Table. 2). Wnt signaling has been demonstrated to be crucial for HF morphogenesis (Schneider, Schmidt-Ullrich, and Paus 2009; Chen et al. 2012; Huelsken et al. 2001; Andl et al. 2002), and the role of IGF in HF development is not clear yet. We then quantitatively compared the phosphoproteomes of cultured fibroblasts before and after exposure to E16.5 skin extract or 3 proteins by immobilized metal affinity chromatography to enrich phosphopeptides followed by LC-MS/MS for quantitation (Tsai et al. 2008; Tsai et al. 2015). KEGG pathway enrichment analysis of all differentially regulated phosphoproteins also revealed that exposure to either E16.5 extract or ApoA1/Lgals1/Lum mix could activate insulin/Igf signaling (Fig. 23).

To dissect the signaling pathways mediated by the E16.5 and defined protein mixture, we analyzed the gene expression of DP and fibroblasts before and after being cultured with either the E16.5 skin extract or the combination of ApoA1, Lgals1 and Lum (Table 2) (Tsai et al. 2015).



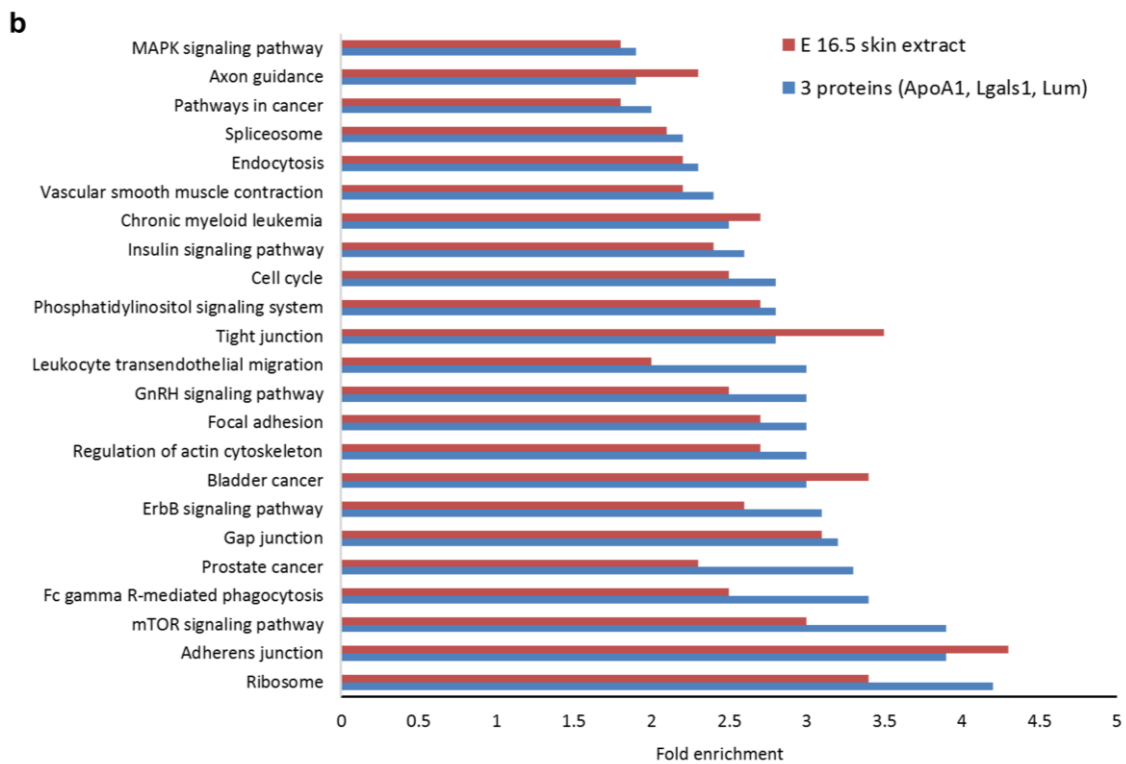
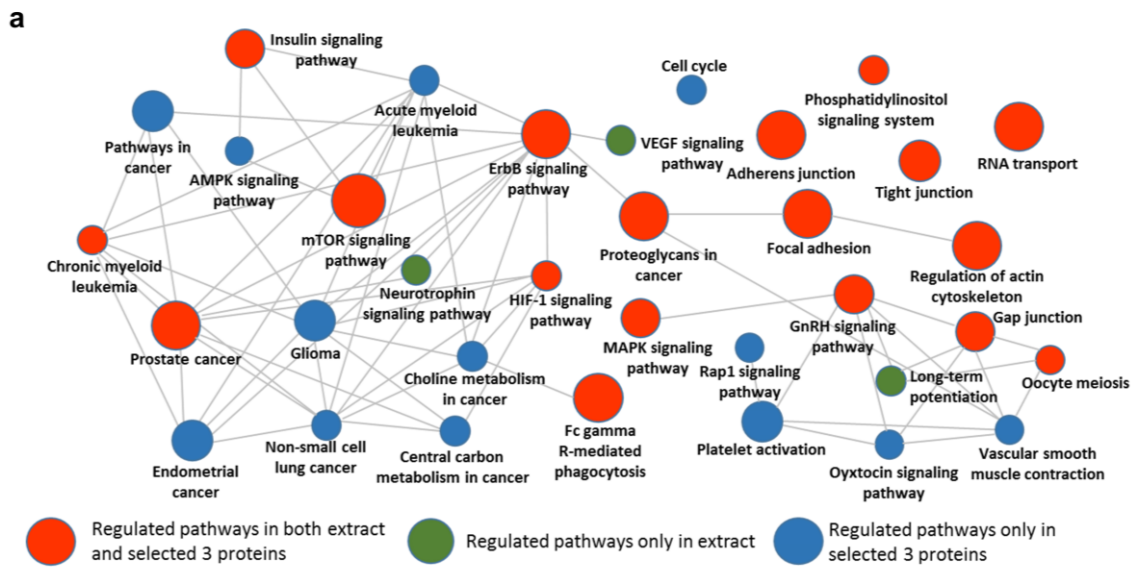


Figure 23 Pathway analysis of all regulated phosphoproteins exposed to E16.5 skin extract or 3 proteins.

(a) KEGG pathway enrichment. Phosphorylated proteins with 1.5-fold increase in comparison with baseline level were analyzed by Cytoscape (version 3.2.1). Larger circles represent involvement of more phosphorylated proteins in each pathway.

(b) Fold changes of the pathways.

Insulin/IGF1 and Wnt Signaling was Required for Hair Follicle Induction Ability of Fibroblasts.

Adult mouse fibroblasts after exposure to E16.5 skin extract express of key DP signature genes was upregulated (Fig. 24), and alkaline phosphatase activity (Fig. 25) was also detected. The results above suggested that adult fibroblasts exposed to E16.5 shifted toward a state most similar to DP cells. Indeed, we found that adult human fibroblasts exposed to rat E16.5 skin extract also became DP-like cells were which express of key DP signature gene was upregulated (Fig. 27), alkaline phosphatase activity (Fig. 27) and capable of inducing HF neogenesis (Fig. 21).

Wnt signaling and IGF signaling were among the shared pathways in Gene expression of adult fibroblasts exposed to E16.5 skin extract and the 3 proteins. Pathway analysis indicated that, in both conditions, IGF signaling and its downstream mTOR signaling were commonly activated (Fig. 25). The result was consistent with the enhanced phosphorylation of IRS2 and upregulated gene and protein expressions of IGF1 in fibroblasts exposed to E16.5 skin extract (Fig. 24 and Fig. 25). Inhibition of insulin/IGF signaling with NVP-AEW541, which is specific for IGF1 receptor kinase, ablated HF induction (Fig. 24).

During HF morphogenesis, both dermal and epidermal Wnt signaling are required (Chen et al. 2012; Huelsken et al. 2001; Andl et al. 2002). E16.5 skin extract increased expression of several Wnt ligands and activated canonical Wnt signaling in fibroblasts (Fig. 24 and Fig. 25). Inhibition of Wnt signaling by XAV-939 also suppressed HF neogenesis (Fig. 24).

Similar to whole-skin extract, the 3 proteins also enhanced IGF1 expression, IGF1 signaling, secretion of Wnt ligands and canonical Wnt signaling in adult fibroblast (Fig. 26). These results demonstrate that partial reprogramming of fibroblasts into DP-like

cells, along with IGF and Wnt activation, constitutes the core mechanism of skin extract-induced HF neogenesis. They also support the notion that IGF signaling may be involved in embryonic HF development.

Conversion of adult murine fibroblasts toward an HF-inductive state by rat E16.5 skin extract suggests that developmental signaling pathways is conserved, and could potentially be applied to humans. The result is similar to the adult mouse fibroblasts, the whole-skin extract and 3 proteins also enhanced IGF1 expression, IGF signaling, secretion of Wnt ligands and canonical Wnt signaling (Fig. 27 and Fig. 28). Indeed, we found that adult human fibroblasts exposed to rat E16.5 skin extract also became DP-like with activation of Wnt and IGF signaling and were capable of inducing HF neogenesis. In addition, we also demonstrated a novel way to induce HF neogenesis by transfecting adult human fibroblasts with of mRNAs of these three genes, *Apoa1/Lgals1/Lum* (Fig. 29).

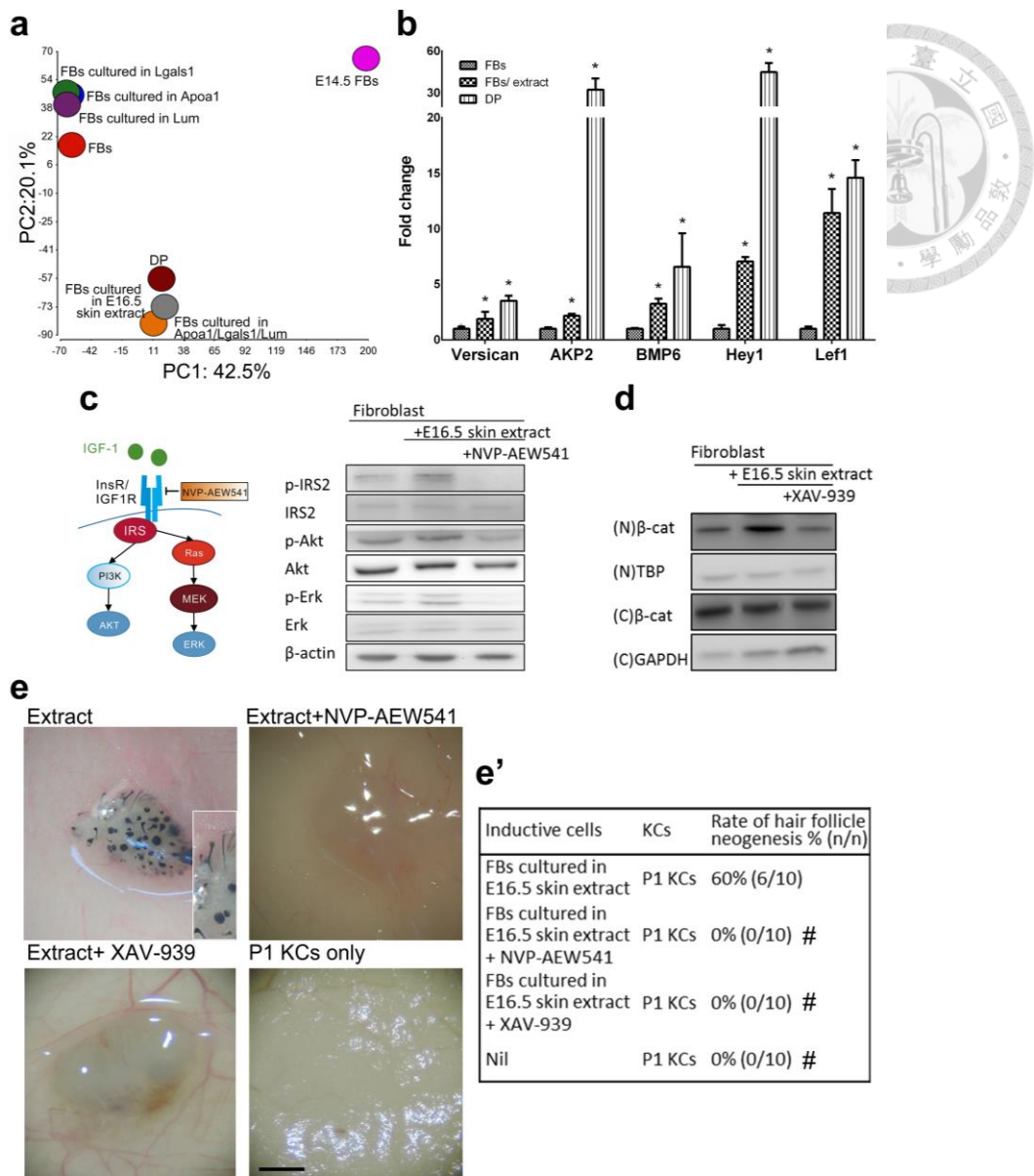
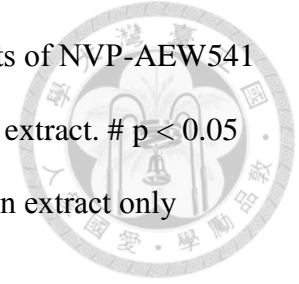


Figure 24 E16.5 skin extract confers adult fibroblasts trichogenic ability through activating IGF and Wnt signaling.

(a) Principal component analysis of the transcriptomes of E14.5 dermal fibroblasts, adult DP cells and fibroblasts before and after exposure to selected proteins or E16.5 skin extract for 6 hr. (b) Effect of a 6-hr exposure to E16.5 skin extract on the expression of the DP signature genes in cultured fibroblasts. * $p < 0.05$ with Student's t-test, compared with fibroblasts ($n = 3$). (c) Western blotting. The effect of E16.5 skin extract on insulin/Igf signaling in fibroblasts was inhibited by NVP-AEW541. (d)

Western blotting. Enhanced Wnt signaling in fibroblasts by E16.5 skin extract was inhibited by XAV-939. N: nuclear; C: cytoplasmic. (e, e') The effects of NVP-AEW541 and XAV-939 on HF induction by fibroblasts exposed to E16.5 skin extract. # $p < 0.05$ with Fisher's test, compared with fibroblasts cultured with E16.5 skin extract only (n=10). Bar: 500 μm . See also



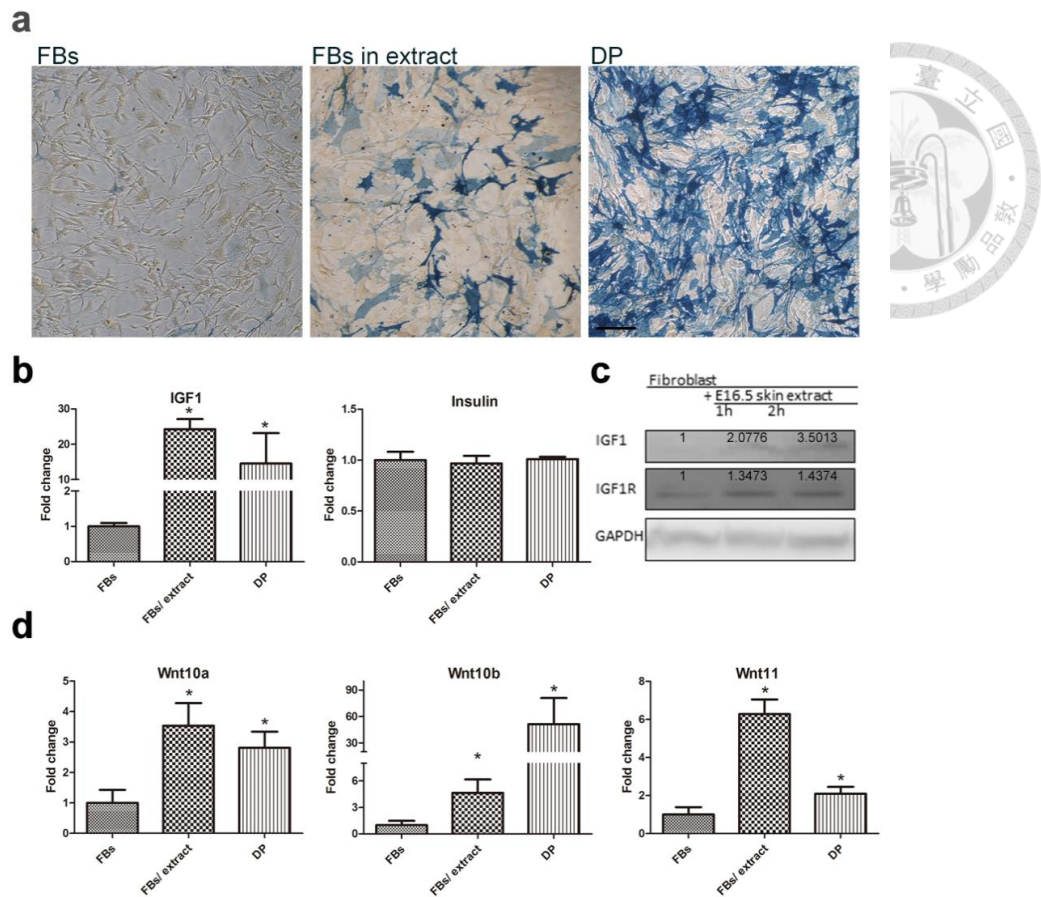


Figure 25 Alkaline phosphatase activity and gene expression of adult fibroblasts cultured in E16.5 skin extract.

(a) Alkaline phosphatase activity. Fibroblasts, originally negative for alkaline phosphatase activity (left panel), showed positive alkaline phosphatase activity after being cultured in E16.5 skin extract for 3 days (middle panel). Primary DP cells had highest alkaline phosphatase activity (right panel). (b) Gene expression of IGF1 and insulin quantified by q-PCR. Expression of IGF1 was increased in fibroblasts exposed to E16.5 skin extract. The expression of insulin was not significantly changed. (c) Western blot showed increased IGF1 production in fibroblasts exposed to E16.5 skin extract. The numbers indicated fold changes of protein expression. (d) q-PCR showed that expression of Wnt ligands including Wnt10a, Wnt10b and Wnt11 was increased in

fibroblasts exposed to E16.5 skin extract. * $p < 0.05$, compared with adult fibroblasts.

Bar: 100 μ m.



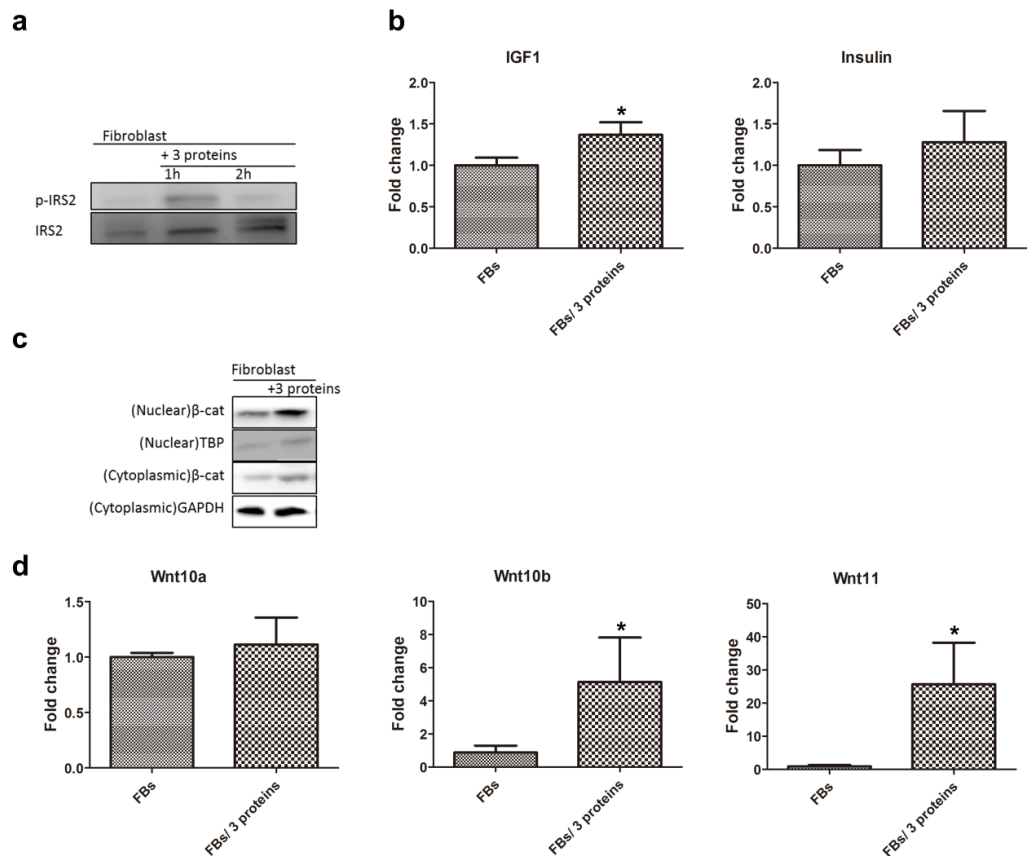


Figure 26 Effect of the combination apolipoprotein-A1, galectin-1 and lumican on IGF and Wnt signaling in adult fibroblasts.

(a) Adult fibroblasts were cultured with the combination of apolipoprotein-A1, galectin-1 and lumican for analysis. (b) Phosphorylation of IRS2 was increased after exposure to the 3 proteins. (b) q-PCR showed increased IGF1 expression by the treatment of the 3 proteins. The expression of insulin was not significantly increased. (c) Western blot showed that nuclear β -catenin (β -cat) was increased by the treatment of the 3 proteins. It indicated enhanced Wnt signaling. TATA-binding protein (TBP) expression was used as a nuclear marker. (d) q-PCR showed that expression of Wnt ligands including Wnt10b and Wnt11 was increased in fibroblasts exposed to the 3 proteins for 2 hr. * $p < 0.05$, compared with adult fibroblasts.

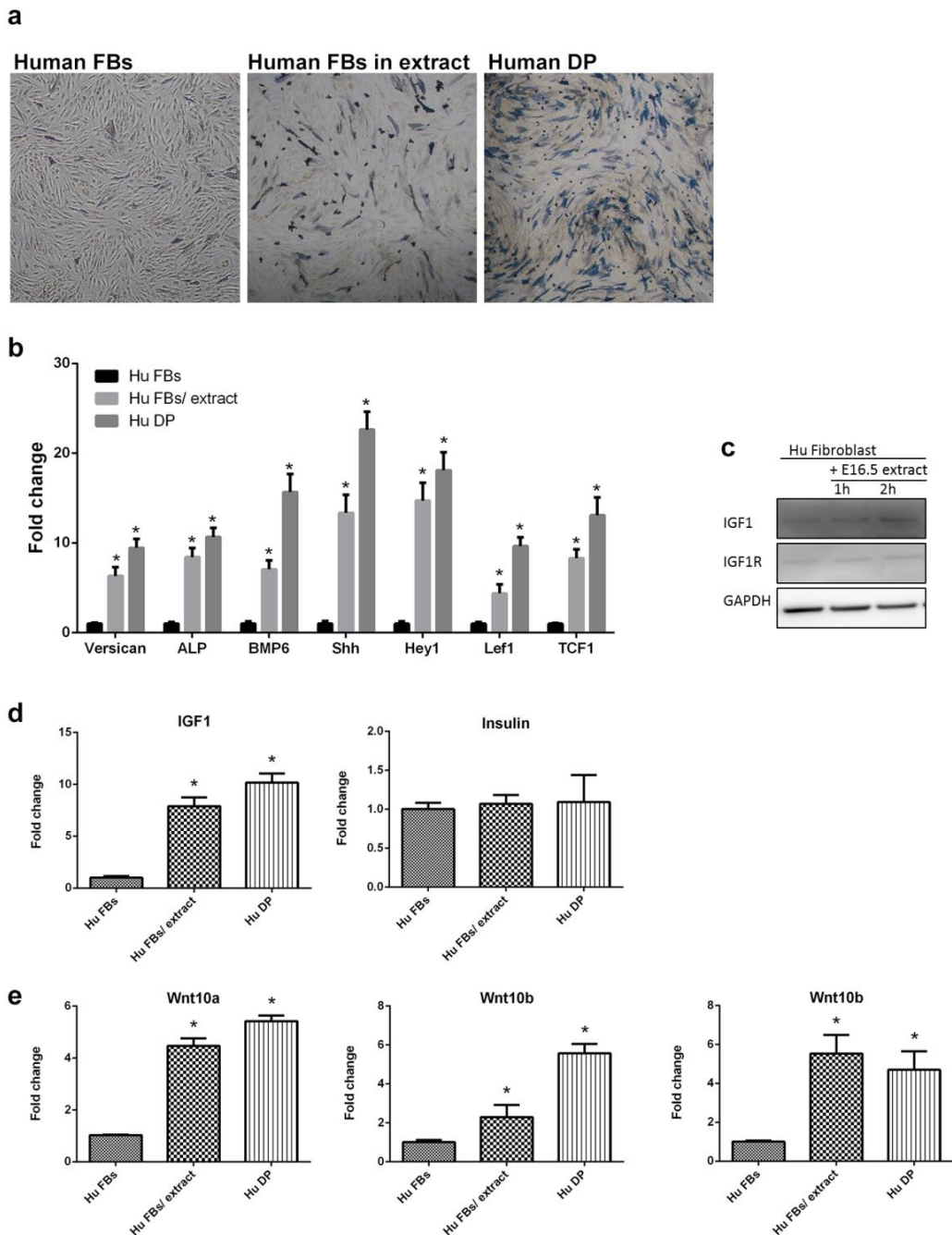
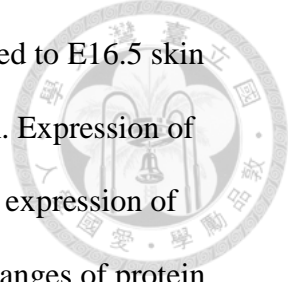


Figure 27 Alkaline phosphatase activity and gene expression of Human adult fibroblasts cultured in E16.5 skin extract.

(a) Alkaline phosphatase activity. Fibroblasts, originally negative for alkaline phosphatase activity (left panel), showed positive alkaline phosphatase activity after being cultured in E16.5 skin extract for 3 days (middle panel). Primary DP cells had highest alkaline phosphatase activity (right panel). (b) Effect of exposure to E16.5 skin

extract for 6hr on the expression of DP signature genes in human adult fibroblast, (c) Western blot showed increased IGF1 production in fibroblasts exposed to E16.5 skin extract (d) Gene expression of IGF1 and insulin quantified by q-PCR. Expression of IGF1 was increased in fibroblasts exposed to E16.5 skin extract. The expression of insulin was not significantly changed. The numbers indicated fold changes of protein expression. (e) q-PCR showed that expression of Wnt ligands including Wnt10a, Wnt10b and Wnt11 was increased in fibroblasts exposed to E16.5 skin extract. * $p < 0.05$, compared with adult fibroblasts. Bar: 100 μ m.



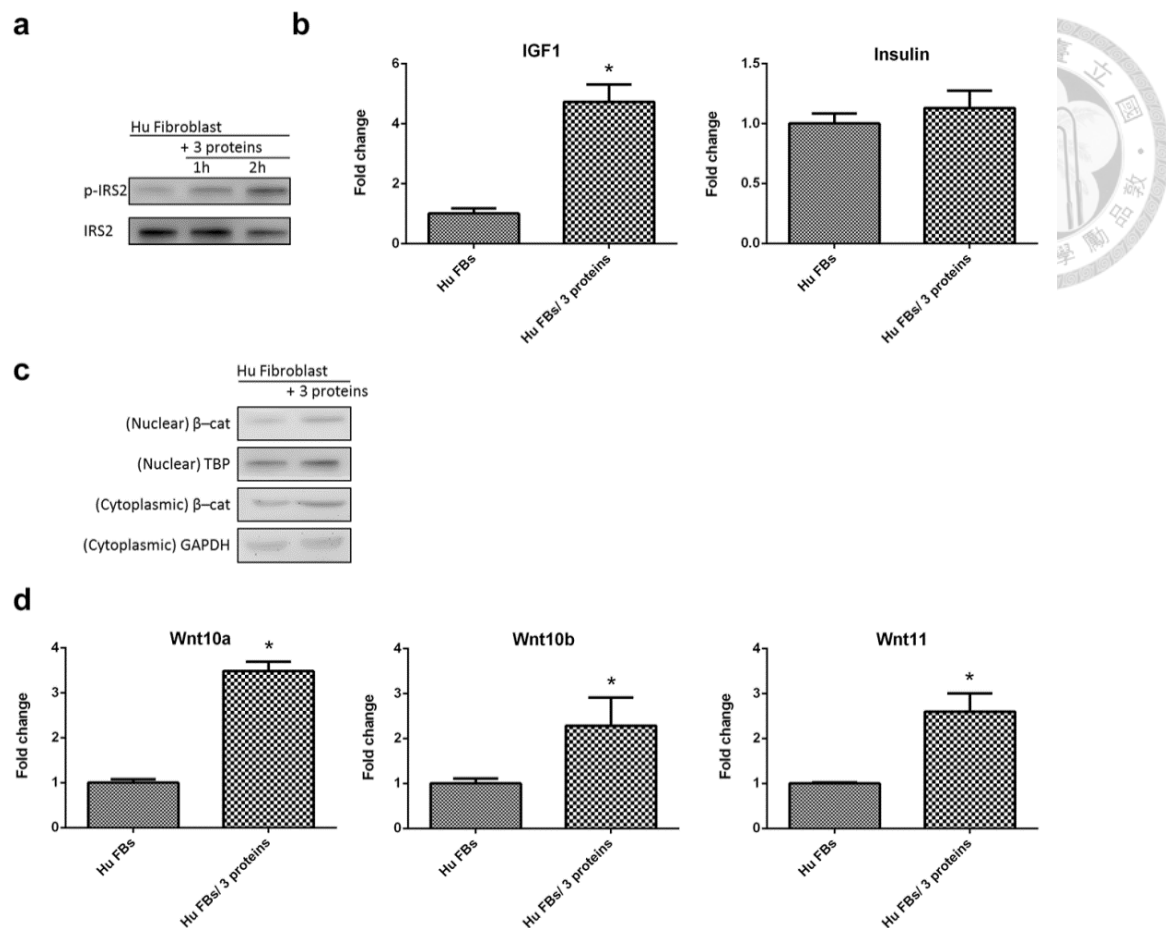
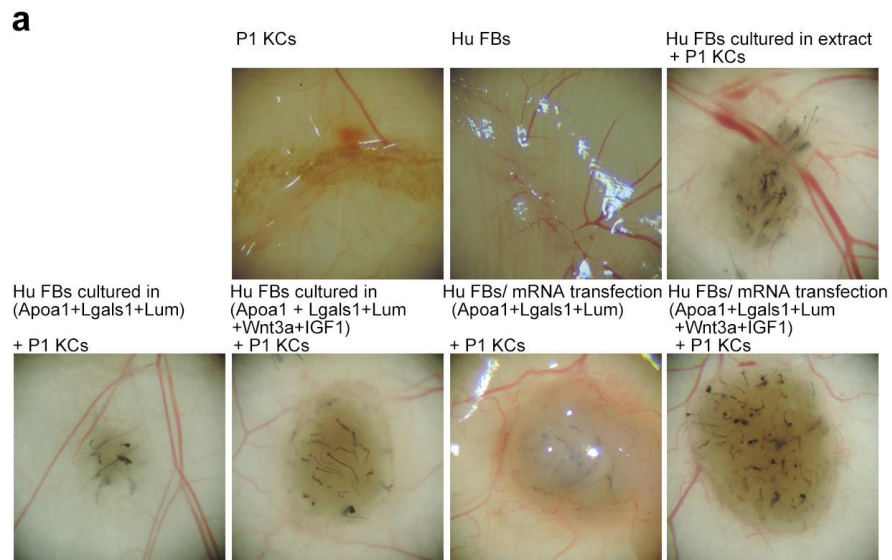


Figure 28 The effect of the 3 proteins on IGF and Wnt signaling in human adult fibroblasts. Adult fibroblasts were cultured with 3 proteins.

(a) Phosphorylation of Irs2 increased after exposure to the 3 proteins. (b) qRT-PCR showed increased *Igf1* following 3 proteins treatment for 6hr. Expression of insulin did not significantly increase. (c) Western blot showed that nuclear β-catenin increased following treatment with the 3 proteins for 6hr. TBP expression was used as the nuclear marker. (d) qRT-PCR showed that the expression of Wnt ligands *Wnt10b* and *Wnt11* increased in fibroblasts exposed to 3 proteins for 2 hr. FB: adult human fibroblast. * $p < 0.05$, compared with adult human fibroblasts ($n = 3$).



b

Inductive cells/ protein	KCs	Rate of hair follicle neogenesis % (n/n)
Nil	P1 KCs	0% (0/10)
Hu-FBs	P1 KCs	0% (0/10)
Hu-FBs cultured in E16.5 skin extract	P1 KCs	40% (4/10)
Hu-FBs cultured in Protein Mixtures (Apoa1+ Lgals1+ Lum)	P1 KCs	10% (1/10)
Hu-FBs cultured in Protein Mixtures (Apoa1+ Lgals1+ Lum+ Wnt3a+ IGF1)	P1 KCs	30% (3/10)
Hu-FBs/ mRNA transfection (Apoa1+ Lgals1+ Lum)	P1 KCs	10% (1/10)
Hu-FBs/ mRNA transfection (Apoa1+ Lgals1+ Lum+ Wnt3a+ IGF1)	P1 KCs	40% (4/10)

Figure 29 Induction of HF neogenesis by defined proteins and mRNAs.

P1 keratinocytes were used for all patch assays. (a) The effect of mRNA transfection of the three genes *Apoa/Lgals1/Lum* to adult human dermal fibroblasts on HF neogenesis. # $p < 0.05$ with Fisher's test, compared with P1 KCs only (n=10). Insets show enlarged images of the regenerated HFs. Bar: 500 μ m.

Discussion

Tissue regeneration depends on the presence of competent cells and an appropriate environment so that cells can initiate intercellular crosstalk to orchestrate morphogenetic events (Longaker and Adzick 1991). To promote regeneration, one can work to increase cell competency and/or make the macroenvironment more permissive.

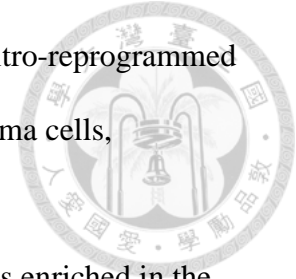
When the limbs of axolotls are amputated, they form a blastema that contains altered ECM and inductive factors that initiate and guide the regeneration of limbs (McGann, Odelberg, and Keating 2001). The tissue regeneration, though limited, after injury observed in several organs showed that cell competency is still preserved in adult mammalian cells. If we can make the environment more permissive while providing inductive signals, we can boot tissue regeneration.

HF regeneration involves follicular epithelium and DP cells, which of epithelial–mesenchymal interactions. Transplantation of those cellular components from mice allows complete hair reconstitution (Ehama et al. 2007). However, regeneration of human hair is not so easy.

Using HK2- cell-free extracts can induce Human bone marrow stromal cells (BMSCs) reprogrammed into renal proximal tubular-like epithelial cells, and the reprogrammed BMSCs can imploded into forming kidney tissue and tubular structures (Papadimou et al. 2015). The process of adult cell reprogramming, which induced by the cell residing in their native environment and re-expressing the developmental regulators to promote their maturation(Ginsberg et al. 2012; Karow et al. 2012; Qin et al. 2005).

Technology for direct cell reprogramming by exposing reversibly permeabilized somatic cells to cell-free extract have emerged. Cell-extract reprogramming was first demonstrated with extract of regenerating newt limbs, which promoted cell-cycle re-

entry and downregulation of myogenic markers in differentiated myotubes (McGann, Odelberg, and Keating 2001). Afterward, this approach yielded in-vitro-reprogrammed somatic cells with the extract from T cells, cardiomyocytes, insulinoma cells, pneumocytes, chromaffin, or embryonic stem cells (Qu et al. 2013).



Through proteomics analysis, we identified 3 secretable proteins enriched in the peri-folliculogenetic cutaneous environment, including apolipoprotein A-1, galectin-1, and lumican, that together were essential and sufficient to induce HF neogenesis.

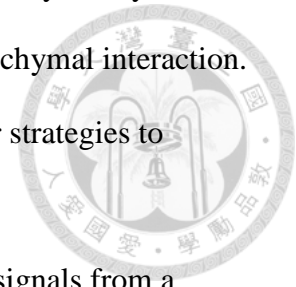
ApoA1 is the major protein component of plasma high-density lipoprotein particles (Brouillette et al. 2001).

Apolipoprotein (apo) A-I, is the major protein component of plasma high-density lipoprotein particles (Brouillette et al. 2001; Rye and Barter 2012). Including enhancement of endothelial repair and improvement of endothelial function (Wu et al. 2015; Spieker et al. 2002; Tso et al. 2006); removal of cholesterol from macrophages (Khera and Rader 2010); and also inhibit vascular inflammation (Nicholls et al. 2005); reduce oxidative stress in macrophages (Tabet et al. 2011); prevent oxidation of low-density lipoproteins (LDLs) (Zerrad-Saadi et al. 2009); reduce thrombosis (Mineo et al. 2006); increase angiogenesis (Sumi et al. 2007) and improve pancreatic β -cell function (Fryirs et al. 2010). Due to their function in lipid metabolism and transport, apolipoproteins are actively involved in tissue healing and regeneration where newly formed lipid membranes are required (van der Vliet et al. 2001; Monnot et al. 1999; Boyles et al. 1989). In addition to lipid metabolism, apolipoproteins also exhibit important functions in regulating morphogen signaling and epithelial-mesenchymal interaction during tissue development and regeneration (Monnot et al. 1999; Kim et al. 2010; Yao et al. 2008).

Lumican is also a member of the small leucine-rich proteoglycan (SLR) family and an ECM glycoprotein widely distributed in mammalian connective tissues include the cornea, sclera, aorta, cartilage, liver, skeletal muscle, kidney, pancreas, brain, placenta, and lung (Chakravarti et al. 1998; Funderburgh et al. 1991; Funderburgh et al. 1993; Grover et al. 1995; Krull and Gressner 1992; Ezura et al. 2000). And many studies have shown that in embryonic development and wound healing process lumican involved in cell migration and proliferation (Saika et al. 2000; Cornuet, Blochberger, and Hassell 1994; Doane et al. 1996; Wilda et al. 2000). Apart from its role in the organization of extracellular matrix, Lum also affects cell signaling, modulates the bioactivity of growth factors through binding and regulates tissue regeneration (Saika et al. 2003; Saika et al. 2000; Nikitovic, Katonis, et al. 2008; Nikitovic, Berdiaki, et al. 2008; Naito 2005).

Galectin-1 is a member of carbohydrate-binding proteins with an affinity for β -galactosides (Camby et al. 2006). Galectin-1 can be characterized as a truly matricellular protein, which serves as an adapter between cells and ECM modulates cell-cell and cell-ECM adhesion, migration, proliferation, and apoptosis (Elola et al. 2005). Galectin-1 also modulates proliferation of normal and malignant cells (Adams, Scott, and Weinberg 1996; van den Brule et al. 2003). Previous studies have described Galectin-1 can increase DNA synthesis in human SMC cultured on ECM (Moiseeva et al. 2000); promotes proliferation in rat pulmonary arterial endothelial cells (Sanford and Harris-Hooker 1990); induces proliferation of hepatic stellate cells (Maeda et al. 2003). Galectin-1 modulates a variety of functions, including cell growth, cell migration, lineage differentiation, immunity and tissue development (Camby et al. 2006; Puche et al. 1996; Andersen et al. 2003; Lutomski et al. 1997; Almkvist and Karlsson 2002; Georgiadis et al. 2007). It also promotes tissue regeneration (Chan et al. 2006; Georgiadis et al. 2007).

Therefore, postnatal organogenesis can be induced by local delivery of key environmental proteins to re-initiate developmental epithelial-mesenchymal interaction. Identification of such factors can potentially be integrated with other strategies to promote regeneration.

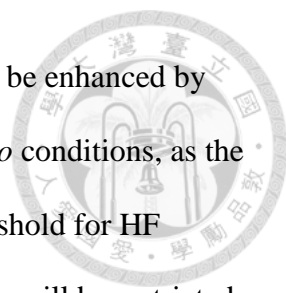


In the hair follicle, the activity of keratinocytes is regulated by signals from a specialized mesenchymal niche (DP). And by FGF and IGF stimulate β -catenin activity in the DP regulates signaling pathways that can mediate the DP's inductive effects. Therefore Wnt/ β -catenin signaling manage the interactions to conduct hair morphogenesis in both epithelial progenitor cells and their mesenchymal niche (Enshell-Seijffers et al. 2010; Nelson and Garza 2015). Another related message, the IGFs is produced by many tissues, it is thought that they function in an autocrine/paracrine fashion (Liu et al. 1993). And by the signaling pathway downstream of IGF1-R contain IRS-2 that regulate the differentiation and proliferation of keratinocytes (Sadagurski et al. 2006). And Dermal fibroblasts through a rich source for mitogens (e.g., IGFs, FGF-7, FGF-10 and epidermal growth factor receptor (EGFR) ligands) then promote facilitate colony formation of human and mouse keratinocytes in vitro (Lewis et al. 2010; Rheinwald and Green 1975; Rendl, Lewis, and Fuchs 2005).

In summary, we demonstrated that postnatal HF organogenesis could be induced by introducing defined extracellular proteins enriched in the embryonic environment. We showed that the minimal combination of the 3 core proteins of Apoa1, Lgals1 and Lum induced HF neogenesis in vivo, and incorporation of other factors could further enhance the trichogenic effect for higher HF inductivity. Tissue regeneration requires both cellular competency and inductive cues. Inductivity for organogenesis has been introduced by transplantation of embryonic mesenchymal cells of developing organs or postnatal organ-specific mesenchymal cells (Ferraris, Chaloin-Dufau, and Dhouailly

1994; Yen, Chan, and Lin 2010; Oliver 1970). The interaction of these mesenchymal cells with competent epithelial cells leads to organ neogenesis. Here, organ regeneration can be launched without the pre-existing inductive mesenchymal cells. Blastema of amputated limbs of axolotls also contains altered ECM and inductive factors to initiate and guide the regeneration of limbs (McGann, Odelberg, and Keating 2001). We expect that inductive factors and ECM can vary among organs for regeneration (Badylak 2005). Identification of defined organ-specific pro-regenerative factors can be a strategy to elicit or enhance regeneration.

Conclusions



In this work, we hypothesized that post-natal organogenesis can be enhanced by modifying the environment with defined protein factors. In the *in vivo* conditions, as the concentration of delivered proteins or mRNAs decays below the threshold for HF regeneration due to either diffusion or degradation, the HF inductivity will be restricted to a narrow post-injection period. We found that adult fibroblasts were stimulated by E16.5 skin extract to a state exhibiting upregulated DP-specific genes. Since the trichogenic ability of the stimulated fibroblasts was lost after a washout period, fibroblasts were not directly converted to a stable DP state. The secreted proteins enriched in the embryonic dermis around the time of HF morphogenesis are able to induce HF neogenesis in postnatal skin. The protein contains Apolipoprotein A-1, galectin-1 and lumican are the three key proteins in embryonic skin extract to re-elicite epithelial-mesenchymal interaction for HF morphogenesis. The cellular change here may not be equal to the direct cell fate reprogramming by transcriptional factors (Pang et al. 2011), in which the involvement of epigenetic rewiring raises safety concern in future clinical application. Adult fibroblasts here were brought to a stimulated condition capable of initiating crosstalk with keratinocytes and perpetuation of this interaction *in vivo* lead to HF neogenesis. The final cell fate conversion here is converted during the re-elicited epithelial-mesenchymal interaction. In addition to Wnt signaling, we also identified IGF signaling as one of the key signaling pathways in this process. Our results supported the notion that IGF signaling may be involved in the embryonic development of HFs (Liu et al. 1993). Pharmacological modulation of these key signaling pathways can potentially enhance regeneration.

Adult cells exposed to these pro-regeneration environmental proteins become competent to re-engage in organogenesis. The concealed regenerative potential of adult

cells can thus be unleashed in an environment reconstituted by defined extracellular protein factors.



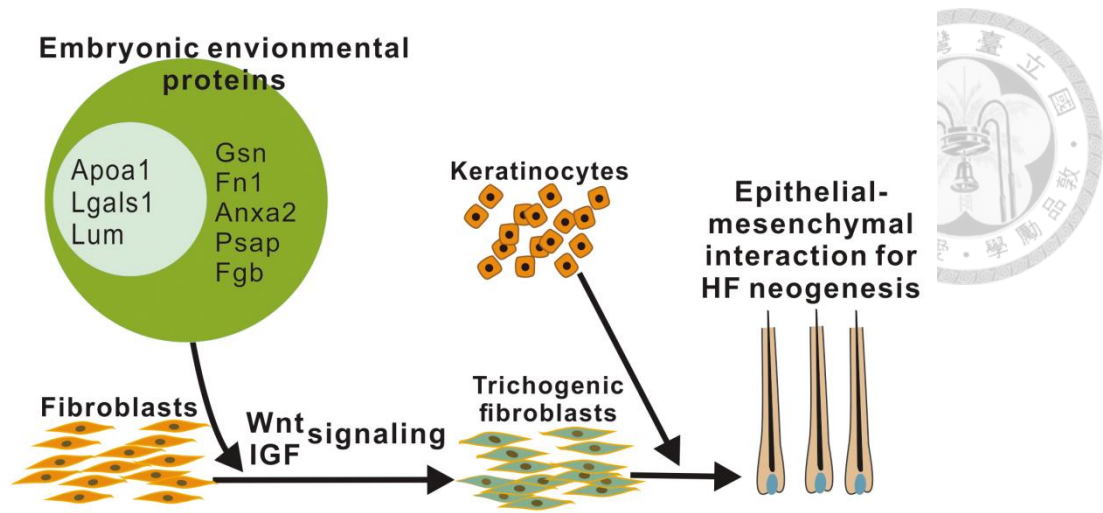
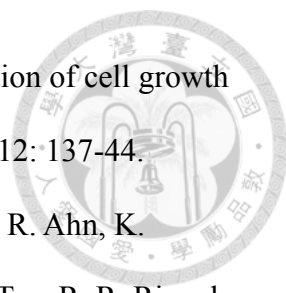


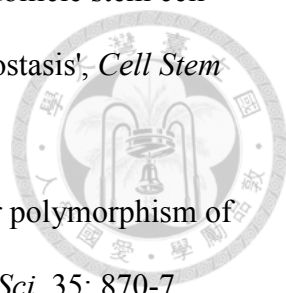
Figure 30 Depiction of the effect of embryonic environmental proteins on HF neogenesis.

Reference

- 
- Adams, L., G. K. Scott, and C. S. Weinberg. 1996. 'Biphasic modulation of cell growth by recombinant human galectin-1', *Biochim Biophys Acta*, 1312: 137-44.
- Ali, N., B. Zirak, R. S. Rodriguez, M. L. Pauli, H. A. Truong, K. Lai, R. Ahn, K. Corbin, M. M. Lowe, T. C. Scharschmidt, K. Taravati, M. R. Tan, R. R. Ricardo-Gonzalez, A. Nosbaum, M. Bertolini, W. Liao, F. O. Nestle, R. Paus, G. Cotsarelis, A. K. Abbas, and M. D. Rosenblum. 2017. 'Regulatory T Cells in Skin Facilitate Epithelial Stem Cell Differentiation', *Cell*, 169: 1119-29 e11.
- Almkvist, J., and A. Karlsson. 2002. 'Galectins as inflammatory mediators', *Glycoconj J*, 19: 575-81.
- Andersen, H., O. N. Jensen, E. P. Moiseeva, and E. F. Eriksen. 2003. 'A proteome study of secreted prostatic factors affecting osteoblastic activity: galectin-1 is involved in differentiation of human bone marrow stromal cells', *J Bone Miner Res*, 18: 195-203.
- Andl, T., S. T. Reddy, T. Gaddapara, and S. E. Millar. 2002. 'WNT signals are required for the initiation of hair follicle development', *Dev Cell*, 2: 643-53.
- Baarsma, H. A., A. I. Spanjer, G. Haitsma, L. H. Engelbertink, H. Meurs, M. R. Jonker, W. Timens, D. S. Postma, H. A. Kerstjens, and R. Gosens. 2011. 'Activation of WNT/beta-catenin signaling in pulmonary fibroblasts by TGF-beta(1) is increased in chronic obstructive pulmonary disease', *PLoS One*, 6: e25450.
- Badylak, S. F. 2005. 'Regenerative medicine and developmental biology: the role of the extracellular matrix', *Anat Rec B New Anat*, 287: 36-41.
- Becker, R. O., S. Chapin, and R. Sherry. 1974. 'Regeneration of the ventricular myocardium in amphibians', *Nature*, 248: 145-7.

- Billingham, R. E., and P. S. Russell. 1956. 'Incomplete wound contracture and the phenomenon of hair neogenesis in rabbits' skin', *Nature*, 177: 791-2.
- Blanpain, C., W. E. Lowry, A. Geoghegan, L. Polak, and E. Fuchs. 2004. 'Self-renewal, multipotency, and the existence of two cell populations within an epithelial stem cell niche', *Cell*, 118: 635-48.
- Borgens, R. B. 1982. 'Mice regrow the tips of their foretoes', *Science*, 217: 747-50.
- Boyles, J. K., C. D. Zoellner, L. J. Anderson, L. M. Kosik, R. E. Pitas, K. H. Weisgraber, D. Y. Hui, R. W. Mahley, P. J. Gebicke-Haerter, M. J. Ignatius, and et al. 1989. 'A role for apolipoprotein E, apolipoprotein A-I, and low density lipoprotein receptors in cholesterol transport during regeneration and remyelination of the rat sciatic nerve', *J Clin Invest*, 83: 1015-31.
- Breedis, C. 1954. 'Regeneration of hair follicles and sebaceous glands from the epithelium of scars in the rabbit', *Cancer Res*, 14: 575-9.
- Brockes, J. P. 1997. 'Amphibian limb regeneration: rebuilding a complex structure', *Science*, 276: 81-7.
- Brouillette, C. G., G. M. Anantharamaiah, J. A. Engler, and D. W. Borhani. 2001. 'Structural models of human apolipoprotein A-I: a critical analysis and review', *Biochim Biophys Acta*, 1531: 4-46.
- Camby, I., M. Le Mercier, F. Lefranc, and R. Kiss. 2006. 'Galectin-1: a small protein with major functions', *Glycobiology*, 16: 137R-57R.
- Castellana, D., R. Paus, and M. Perez-Moreno. 2014. 'Macrophages contribute to the cyclic activation of adult hair follicle stem cells', *PLoS Biol*, 12: e1002002.
- Chakravarti, S., T. Magnuson, J. H. Lass, K. J. Jepsen, C. LaMantia, and H. Carroll. 1998. 'Lumican regulates collagen fibril assembly: skin fragility and corneal opacity in the absence of lumican', *J Cell Biol*, 141: 1277-86.

- Chan, C. C., S. M. Fan, W. H. Wang, Y. F. Mu, and S. J. Lin. 2015. 'A Two-Stepped Culture Method for Efficient Production of Trichogenic Keratinocytes', *Tissue Eng Part C Methods*, 21: 1070-9.
- Chan, J., K. O'Donoghue, M. Gavina, Y. Torrente, N. Kennea, H. Mehmet, H. Stewart, D. J. Watt, J. E. Morgan, and N. M. Fisk. 2006. 'Galectin-1 induces skeletal muscle differentiation in human fetal mesenchymal stem cells and increases muscle regeneration', *Stem Cells*, 24: 1879-91.
- Chen, C. C., and C. M. Chuong. 2012. 'Multi-layered environmental regulation on the homeostasis of stem cells: the saga of hair growth and alopecia', *J Dermatol Sci*, 66: 3-11.
- Chen, C. C., M. V. Plikus, P. C. Tang, R. B. Widelitz, and C. M. Chuong. 2016. 'The Modulatable Stem Cell Niche: Tissue Interactions during Hair and Feather Follicle Regeneration', *J Mol Biol*, 428: 1423-40.
- Chen, C. C., L. Wang, M. V. Plikus, T. X. Jiang, P. J. Murray, R. Ramos, C. F. Guerrero-Juarez, M. W. Hughes, O. K. Lee, S. Shi, R. B. Widelitz, A. D. Lander, and C. M. Chuong. 2015. 'Organ-level quorum sensing directs regeneration in hair stem cell populations', *Cell*, 161: 277-90.
- Chen, D., A. Jarrell, C. Guo, R. Lang, and R. Atit. 2012. 'Dermal beta-catenin activity in response to epidermal Wnt ligands is required for fibroblast proliferation and hair follicle initiation', *Development*, 139: 1522-33.
- Chen, R. N., H. O. Ho, Y. T. Tsai, and M. T. Sheu. 2004. 'Process development of an acellular dermal matrix (ADM) for biomedical applications', *Biomaterials*, 25: 2679-86.
- Choi, Y. S., Y. Zhang, M. Xu, Y. Yang, M. Ito, T. Peng, Z. Cui, A. Nagy, A. K. Hadjantonakis, R. A. Lang, G. Cotsarelis, T. Andl, E. E. Morrisey, and S. E.

- 
- Millar. 2013. 'Distinct functions for Wnt/beta-catenin in hair follicle stem cell proliferation and survival and interfollicular epidermal homeostasis', *Cell Stem Cell*, 13: 720-33.
- Cornuet, P. K., T. C. Blochberger, and J. R. Hassell. 1994. 'Molecular polymorphism of lumican during corneal development', *Invest Ophthalmol Vis Sci*, 35: 870-7.
- Cotsarelis, G., T. T. Sun, and R. M. Lavker. 1990. 'Label-retaining cells reside in the bulge area of pilosebaceous unit: implications for follicular stem cells, hair cycle, and skin carcinogenesis', *Cell*, 61: 1329-37.
- Cox, J., and M. Mann. 2008. 'MaxQuant enables high peptide identification rates, individualized p.p.b.-range mass accuracies and proteome-wide protein quantification', *Nat Biotechnol*, 26: 1367-72.
- Cox, J., N. Neuhauser, A. Michalski, R. A. Scheltema, J. V. Olsen, and M. Mann. 2011. 'Andromeda: a peptide search engine integrated into the MaxQuant environment', *J Proteome Res*, 10: 1794-805.
- Dellgren, G., M. J. Eriksson, L. A. Brodin, and K. Radegran. 2002. 'Eleven years' experience with the Biocor stentless aortic bioprosthesis: clinical and hemodynamic follow-up with long-term relative survival rate', *Eur J Cardiothorac Surg*, 22: 912-21.
- Dhouailly, D. 1973. 'Dermo-epidermal interactions between birds and mammals: differentiation of cutaneous appendages', *J Embryol Exp Morphol*, 30: 587-603.
- Diani, A. R., M. J. Mulholland, K. L. Shull, M. F. Kubicek, G. A. Johnson, H. J. Schostarez, M. N. Brunden, and A. E. Buhl. 1992. 'Hair growth effects of oral administration of finasteride, a steroid 5 alpha-reductase inhibitor, alone and in combination with topical minoxidil in the balding stump-tail macaque', *J Clin Endocrinol Metab*, 74: 345-50.

- Doane, K. J., W. H. Ting, J. S. McLaughlin, and D. E. Birk. 1996. 'Spatial and temporal variations in extracellular matrix of periocular and corneal regions during corneal stromal development', *Experimental Eye Research*, 62: 271-83.
- Dobin, A., C. A. Davis, F. Schlesinger, J. Drenkow, C. Zaleski, S. Jha, P. Batut, M. Chaisson, and T. R. Gingeras. 2013. 'STAR: ultrafast universal RNA-seq aligner', *Bioinformatics*, 29: 15-21.
- Ehama, R., Y. Ishimatsu-Tsuji, S. Iriyama, R. Ideta, T. Soma, K. Yano, C. Kawasaki, S. Suzuki, Y. Shirakata, K. Hashimoto, and J. Kishimoto. 2007. 'Hair follicle regeneration using grafted rodent and human cells', *J Invest Dermatol*, 127: 2106-15.
- Elola, M. T., M. E. Chiesa, A. F. Alberti, J. Mordoh, and N. E. Fink. 2005. 'Galectin-1 receptors in different cell types', *J Biomed Sci*, 12: 13-29.
- Enshell-Seijffers, D., C. Lindon, M. Kashiwagi, and B. A. Morgan. 2010. 'beta-catenin activity in the dermal papilla regulates morphogenesis and regeneration of hair', *Dev Cell*, 18: 633-42.
- Ezura, Y., S. Chakravarti, A. Oldberg, I. Chervoneva, and D. E. Birk. 2000. 'Differential expression of lumican and fibromodulin regulate collagen fibrillogenesis in developing mouse tendons', *J Cell Biol*, 151: 779-88.
- Ferraris, C., B. A. Bernard, and D. Dhouailly. 1997. 'Adult epidermal keratinocytes are endowed with pilosebaceous forming abilities', *Int J Dev Biol*, 41: 491-8.
- Ferraris, C., C. Chaloin-Dufau, and D. Dhouailly. 1994. 'Transdifferentiation of embryonic and postnatal rabbit corneal epithelial cells', *Differentiation*, 57: 89-96.

- Festa, E., J. Fretz, R. Berry, B. Schmidt, M. Rodeheffer, M. Horowitz, and V. Horsley. 2011. 'Adipocyte lineage cells contribute to the skin stem cell niche to drive hair cycling', *Cell*, 146: 761-71.
- Fryirs, M. A., P. J. Barter, M. Appavoo, B. E. Tuch, F. Tabet, A. K. Heather, and K. A. Rye. 2010. 'Effects of high-density lipoproteins on pancreatic beta-cell insulin secretion', *Arterioscler Thromb Vasc Biol*, 30: 1642-8.
- Funderburgh, J. L., M. L. Funderburgh, S. J. Brown, J. P. Vergnes, J. R. Hassell, M. M. Mann, and G. W. Conrad. 1993. 'Sequence and structural implications of a bovine corneal keratan sulfate proteoglycan core protein. Protein 37B represents bovine lumican and proteins 37A and 25 are unique', *J Biol Chem*, 268: 11874-80.
- Funderburgh, J. L., M. L. Funderburgh, M. M. Mann, and G. W. Conrad. 1991. 'Arterial lumican. Properties of a corneal-type keratan sulfate proteoglycan from bovine aorta', *J Biol Chem*, 266: 24773-7.
- Gay, D., O. Kwon, Z. Zhang, M. Spata, M. V. Plikus, P. D. Holler, M. Ito, Z. Yang, E. Treffeisen, C. D. Kim, A. Nace, X. Zhang, S. Baratono, F. Wang, D. M. Ornitz, S. E. Millar, and G. Cotsarelis. 2013. 'Fgf9 from dermal gammadelta T cells induces hair follicle neogenesis after wounding', *Nat Med*, 19: 916-23.
- Georgiadis, V., H. J. Stewart, H. J. Pollard, Y. Tavsanoglu, R. Prasad, J. Horwood, L. Deltour, K. Goldring, F. Poirier, and D. J. Lawrence-Watt. 2007. 'Lack of galectin-1 results in defects in myoblast fusion and muscle regeneration', *Dev Dyn*, 236: 1014-24.
- Gerecht-Nir, S., M. Radisic, H. Park, C. Cannizzaro, J. Boublik, R. Langer, and G. Vunjak-Novakovic. 2006. 'Biophysical regulation during cardiac development and application to tissue engineering', *Int J Dev Biol*, 50: 233-43.

- Gilbert, T. W., T. L. Sellaro, and S. F. Badylak. 2006. 'Decellularization of tissues and organs', *Biomaterials*, 27: 3675-83.
- Ginsberg, M., D. James, B. S. Ding, D. Nolan, F. Geng, J. M. Butler, W. Schachterle, V. R. Pulijaal, S. Mathew, S. T. Chasen, J. Xiang, Z. Rosenwaks, K. Shido, O. Elemento, S. Y. Rabbany, and S. Rafii. 2012. 'Efficient direct reprogramming of mature amniotic cells into endothelial cells by ETS factors and TGFbeta suppression', *Cell*, 151: 559-75.
- Greco, V., T. Chen, M. Rendl, M. Schober, H. A. Pasolli, N. Stokes, J. Dela Cruz-Racelis, and E. Fuchs. 2009. 'A two-step mechanism for stem cell activation during hair regeneration', *Cell Stem Cell*, 4: 155-69.
- Grover, J., X. N. Chen, J. R. Korenberg, and P. J. Roughley. 1995. 'The human lumican gene. Organization, chromosomal location, and expression in articular cartilage', *J Biol Chem*, 270: 21942-9.
- Hardy, M. H. 1992. 'The secret life of the hair follicle', *Trends Genet*, 8: 55-61.
- Headington, J. T. 1987. 'Hair follicle biology and topical minoxidil: possible mechanisms of action', *Dermatologica*, 175 Suppl 2: 19-22.
- Higgins, C. A., J. C. Chen, J. E. Cerise, C. A. Jahoda, and A. M. Christiano. 2013. 'Microenvironmental reprogramming by three-dimensional culture enables dermal papilla cells to induce de novo human hair-follicle growth', *Proc Natl Acad Sci U S A*, 110: 19679-88.
- Horne, K. A., C. A. Jahoda, and R. F. Oliver. 1986. 'Whisker growth induced by implantation of cultured vibrissa dermal papilla cells in the adult rat', *J Embryol Exp Morphol*, 97: 111-24.
- Huang, Y. C., C. C. Chan, W. T. Lin, H. Y. Chiu, R. Y. Tsai, T. H. Tsai, J. Y. Chan, and S. J. Lin. 2013. 'Scalable production of controllable dermal papilla spheroids on

PVA surfaces and the effects of spheroid size on hair follicle regeneration',
Biomaterials, 34: 442-51.

Huelsken, J., R. Vogel, B. Erdmann, G. Cotsarelis, and W. Birchmeier. 2001. 'beta-Catenin controls hair follicle morphogenesis and stem cell differentiation in the skin', *Cell*, 105: 533-45.

Hughes, M. W., T. X. Jiang, S. J. Lin, Y. Leung, K. Kobiela, R. B. Widelitz, and C. M. Chuong. 2014. 'Disrupted ectodermal organ morphogenesis in mice with a conditional histone deacetylase 1, 2 deletion in the epidermis', *J Invest Dermatol*, 134: 24-32.

Ihaka, Ross, and Robert Gentleman. 1996. 'R: A Language for Data Analysis and Graphics', *Journal of Computational and Graphical Statistics*, 5: 299-314.

Inamatsu, M., T. Tochio, A. Makabe, T. Endo, S. Oomizu, E. Kobayashi, and K. Yoshizato. 2006. 'Embryonic dermal condensation and adult dermal papilla induce hair follicles in adult glabrous epidermis through different mechanisms', *Dev Growth Differ*, 48: 73-86.

Ito, M., Z. Yang, T. Andl, C. Cui, N. Kim, S. E. Millar, and G. Cotsarelis. 2007. 'Wnt-dependent de novo hair follicle regeneration in adult mouse skin after wounding', *Nature*, 447: 316-20.

Jaenisch, R., and R. Young. 2008. 'Stem cells, the molecular circuitry of pluripotency and nuclear reprogramming', *Cell*, 132: 567-82.

Jahoda, C. A., K. A. Horne, and R. F. Oliver. 1984. 'Induction of hair growth by implantation of cultured dermal papilla cells', *Nature*, 311: 560-2.

Jahoda, C. A., A. J. Reynolds, and R. F. Oliver. 1993. 'Induction of hair growth in ear wounds by cultured dermal papilla cells', *J Invest Dermatol*, 101: 584-90.



- Johnson, S. L., and J. A. Weston. 1995. 'Temperature-sensitive mutations that cause stage-specific defects in Zebrafish fin regeneration', *Genetics*, 141: 1583-95.
- Kandyba, E., Y. Leung, Y. B. Chen, R. Widelitz, C. M. Chuong, and K. Kobiela. 2013. 'Competitive balance of intrabulge BMP/Wnt signaling reveals a robust gene network ruling stem cell homeostasis and cyclic activation', *Proc Natl Acad Sci U S A*, 110: 1351-6.
- Karow, M., R. Sanchez, C. Schichor, G. Masserdotti, F. Ortega, C. Heinrich, S. Gascon, M. A. Khan, D. C. Lie, A. Dellavalle, G. Cossu, R. Goldbrunner, M. Gotz, and B. Berninger. 2012. 'Reprogramming of pericyte-derived cells of the adult human brain into induced neuronal cells', *Cell Stem Cell*, 11: 471-6.
- Kaufman, K. D., and R. P. Dawber. 1999. 'Finasteride, a Type 2 5alpha-reductase inhibitor, in the treatment of men with androgenetic alopecia', *Expert Opin Investig Drugs*, 8: 403-15.
- Ketchedjian, A., A. L. Jones, P. Krueger, E. Robinson, K. Crouch, L. Wolfenbarger, Jr., and R. Hopkins. 2005. 'Recellularization of decellularized allograft scaffolds in ovine great vessel reconstructions', *Ann Thorac Surg*, 79: 888-96; discussion 96.
- Khera, A. V., and D. J. Rader. 2010. 'Future therapeutic directions in reverse cholesterol transport', *Curr Atheroscler Rep*, 12: 73-81.
- Kim, T. H., Y. H. Lee, K. H. Kim, S. H. Lee, J. Y. Cha, E. K. Shin, S. Jung, A. S. Jang, S. W. Park, S. T. Uh, Y. H. Kim, J. S. Park, H. G. Sin, W. Youm, E. S. Koh, S. Y. Cho, Y. K. Paik, T. Y. Rhim, and C. S. Park. 2010. 'Role of lung apolipoprotein A-I in idiopathic pulmonary fibrosis: antiinflammatory and antifibrotic effect on experimental lung injury and fibrosis', *Am J Respir Crit Care Med*, 182: 633-42.
- Kligman, A. M., and J. S. Strauss. 1956. 'The formation of vellus hair follicles from human adult epidermis', *J Invest Dermatol*, 27: 19-23.

- Kobiela, K., N. Stokes, J. de la Cruz, L. Polak, and E. Fuchs. 2007. 'Loss of a quiescent niche but not follicle stem cells in the absence of bone morphogenetic protein signaling', *Proc Natl Acad Sci U S A*, 104: 10063-8.
- Kreindler, T. G. 1987. 'Topical minoxidil in early androgenetic alopecia', *J Am Acad Dermatol*, 16: 718-24.
- Krull, N. B., and A. M. Gressner. 1992. 'Differential expression of keratan sulphate proteoglycans fibromodulin, lumican and aggrecan in normal and fibrotic rat liver', *FEBS Lett*, 312: 47-52.
- Lacassagne, A., and R. Latarjet. 1946. 'Action of methylcholanthrene on certain scars of the skin in mice', *Cancer Res*, 6: 183-8.
- Lei, M., L. J. Schumacher, Y. C. Lai, W. T. Juan, C. Y. Yeh, P. Wu, T. X. Jiang, R. E. Baker, R. B. Widelitz, L. Yang, and C. M. Chuong. 2017. 'Self-organization process in newborn skin organoid formation inspires strategy to restore hair regeneration of adult cells', *Proc Natl Acad Sci U S A*, 114: E7101-E10.
- Lewis, D. A., J. B. Travers, A. K. Somani, and D. F. Spandau. 2010. 'The IGF-1/IGF-1R signaling axis in the skin: a new role for the dermis in aging-associated skin cancer', *Oncogene*, 29: 1475-85.
- Li, Y. C., M. W. Lin, M. H. Yen, S. M. Fan, J. T. Wu, T. H. Young, J. Y. Cheng, and S. J. Lin. 2015. 'Programmable Laser-Assisted Surface Microfabrication on a Poly(Vinyl Alcohol)-Coated Glass Chip with Self-Changing Cell Adhesivity for Heterotypic Cell Patterning', *ACS Appl Mater Interfaces*, 7: 22322-32.
- Lichti, U., J. Anders, and S. H. Yuspa. 2008. 'Isolation and short-term culture of primary keratinocytes, hair follicle populations and dermal cells from newborn mice and keratinocytes from adult mice for in vitro analysis and for grafting to immunodeficient mice', *Nat Protoc*, 3: 799-810.

- Lichti, U., W. C. Weinberg, L. Goodman, S. Ledbetter, T. Dooley, D. Morgan, and S. H. Yuspa. 1993. 'In vivo regulation of murine hair growth: insights from grafting defined cell populations onto nude mice', *J Invest Dermatol*, 101: 124S-29S.
- Lin, M. H., N. Sugiyama, and Y. Ishihama. 2015. 'Systematic profiling of the bacterial phosphoproteome reveals bacterium-specific features of phosphorylation', *Sci Signal*, 8: rs10.
- Lin, S. J., J. Foley, T. X. Jiang, C. Y. Yeh, P. Wu, A. Foley, C. M. Yen, Y. C. Huang, H. C. Cheng, C. F. Chen, B. Reeder, S. H. Jee, R. B. Widelitz, and C. M. Chuong. 2013. 'Topology of feather melanocyte progenitor niche allows complex pigment patterns to emerge', *Science*, 340: 1442-5.
- Liu, J. P., J. Baker, A. S. Perkins, E. J. Robertson, and A. Efstratiadis. 1993. 'Mice carrying null mutations of the genes encoding insulin-like growth factor I (Igf-1) and type 1 IGF receptor (Igf1r)', *Cell*, 75: 59-72.
- Lobe, C. G., K. E. Koop, W. Kreppner, H. Lomeli, M. Gertsenstein, and A. Nagy. 1999. 'Z/AP, a double reporter for cre-mediated recombination', *Dev Biol*, 208: 281-92.
- Longaker, M. T., and N. S. Adzick. 1991. 'The biology of fetal wound healing: a review', *Plast Reconstr Surg*, 87: 788-98.
- Lutowski, D., M. Fouillit, P. Bourin, D. Mellottee, N. Denize, M. Pontet, D. Bladier, M. Caron, and R. Joubert-Caron. 1997. 'Externalization and binding of galectin-1 on cell surface of K562 cells upon erythroid differentiation', *Glycobiology*, 7: 1193-9.
- Maeda, N., N. Kawada, S. Seki, T. Arakawa, K. Ikeda, H. Iwao, H. Okuyama, J. Hirabayashi, K. Kasai, and K. Yoshizato. 2003. 'Stimulation of proliferation of rat hepatic stellate cells by galectin-1 and galectin-3 through different intracellular signaling pathways', *J Biol Chem*, 278: 18938-44.

- Martin, P. 1997. 'Wound healing--aiming for perfect skin regeneration', *Science*, 276: 75-81.
- Maurel, D., C. Coutant, and J. Boissin. 1987. 'Thyroid and gonadal regulation of hair growth during the seasonal molt in the male European badger, *Meles meles L*', *Gen Comp Endocrinol*, 65: 317-27.
- McGann, C. J., S. J. Odelberg, and M. T. Keating. 2001. 'Mammalian myotube dedifferentiation induced by newt regeneration extract', *Proc Natl Acad Sci U S A*, 98: 13699-704.
- Messenger, A. G., D. N. Slater, and S. S. Bleehen. 1986. 'Alopecia areata: alterations in the hair growth cycle and correlation with the follicular pathology', *Br J Dermatol*, 114: 337-47.
- Millar, S. E. 2002. 'Molecular mechanisms regulating hair follicle development', *J Invest Dermatol*, 118: 216-25.
- Mineo, C., H. Deguchi, J. H. Griffin, and P. W. Shaul. 2006. 'Endothelial and antithrombotic actions of HDL', *Circ Res*, 98: 1352-64.
- Moiseeva, E. P., Q. Javed, E. L. Spring, and D. P. de Bono. 2000. 'Galectin 1 is involved in vascular smooth muscle cell proliferation', *Cardiovasc Res*, 45: 493-502.
- Monnot, M. J., P. J. Babin, G. Poleo, M. Andre, L. Laforest, C. Ballagny, and M. A. Akimenko. 1999. 'Epidermal expression of apolipoprotein E gene during fin and scale development and fin regeneration in zebrafish', *Dev Dyn*, 214: 207-15.
- Morris, R. J., Y. Liu, L. Marles, Z. Yang, C. Trempus, S. Li, J. S. Lin, J. A. Sawicki, and G. Cotsarelis. 2004. 'Capturing and profiling adult hair follicle stem cells', *Nat Biotechnol*, 22: 411-7.
- Muller-Rover, S., B. Handjiski, C. van der Veen, S. Eichmuller, K. Foitzik, I. A. McKay, K. S. Stenn, and R. Paus. 2001. 'A comprehensive guide for the accurate

- classification of murine hair follicles in distinct hair cycle stages', *J Invest Dermatol*, 117: 3-15.
- Naito, Z. 2005. 'Role of the small leucine-rich proteoglycan (SLRP) family in pathological lesions and cancer cell growth', *J Nippon Med Sch*, 72: 137-45.
- Nelson, A. M., and L. A. Garza. 2015. 'Bad Hair Day: Testosterone and Wnts', *J Invest Dermatol*, 135: 2567-69.
- Nelson, A. M., S. K. Reddy, T. S. Ratliff, M. Z. Hossain, A. S. Katseff, A. S. Zhu, E. Chang, S. R. Resnik, C. Page, D. Kim, A. J. Whittam, L. S. Miller, and L. A. Garza. 2015. 'dsRNA Released by Tissue Damage Activates TLR3 to Drive Skin Regeneration', *Cell Stem Cell*, 17: 139-51.
- Nicholls, S. J., G. J. Dusting, B. Cutri, S. Bao, G. R. Drummond, K. A. Rye, and P. J. Barter. 2005. 'Reconstituted high-density lipoproteins inhibit the acute pro-oxidant and proinflammatory vascular changes induced by a periarterial collar in normocholesterolemic rabbits', *Circulation*, 111: 1543-50.
- Nikitovic, D., A. Berdiaki, A. Zafiroopoulos, P. Katonis, A. Tsatsakis, N. K. Karamanos, and G. N. Tzanakakis. 2008. 'Lumican expression is positively correlated with the differentiation and negatively with the growth of human osteosarcoma cells', *FEBS J*, 275: 350-61.
- Nikitovic, D., P. Katonis, A. Tsatsakis, N. K. Karamanos, and G. N. Tzanakakis. 2008. 'Lumican, a small leucine-rich proteoglycan', *IUBMB Life*, 60: 818-23.
- Norwood, O. T. 1975. 'Male pattern baldness: classification and incidence', *South Med J*, 68: 1359-65.
- O'Connor, N.E. , J.B. Mulliken, S. Banks-Schlegel, O. Kehinde, and H. Green. 'Grafting of burns with cultured epithelium prepared from autologous epidermal cells', *Lancet*, 1: 4.

- Ohyama, M., Y. Zheng, R. Paus, and K. S. Stenn. 2010. 'The mesenchymal component of hair follicle neogenesis: background, methods and molecular characterization', *Exp Dermatol*, 19: 89-99.
- Oliver, R. F. 1966. 'Whisker growth after removal of the dermal papilla and lengths of follicle in the hooded rat', *J Embryol Exp Morphol*, 15: 331-47.
- . 1970. 'The induction of hair follicle formation in the adult hooded rat by vibrissa dermal papillae', *J Embryol Exp Morphol*, 23: 219-36.
- Osada, A., T. Iwabuchi, J. Kishimoto, T. S. Hamazaki, and H. Okochi. 2007. 'Long-term culture of mouse vibrissal dermal papilla cells and de novo hair follicle induction', *Tissue Eng*, 13: 975-82.
- Oshimori, N., and E. Fuchs. 2012. 'Paracrine TGF-beta signaling counterbalances BMP-mediated repression in hair follicle stem cell activation', *Cell Stem Cell*, 10: 63-75.
- Ott, H. C., T. S. Matthiesen, S. K. Goh, L. D. Black, S. M. Kren, T. I. Netoff, and D. A. Taylor. 2008. 'Perfusion-decellularized matrix: using nature's platform to engineer a bioartificial heart', *Nat Med*, 14: 213-21.
- Pang, Z. P., N. Yang, T. Vierbuchen, A. Ostermeier, D. R. Fuentes, T. Q. Yang, A. Citri, V. Sebastiano, S. Marro, T. C. Sudhof, and M. Wernig. 2011. 'Induction of human neuronal cells by defined transcription factors', *Nature*, 476: 220-3.
- Papadimou, E., M. Morigi, P. Iatropoulos, C. Xinaris, S. Tomasoni, V. Benedetti, L. Longaretti, C. Rota, M. Todeschini, P. Rizzo, M. Introna, M. Grazia de Simoni, G. Remuzzi, M. S. Goligorsky, and A. Benigni. 2015. 'Direct reprogramming of human bone marrow stromal cells into functional renal cells using cell-free extracts', *Stem Cell Reports*, 4: 685-98.



- Plikus, M. V., J. A. Mayer, D. de la Cruz, R. E. Baker, P. K. Maini, R. Maxson, and C. M. Chuong. 2008. 'Cyclic dermal BMP signalling regulates stem cell activation during hair regeneration', *Nature*, 451: 340-4.
- Porrello, E. R., A. I. Mahmoud, E. Simpson, J. A. Hill, J. A. Richardson, E. N. Olson, and H. A. Sadek. 2011. 'Transient regenerative potential of the neonatal mouse heart', *Science*, 331: 1078-80.
- Puche, A. C., F. Poirier, M. Hair, P. F. Bartlett, and B. Key. 1996. 'Role of galectin-1 in the developing mouse olfactory system', *Dev Biol*, 179: 274-87.
- Qiao, J., A. Zawadzka, E. Philips, A. Turetsky, S. Batchelor, J. Peacock, S. Durrant, D. Garlick, P. Kemp, and J. Teumer. 2009. 'Hair follicle neogenesis induced by cultured human scalp dermal papilla cells', *Regen Med*, 4: 667-76.
- Qin, M., G. Tai, P. Collas, J. M. Polak, and A. E. Bishop. 2005. 'Cell extract-derived differentiation of embryonic stem cells', *Stem Cells*, 23: 712-8.
- Qu, T., G. Shi, K. Ma, H. N. Yang, W. M. Duan, and G. D. Pappas. 2013. 'Targeted cell reprogramming produces analgesic chromaffin-like cells from human mesenchymal stem cells', *Cell Transplant*, 22: 2257-66.
- Rendl, M., L. Lewis, and E. Fuchs. 2005. 'Molecular dissection of mesenchymal-epithelial interactions in the hair follicle', *PLoS Biol*, 3: e331.
- Reynolds, A. J., and C. A. Jahoda. 1992. 'Cultured dermal papilla cells induce follicle formation and hair growth by transdifferentiation of an adult epidermis', *Development*, 115: 587-93.
- Rheinwald, J. G., and H. Green. 1975. 'Serial cultivation of strains of human epidermal keratinocytes: the formation of keratinizing colonies from single cells', *Cell*, 6: 331-43.

- Rieder, E., M. T. Kasimir, G. Silberhumer, G. Seebacher, E. Wolner, P. Simon, and G. Weigel. 2004. 'Decellularization protocols of porcine heart valves differ importantly in efficiency of cell removal and susceptibility of the matrix to recellularization with human vascular cells', *J Thorac Cardiovasc Surg*, 127: 399-405.
- Rye, K. A., and P. J. Barter. 2012. 'Predictive value of different HDL particles for the protection against or risk of coronary heart disease', *Biochim Biophys Acta*, 1821: 473-80.
- Sadagurski, M., S. Yakar, G. Weingarten, M. Holzenberger, C. J. Rhodes, D. Breitkreutz, D. Leroith, and E. Wertheimer. 2006. 'Insulin-like growth factor 1 receptor signaling regulates skin development and inhibits skin keratinocyte differentiation', *Mol Cell Biol*, 26: 2675-87.
- Saika, S., T. Miyamoto, S. Tanaka, T. Tanaka, I. Ishida, Y. Ohnishi, A. Ooshima, T. Ishiwata, G. Asano, T. Chikama, A. Shiraishi, C. Y. Liu, C. W. Kao, and W. W. Kao. 2003. 'Response of lens epithelial cells to injury: role of lumican in epithelial-mesenchymal transition', *Invest Ophthalmol Vis Sci*, 44: 2094-102.
- Saika, S., A. Shiraishi, C. Y. Liu, J. L. Funderburgh, C. W. Kao, R. L. Converse, and W. W. Kao. 2000. 'Role of lumican in the corneal epithelium during wound healing', *J Biol Chem*, 275: 2607-12.
- Sanford, G. L., and S. Harris-Hooker. 1990. 'Stimulation of vascular cell proliferation by beta-galactoside specific lectins', *FASEB J*, 4: 2912-8.
- Schmidt-Ullrich, R., and R. Paus. 2005. 'Molecular principles of hair follicle induction and morphogenesis', *Bioessays*, 27: 247-61.
- Schneider, M. R., R. Schmidt-Ullrich, and R. Paus. 2009. 'The hair follicle as a dynamic miniorgan', *Curr Biol*, 19: R132-42.

Segers, V. F., and R. T. Lee. 2008. 'Stem-cell therapy for cardiac disease', *Nature*, 451: 937-42.

Seifert, A. W., S. G. Kiama, M. G. Seifert, J. R. Goheen, T. M. Palmer, and M. Maden. 2012. 'Skin shedding and tissue regeneration in African spiny mice (*Acomys*)', *Nature*, 489: 561-5.

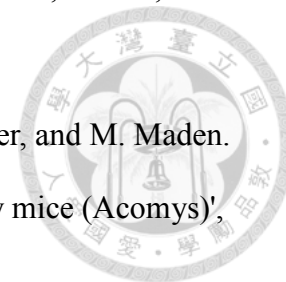
Spieker, L. E., I. Sudano, D. Hurlimann, P. G. Lerch, M. G. Lang, C. Binggeli, R. Corti, F. Ruschitzka, T. F. Luscher, and G. Noll. 2002. 'High-density lipoprotein restores endothelial function in hypercholesterolemic men', *Circulation*, 105: 1399-402.

Sumi, M., M. Sata, S. Miura, K. A. Rye, N. Toya, Y. Kanaoka, K. Yanaga, T. Ohki, K. Saku, and R. Nagai. 2007. 'Reconstituted high-density lipoprotein stimulates differentiation of endothelial progenitor cells and enhances ischemia-induced angiogenesis', *Arterioscler Thromb Vasc Biol*, 27: 813-8.

Tabet, F., G. Lambert, L. F. Cuesta Torres, L. Hou, I. Sotirchos, R. M. Touyz, A. J. Jenkins, P. J. Barter, and K. A. Rye. 2011. 'Lipid-free apolipoprotein A-I and discoidal reconstituted high-density lipoproteins differentially inhibit glucose-induced oxidative stress in human macrophages', *Arterioscler Thromb Vasc Biol*, 31: 1192-200.

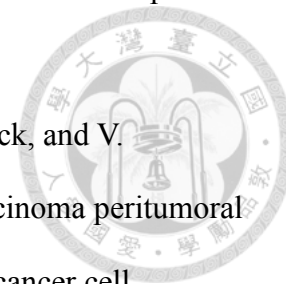
Takahashi, K., and S. Yamanaka. 2006. 'Induction of pluripotent stem cells from mouse embryonic and adult fibroblast cultures by defined factors', *Cell*, 126: 663-76.

Tam, P. P., M. Parameswaran, S. J. Kinder, and R. P. Weinberger. 1997. 'The allocation of epiblast cells to the embryonic heart and other mesodermal lineages: the role of ingression and tissue movement during gastrulation', *Development*, 124: 1631-42.

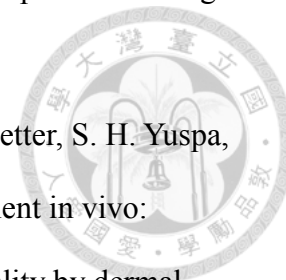


- Toyoshima, K. E., K. Asakawa, N. Ishibashi, H. Toki, M. Ogawa, T. Hasegawa, T. Irie, T. Tachikawa, A. Sato, A. Takeda, and T. Tsuji. 2012. 'Fully functional hair follicle regeneration through the rearrangement of stem cells and their niches', *Nat Commun*, 3: 784.
- Trapnell, C., A. Roberts, L. Goff, G. Pertea, D. Kim, D. R. Kelley, H. Pimentel, S. L. Salzberg, J. L. Rinn, and L. Pachter. 2012. 'Differential gene and transcript expression analysis of RNA-seq experiments with TopHat and Cufflinks', *Nat Protoc*, 7: 562-78.
- Tsai, C. F., C. C. Hsu, J. N. Hung, Y. T. Wang, W. K. Choong, M. Y. Zeng, P. Y. Lin, R. W. Hong, T. Y. Sung, and Y. J. Chen. 2014. 'Sequential phosphoproteomic enrichment through complementary metal-directed immobilized metal ion affinity chromatography', *Anal Chem*, 86: 685-93.
- Tsai, C. F., Y. T. Wang, Y. R. Chen, C. Y. Lai, P. Y. Lin, K. T. Pan, J. Y. Chen, K. H. Khoo, and Y. J. Chen. 2008. 'Immobilized metal affinity chromatography revisited: pH/acid control toward high selectivity in phosphoproteomics', *J Proteome Res*, 7: 4058-69.
- Tsai, C. F., Y. T. Wang, H. Y. Yen, C. C. Tsou, W. C. Ku, P. Y. Lin, H. Y. Chen, A. I. Nesvizhskii, Y. Ishihama, and Y. J. Chen. 2015. 'Large-scale determination of absolute phosphorylation stoichiometries in human cells by motif-targeting quantitative proteomics', *Nat Commun*, 6: 6622.
- Tso, C., G. Martinic, W. H. Fan, C. Rogers, K. A. Rye, and P. J. Barter. 2006. 'High-density lipoproteins enhance progenitor-mediated endothelium repair in mice', *Arterioscler Thromb Vasc Biol*, 26: 1144-9.
- Tsou, C. C., C. F. Tsai, Y. H. Tsui, P. R. Sudhir, Y. T. Wang, Y. J. Chen, J. Y. Chen, T. Y. Sung, and W. L. Hsu. 2010. 'IDEAL-Q, an automated tool for label-free

- quantitation analysis using an efficient peptide alignment approach and spectral data validation', *Mol Cell Proteomics*, 9: 131-44.
- van den Brule, F., S. Califice, F. Garnier, P. L. Fernandez, A. Berchuck, and V. Castronovo. 2003. 'Galectin-1 accumulation in the ovary carcinoma peritumoral stroma is induced by ovary carcinoma cells and affects both cancer cell proliferation and adhesion to laminin-1 and fibronectin', *Lab Invest*, 83: 377-86.
- van der Vliet, H. N., M. G. Sammels, A. C. Leegwater, J. H. Levels, P. H. Reitsma, W. Boers, and R. A. Chamuleau. 2001. 'Apolipoprotein A-V: a novel apolipoprotein associated with an early phase of liver regeneration', *J Biol Chem*, 276: 44512-20.
- Veves, A., V. Falanga, D. G. Armstrong, M. L. Sabolinski, and Study Apligraf Diabetic Foot Ulcer. 2001. 'Graftskin, a human skin equivalent, is effective in the management of noninfected neuropathic diabetic foot ulcers: a prospective randomized multicenter clinical trial', *Diabetes Care*, 24: 290-5.
- Vierbuchen, T., A. Ostermeier, Z. P. Pang, Y. Kokubu, T. C. Sudhof, and M. Wernig. 2010. 'Direct conversion of fibroblasts to functional neurons by defined factors', *Nature*, 463: 1035-41.
- Vizcaino, J. A., E. W. Deutsch, R. Wang, A. Csordas, F. Reisinger, D. Rios, J. A. Dienes, Z. Sun, T. Farrah, N. Bandeira, P. A. Binz, I. Xenarios, M. Eisenacher, G. Mayer, L. Gatto, A. Campos, R. J. Chalkley, H. J. Kraus, J. P. Albar, S. Martinez-Bartolome, R. Apweiler, G. S. Omenn, L. Martens, A. R. Jones, and H. Hermjakob. 2014. 'ProteomeXchange provides globally coordinated proteomics data submission and dissemination', *Nat Biotechnol*, 32: 223-6.
- Wang, Y. T., C. F. Tsai, T. C. Hong, C. C. Tsou, P. Y. Lin, S. H. Pan, T. M. Hong, P. C. Yang, T. Y. Sung, W. L. Hsu, and Y. J. Chen. 2010. 'An informatics-assisted



- label-free quantitation strategy that depicts phosphoproteomic profiles in lung cancer cell invasion', *J Proteome Res*, 9: 5582-97.
- Weinberg, W. C., L. V. Goodman, C. George, D. L. Morgan, S. Ledbetter, S. H. Yuspa, and U. Lichti. 1993. 'Reconstitution of hair follicle development in vivo: determination of follicle formation, hair growth, and hair quality by dermal cells', *J Invest Dermatol*, 100: 229-36.
- Wickham, Hadley. 2006. 'ggplot: An Implementation of the Grammar of Graphics.', *R package version 0.4. 0*.
- Wilda, M., D. Bachner, W. Just, C. Geerkens, P. Kraus, W. Vogel, and H. Hameister. 2000. 'A comparison of the expression pattern of five genes of the family of small leucine-rich proteoglycans during mouse development', *J Bone Miner Res*, 15: 2187-96.
- Wu, B. J., S. Shrestha, K. L. Ong, D. Johns, L. Hou, P. J. Barter, and K. A. Rye. 2015. 'Cholesteryl ester transfer protein inhibition enhances endothelial repair and improves endothelial function in the rabbit', *Arterioscler Thromb Vasc Biol*, 35: 628-36.
- Wynn, T. A., and T. R. Ramalingam. 2012. 'Mechanisms of fibrosis: therapeutic translation for fibrotic disease', *Nat Med*, 18: 1028-40.
- Xiang, Y., C. Q. Zhang, and K. Huang. 2012. 'Predicting glioblastoma prognosis networks using weighted gene co-expression network analysis on TCGA data', *BMC Bioinformatics*, 13 Suppl 2: S12.
- Yang, C. C., and G. Cotsarelis. 2010. 'Review of hair follicle dermal cells', *J Dermatol Sci*, 57: 2-11.
- Yao, Y., E. S. Shao, M. Jumabay, A. Shahbazian, S. Ji, and K. I. Bostrom. 2008. 'High-density lipoproteins affect endothelial BMP-signaling by modulating expression



of the activin-like kinase receptor 1 and 2', *Arterioscler Thromb Vasc Biol*, 28: 2266-74.

Yen, C. M., C. C. Chan, and S. J. Lin. 2010. 'High-throughput reconstitution of epithelial-mesenchymal interaction in folliculoid microtissues by biomaterial-facilitated self-assembly of dissociated heterotypic adult cells', *Biomaterials*, 31: 4341-52.

Zerrad-Saadi, A., P. Therond, S. Chantepie, M. Couturier, K. A. Rye, M. J. Chapman, and A. Kontush. 2009. 'HDL3-mediated inactivation of LDL-associated phospholipid hydroperoxides is determined by the redox status of apolipoprotein A-I and HDL particle surface lipid rigidity: relevance to inflammation and atherogenesis', *Arterioscler Thromb Vasc Biol*, 29: 2169-75.

Zheng, Y., X. Du, W. Wang, M. Boucher, S. Parimoo, and K. Stenn. 2005. 'Organogenesis from dissociated cells: generation of mature cycling hair follicles from skin-derived cells', *J Invest Dermatol*, 124: 867-76.

Zhou, Q., and D. A. Melton. 2008. 'Extreme makeover: converting one cell into another', *Cell Stem Cell*, 3: 382-8.

